University of Alberta

Electrophysiological Properties of a Quail Neuroretina Cell Line (QNR/D): Effects of Growth Hormone?

By

Alexis Andres

A thesis submitted to the Faculty of Graduated Studies and Research in partial fulfillment of the requirements for the degree of

Master of Science

Department of Physiology

Fall 2012

Edmonton, Alberta

ABSTRACT

The QNR/D cell line was derived from the embryonic quail retina with the purpose of creating an experimental model of retinal ganglion cell physiology. However, the validity of this model has not been demonstrated since expression of retinal ganglion cell protein markers and the electrophysiological properties of this cell line have not been evaluated. In this study, the expression of retinal ganglion cell protein markers and voltage-gated ion channels in QNR/D cells was investigated using immunocytochemistry and the whole cell patch clamp technique, respectively. Additionally, since these cells express growth hormone and growth hormone receptor, the effects of exogenous growth hormone treatment on ion channel expression were also investigated.

Using immunocytochemistry, it was determined that QNR/D cells express retinal ganglion cell markers Islet-1 homeobox transcription factor, R4A antigenicity, neurofilament proteins as well as growth hormone and growth hormone receptor. It was also determined that these cells express vimentin filaments which are expressed *in vivo* in retinal ganglion cell precursors.

Using the whole cell patch clamp technique, it was determined that QNR/D cells are incapable of firing action potentials. However, the expression of a variety of voltage-gated currents was observed using this technique. These currents include T-type Ca^{2+} currents, A-type K^+ currents and delayed rectifier K^+ currents. It was determined that the inward Ca^{2+} current was conducted by T-type voltage-gated calcium channels since these currents were completely inhibited by 5 μm mibefradil, a T-type selective antagonist. The A-type K^+ current was

identified by its transient nature and complete inactivation at a holding potential of -40 mV, while the delayed rectifier was identified by its lack of inactivation and outwardly rectifying current voltage relationship. Exogenous growth hormone treatment did not significantly alter the density of these currents or induce the expression of any other current types after 72 hours of exposure.

These results indicate that QNR/D are representative of retinal ganglion cells in the specificity stage of differentiation rather than mature retinal ganglion cells. Nonetheless, these cells do express a variety of voltage-gated currents, making the QNR/D cell line, from an electrophysiological perspective, the most suitable cell line model of retinal ganglion cells currently available.

ELECTROPHYSIOLOGICAL PROPERTIES OF A QUAIL NEURORETINA CELL LINE (QNR/D): EFFECTS OF GROWTH HORMONE?

TABLE OF CONTENTS

LIST OF TABLES

LIST OF FIGURES

LIST OF ABBREVIATIONS

AMPA	2-amino-3-(5-methyl-3-oxo-1,2-oxazol-4-yl) Propanoic Acid
ATCC	American Type Culture Collection
cAMP	Cyclic Adenosine Monophosphate
CNS	Central Nervous System
CREB	Cyclic Adenosine Monophosphate Response Element-binding
DAPI	4'-6-diamidino-2-phenylindol
DMEM	Dulbecco's Modified Eagles Medium
DMSO	Dimethyl Sulfoxide
ED	Embryonic Day
EDTA	Ethylenediaminetetraacetic Acid
EGF	Epidermal Growth Factor
ELISA	Enzyme-linked Immunosorbent Assay
EPSP	Excitatory Post Synaptic Potential
FBS	Fetal Bovine Serum
FGF	Fibroblast Growth Factor
GABA	γ-Aminobutyric Acid
GH	Growth Hormone
GHD	Growth Hormone Deficient
GHR	Growth Hormone Receptor
$GHR^{-/-}$	Growth Hormone Receptor Knockout
GHRH	Growth Hormone Releasing Hormone

HVA	High Voltage Activated
IGF	Insulin-like Growth Factor
IPL	Inner Plexiform Layer
LGN	Lateral Geniculate Nucleus
LTD	Long-term Depression
LTP	Long-term Potentiation
LVA	Low Voltage Activated
MAPK	Mitogen-activated Protein Kinase
mRNA	Messenger Ribonucleic Acid
NGF	Nerve Growth Factor
NGS	Normal Goat Serum
NMDA	N-methyl-D-aspartic Acid
P	Postnatal Day
PBS	Phosphate Buffed Saline
PI3K	Phosphatidylinositol 3'-kinase
PKA	Protein Kinase A
rANOVA	Repeated Measures Analysis of Variance
RT-PCR	Reverse Transcription Polymerase Chain Reaction
RGC	Retinal Ganglion Cell
scGH	Small Chicken Growth Hormone
SEA	Spontaneous Electrical Activity
Shh	Sonic Hedgehog
siRNA	Small Interfering Ribonucleic Acid

TGF	Transforming Growth Factor

CHAPTER ONE

LITERATURE REVIEW

I. GENERAL INTRODUCTION

The retinal ganglion cell (RGC) is the output neuron of the retina. It receives visual information from bipolar cells and amacrine cells, integrates these inputs and transmits this information over great distances to the visual centres in the central nervous system (CNS). This transmission is accomplished by the firing of action potentials which themselves are the product of ionic currents conducted by voltage gated ion channels. With this mechanism of operation in mind, it is clear that the expression of ion channels and the ability to fire action potentials is a RGC phenotype of utmost importance and hence any valid experimental model representing RGCs must exhibit robust ion channel expression.

Cell lines have been used extensively in the study of retinal ganglion cells. In fact, a pubmed search reveals over 150 publications in which the RGC-5 cell line was used as a model for retinal ganglion cells. This cell line was reportedly derived from the rat retina and yet does not display the single most important phenotypic characteristic of retinal ganglion cells, the expression of voltage-gated ion channels (Moorhouse *et al*, 2004). Furthermore, recent studies cast doubt on the reported origin of these cells (Van Bergen *et al*, 2009, Wood *et al*, 2010).

The QNR/D cell line is also employed as a model of retinal ganglion cells. This cell line is derived from the embryonic quail retina and could be a useful model of avian embryonic retinal ganglion cells. However, the validity of this model has not been demonstrated since expression of retinal ganglion cell protein markers and the electrophysiological properties of this cell line have not been evaluated. In this study, the expression of protein markers of retinal ganglion cells

and the expression of voltage-gated ion channels were investigated in QNR/D cells using immunocytochemistry and the whole cell patch clamp technique, respectively. Furthermore, the presence of GH and growth hormone receptor (GHR) in QNR/D cells suggests GH might have local electrophysiological actions in these cells, especially as GH had electrophysiological effects in the chicken brain (Lea and Harvey, 1993). Therefore, the effect of growth hormone (GH) on the expression of voltage-gated ion channels in the QNR/D cell line was investigated.

In this chapter a brief review of the scientific literature pertinent to these aims will be conducted. The pertinent topics are (1) the competence model of RGC differentiation, (2) the electrophysiological properties of RGCs, (3) cell lines as a model of RGC physiology and (4) growth hormone expression and activity in the avian neuroretina.

II. THE COMPETENCE MODEL OF RETINAL GANGLION CELL DIFFERENTIATION

Background

RGCs are the output neurons of the retina. These cells have a large soma, a single axon and a complex dentritic arbour that varies in breadth depending on RGC cell type. RGCs receive input from bipolar and amacrine cells and transmit the summation of this information along their axons in the form of action potential trains. These axons, which together constitute the optic nerve, ultimately synapse with neurons in the visual centres of the CNS.

RGCs are the first retinal cell type to differentiate. This is a complex process regulated by a number of intrinsic (transcription factors and growth factor receptors) and extrinsic (paracrine growth factors) factors. Initially the neuroepithelial cells that constitute the developing retina are mitotic multipotent progenitors capable of becoming any of the retinal cell types (Adler, 2000; Marquardt and Gruss, 2002; Mu and Klein, 2004). These multipotent precursors then progress through a number of developmental states. The chronological order of these states is (i) multipoentency (the capability to become any cell type within the retina), (ii) competency (the capability to become a specific cell type without being fully committed to that specific fate), (iii) specificity (the commitment to becoming a specific cell type without the expression of specific phenotypic characteristics of that cell type) and finally (iv) differentiation (the expression and functionality of those defining characteristics) (Adler, 2000; Marquardt and Gruss, 2002; Mu and Klein, 2004).

This process is first initiated in the centre of the immature retina and

spreads outward toward the periphery (Mu and Klein, 2004; Wallace, 2008). This concentric development pattern suggests that an inductive factor produced in the optic stalk triggers this development. Some evidence suggests that sonic hedgehog (Shh) is responsible for initiation of this development (Marquardt and Gruss, 2002; Wallace, 2008), however studies corroborating this in higher vertebrates are lacking.

Multipotency

Immediately after invagination of the optic vesicle, the cells composing the primordial retina are neuroepithelial cells in a multipotent state. Proliferation of these cells is promoted by both extrinsic growth factors: epidermal growth factor (EGF) (Anchan *et al*, 1997; James *et al*, 2004), fibroblast growth factor (FGF) (James *et al*, 2004) TGF (Anchan *et al*, 1997) and the membrane-bound Notch ligand Delta (James *et al*, 2004; Ohsawa and Kageyama, 2008) as well as the intrinsic transcription factors Hes1, Hes5 (Ohsawa and Kageyama, 2008) and Sox2 (Lin *et al*, 2009). Sox2 has been shown to increase the proliferation of retinal progenitor cells and to prevent their exit from the cell cycle (Lin *et al*, 2009). This proliferative activity results, at least in part, from Sox2 enhancement of Notch transcription (Taranova *et al*, 2006). When Notch combines with its ligand Delta, the transcription of Hes is then increased (Ohsawa and Kageyama, 2008). Hes transcription factors are basic helix-loop-helix (bHLH) transcriptional repressors and have been shown to inhibit neural differentiation by binding to corepressor Groucho and repressing ath3, ath5 and ash1 genes (Ohsawa and Kageyama, 2008). This process increases the number of retinal progenitors

and as a result increases the number of Muller cells in the mature retina (Furukawa *et al*, 2000; Ohsawa and Kageyama, 2008). Furthermore, the transcription factor Lhx2, which is also expressed at this stage, promotes expression of Six3 and Rx (Tetreault *et al*, 2009) which are important factors in the differentiation of the neural retina from retinal pigment epithelial tissue (Bailey *et al*, 2004; Eiraku *et al*, 2011; Liu *et al*, 2010; Lom et al, 2002; Marquardt and Gruss, 2002). Rx and Six3 accomplish this by antagonizing the Wnt signaling pathway, which normally promotes the differentiation of the retinal pigment epithelium (Eiraku *et al*, 2011; Liu *et al*, 2010).

Competency

At the competency stage retinal precursors become postmitotic and begin to migrate to specific layers within the developing retina. Competency is also marked by the expression of homeobox-containing transcription factors Pax6 and Chx10 (Adler 2000; Eiraku *et al*, 2011; Marquardt and Gruss, 2002; Mu and Klein, 2004). These transcription factors permit competency for different cell types within the retina. Pax6 is critical for RGC competency as well as for the competency of every cell type within the retina (Adler 2000; Eiraku *et al*, 2011; Mu and Klein, 2004) and its activity is initiated by the expression of Lhx2 and Sox2 (Lin *et al*, 2009). Pax6 promotes the expression of the proneural bHLH transcription factor ath5 (Marquardt and Gruss, 2002; Mu *et al*, 2008) that either directly (as shown in *Xenopus laevis*) (Hutcheson *et al*, 2001) or indirectly, via unidentified intermediates, promotes the expression of both the Brn3b and Isl1 transcription factors (Mu *et al*, 2008; Mu and Klein, 2004).

Specificity

Once retinal cell precursors reach their appropriate layers they enter the specificity phase. This transition from competency to specificity is marked by the expression of Brn3 (Qiu *et al*, 2008) and Isl transription factor families (Pan *et al*, 2008). Furthermore, this stage is also accompanied by the loss of expression of transcription factors permissive to the development of other retinal cell types. Indeed, Brn3 transcription factors establish RGC specificity by repressing the expression of the transcription factors Crx, NeuroD and Otx2 that are required for the differentiation of cone photoreceptors, amacrine cells and rod photoreceptors, respectively (Qiu *et al*, 2008). Also, during this developmental period the expression of Rx and Chx10 is limited to developing photoreceptors and bipolar cells (Marquardt and Gruss, 2002), respectively, where they play a permissive role in the differentiation of these cells (Livesey and Cepko, 2001). However, transcription factors promoting RGC competency, namely Pax6 and Six3, are continued to be expressed in RGC specific precursors (Marquardt and Gruss, 2002).

The transcription factors Brn3b and Isl1 are essential for RGC survival. Genetic knock-down of these proteins results in extensive apoptosis prior to the natural period of programmed RGC death (Mu *et al*, 2008; Qiu *et al*, 2008). Additionally, these transcription factors feed forward to initiate the expression of other members of their own family, namely Brn3a, Brn3c and Isl2 (Mu *et al*, 2008; Pan *et al*, 2008). Members of both families are continually expressed during RGC differentiation and maturity. They are the foundations of two separate, yet

overlapping, gene regulatory networks that control transcription of most of the proteins essential for RGC differentiation and function, including neurofilament proteins and nerve growth factor receptors (Mu *et al*, 2008). As such, Brn3b and Isl1 are the transcription factors most frequently sited by researches as markers of RGC cell type.

Differentiation

In developmental biology, differentiation is the process by which cells become specialized to perform a specific physiological role. For the RGC this role is to receive chemical input from upstream retinal cells, convert this information into an electrical output and transmit this output to the brain. For this role to be fulfilled the RGC must develop the proper connectivity with its input and output neurons so that it is physically positioned in space to communicate with these cells. Also, the cell must develop the proper excitability so that it is receptive to its chemical inputs and can convert those inputs into electrical outputs in the form of action potentials. The axonal and dendritic outgrowth, pathfinding and pruning required to achieve the proper connectivity is an immense and growing field of study that is outside the scope of this investigation and will, therefore, not be discussed in detail. However, the gain of excitability, or the electrical differentiation of RGCs, is highly relevant and will be discussed in depth in the section III.

Regulation of Differentiation

Because the various retinal cell types all differentiate from the same pool of post mitotic progenitors, over production of any one cell type occurs at the

expense of another. Furthermore, since RGCs are the first cell type to differentiate, there must be a mechanism to prevent overproduction of these cells. Therefore, RGCs employ an elaborate system of negative feedback to prevent their overproduction.

Notch protein is a membrane bound receptor which functions as a key negative regulator of RGC differentiation. Transcription of Notch is regulated by the transcription factor Sox2 (Taranova *et al*, 2006) and is therefore present in RGC precursors (Austin *et al*, 1995; Silva *et al*, 2003; Taranova *et al*, 2006). When Notch is activated, its intracellular C-terminus is cleaved and translocates to the cell nucleus (Ohsawa and Kageyama, 2008). Here the Notch fragment binds to the transcription factor complex RBP-J and initiates the expression of Hes1 and Hes5 (Ohsawa and Kageyama, 2008). The Hes proteins then bind with corepressor Groucho and together they inhibit the transcription of ash1, ath3 and ath5 transcription factors (Ohsawa and Kageyama, 2008) that are required for RGC differentiation (Lin *et al*, 2004; Marquardt and Gruss, 2002; Mu *et al*, 2008; Mu and Klein, 2004). The ligand which activates Notch and therefore initiates this transcription factor cascade is Delta (Austin *et al*, 1995; Ohsawa and Kageyama, 2008; Qiu *et al*, 2008; Silva *et al*, 2003; Taranova *et al*, 2006). Delta is a membrane bound protein that is highly expressed on newly differentiated RGCs (Ohsawa and Kageyama, 2008; Rapaport amd Dorsky, 1998; Silva *et al*, 2003). Because it is membrane bound, Delta can only activate Notch signalling (and therefore inhibit differentiation) of adjacent cells. This type of signalling, referred to as lateral inhibition, (Rapaport and Dorsky, 1998) prevents overproduction of

RGCs in a single area and ensures that differentiated RGCs exist in a thin layer rather than a globular sphere.

However, experiments have demonstrated that treatment of immature RGC precursors with media conditioned by differentiated RGCs results in diminished production of RGC (Waid and McLoon, 1998). These results suggest one or multiple diffusible factors may also operate in a paracrine negative feedback system to prevent RGC overproduction. These diffusible molecules have not been identified, but Shh may be one candidate molecule for this role since Brn3b enhances expression of Shh and Shh in turn regulates the transcription of cell cycle regulatory proteins Gli1 and Cyclin D1 (Mu *et al*, 2008).

III. DEVELOPMENT OF THE ELECTROPHYSIOLOGICAL PROPERTIES OF RETINAL GANGLION CELLS

Background

The principal purpose of the RGC is to integrate electrochemical inputs from bipolar cells and amacrine cells and transmit this information over great distances to the brain. The ability to fire successive action potentials at high frequency is essential for fulfillment of this. With the exception of one amacrine cell subtype, RGCs are the only neurons within the retina that are capable of generating action potentials. Photoreceptors, bipolar cells and the vast majority of amacrine cells produce only graded responses to light. As the output neuron of the retina, RGCs must receive and integrate these graded inputs and transform them into action potential trains. Integration occurs within the dendrites of RGCs. Here, excitatory post-synaptic potentials (EPSPs) created by synaptic neurotransmission activate voltage-gated ion channels that produce an amplification of the EPSPs. These amplified EPSPs then combine with EPSPs from other branches of the dentritic arbour. If this amplified and summated depolarization reaches the initial segment of the RGC axon, and is of a magnitude greater than a certain threshold, an action potential is produced. Not only is this spiking ability critical for relaying luminance information to the visual centres of the CNS, but it is hypothesized that the spontaneous spiking that moves in waves across the developing RGC layer prior to eye opening is also integral to the refinement of immature RGC projection patterns and dentritic circuitry.

Action Potentials in Retinal Ganglion Cells

The ability to generate trains of action potentials is critical for RGCs to

fulfill their role as the output neurons of the retina. The action potential is a rapid depolarization and repolarization of the plasma membrane. It is an all or nothing event that is capable of traveling great distances very rapidly without diminishing in amplitude. The waveform of an action potential can be broken down into a number of phases, each of which involves different ionic currents and therefore the activation of different ion channels. These phases, in order, are the stimulation phase, the depolarizing phase, the repolarizing phase and the hyperpolarization phase (Bean, 2007).

The stimulation phase, although not technically part of the action potential proper, is critical for the determination if an action potential will fire. This phase is essentially concerned with bridging the gap between two important membrane potentials, the resting potential (between -75 mV and -60 mV) and the threshold potential (approximately -55 to -50 mV) (Bean, 2007). Small EPSPs will result in small depolarizing pulses in the membrane potential that will open both Na^+ and K^+ channels. At these voltages, the Na^+ current from the few Na^+ channels that open are overwhelmed by the K^+ current (conducted through inwardly rectifying K^+ channels and tandem pore-domain K^+ channels and caused by the shift in membrane potential away from the K^+ equilibrium potential) and no action potential is elicited. Larger depolarizations however, will open enough Na^+ channels to overwhelm this K^+ current. This results in a positive feedback scenario in which depolarization activates Na^+ channels resulting in an inward current and greater depolarization which in turn results in more Na^+ channel activation and more inward current and depolarization. The level of deloparization

that must occur before this positive feedback scenario results is the threshold potential. This potential is usually between -55 and -45 mV and depends on the density of Na^+ channel expression and the relationship between the membrane potential and open probability of those channels—a phenomenon known as channel gating (Bean, 2007).

Another factor that depends on Na^+ channel expression is the depolarizing phase of the action potential. This is the rapid depolarization resulting from the positive feedback scenario previously described. The slope of the increase in the membrane potential (when it is plotted against time) is determined by the very rapid Na^+ channel activation kinetics (Bean, 2007). This rise in membrane potential continues until the number of open Na^+ channels is maximized and the delayed rectifier voltage-gated K^+ channels begin to activate. Like voltage-gated Na+ channels, voltage-gated K^+ channels are activated by the increase in membrane potential (Bean, 2007). However, these channels, as their name suggests, do not activate immediately. This delay is important since it allows the depolarizing phase to occur. Simultaneous with the activation of voltage-gated K^+ channels is the inactivation of voltage-gated Na^+ channels, reducing the Na^+ current. This increase in K^+ current and decrease in Na^+ current results in the peak of the action potential occurring at an instance when the Na^+ and K^+ currents are momentarily equal, negating any effect on membrane potential.

As more K^+ channels activate and more Na^+ channels inactivate, the K^+ current begins to overwhelm the Na^+ current and the membrane potential rapidly begins to drop. This is the repolarizing phase. The rate of repolarization is

determined by the density of K^+ channels expressed in the plasma membrane. Unlike Na^+ channels, K^+ channels do not inactivate and remain open after the membrane potential has returned to resting levels (Bean, 2007). This long-term activation results in after-hyperpolarization, a drop in the membrane potential below resting levels (Bean, 2007). After-hyperpolarization is important because it relieves the inactivation of the Na^+ channels making them capable of initiating another action potential (Bean, 2007). The period of inactivation prevents a subsequent action potential and is therefore referred to as the refractory period (Bean, 2007). The refractory period is also largely responsible for the unidirectional nature of action potentials since Na^+ channels behind the propagating wave of depolarization cannot activate and initiate more depolarization.

Development of Spiking Ability

Electrical maturation of RGCs generally conforms to the same developmental pattern across many species. At early developmental stages prior to axonal projection and dentritic arbourization, RGCs are incapable of firing action potentials. Once axonal projections have reached their central targets, RGCs are capable of firing single action potentials. Finally, in the mature visual system the RGCs is capable of firing robust trains of high frequency action potentials. This change in excitability occurs as a direct result of changes in the intrinsic membrane properties, or in other words, in the expression patterns and activity of ion channels.

Prior to synaptogenesis with their CNS targets, RGCs are incapable of

generating action potentials (Robinson and Wang, 1998). At this point in development (embryonic day (ED)14/15 in rodents and ED4/5 in chicks) neither Na^+ channels (Schmid and Guenther, 1996; Schmid and Guenther, 1998), K^+ channels (Reiff and Guenther, 1999) or Ca^{2+} channels are expressed (Schmid and Guenther, 1996; Schmid and Guenther, 1999). This creates a condition in which the cell membrane is highly impermeable to ions; indeed the membrane resistance of these cells is greater than one gigaohm (Rothe *et al*, 1999). According to the Goldman-Hodgkins-Katz Equation, this low permeability results in very high resting membrane potentials—approximately 0 mV at this stage of development in rodents (Reiff and Guenther, 1999). As RGCs sprout axons and generate synapses with their CNS targets (ED16 in rodents, ED6 in chicks) they also begin to express ion channels (Reiff and Guenther, 1999; Robinson and Wang, 1998; Schmid and Guenther, 1996; Schmid and Guenther, 1998). At this developmental period, Na^+, K^+ and Ca^{2+} channels are all expressed but the channel subtypes and density of expression are vastly different than that observed at maturity. Initially, Na^+ channels are expressed at very low levels. In rat RGCs at ED17/18 Schmid *et al* observed an inward Na^+ current density of 80 pA/pF (compared to > 600 pA/pF at maturity) (Schmid and Guenther, 1998). Furthermore, the activation potential (the potential at which half of the Na^+ current is activated) of these early Na^+ channels is only -15mV compared with -50 mV at maturity (Schmid and Guenther, 1998). This shifted activation potential results in low excitability since a large depolarization is required in order to activate these Na^+ channels, and most Na^+ channels exist in the inactivated conformation at the resting membrane

potential. These effects, combined with the sparse expression pattern of Na^+ channels at this time point, result in these cells being capable of generating only broad single action potentials.

The expression of K^+ channels at this stage is also much different than that observed at maturity. Once axonal projections reach the brain both delayed rectifier and A-type K^+ currents are expressed, albeit at very low levels (Reiff and Guenther, 1999; Robinson and Wang, 1998; Skaliora *et al*, 1995). Furthermore, the A-type K^+ current comprises a much larger proportion of the total current than it does at maturity (Reiff and Guenther, 1999; Robinson and Wang, 1998; Skaliora *et al*, 1995). This expression pattern has a multitude of implications for RGC electrical activity. K^+ channel expression, even at low levels, increases the K^+ permeability, thereby lowering both the membrane resistance and the resting membrane potential. This drop in the resting membrane potential, although limited, is important since it relieves the inactivation of Na^+ channels enough to produce slow rising depolarizations. Furthermore, activation of these K^+ channels allows for repolarization thereby generating a broad rudimentary action potential.

Ca^{2+} channels are also first expressed at this period, and again the expression pattern is much different compared to that at maturity. Initially, only low voltage activated (LVA) T-type Ca^{2+} channels are present in RGCs (Schmid and Guenther, 1996; Schmid and Guenther, 1999). Since these channels activate at relatively low membrane potentials, and since the resting membrane potential at this stage is still relatively high (due to low K^+ channel density), these channels have a high probability of being open at the resting state. It is hypothesized that

the influx of Ca^{2+} created by these conditions is an important regulator of a number of developmental processes such as dentritic arbourization (Lohmann *et al*, 2002), cell death/cell survival and further expression of both the voltage-gated and ligand-gated ion channels (Schmid and Guenther, 1996; Schmid and Guenther, 1999).

The next phase in the electrical maturation of RGCs involves gaining the ability to fire multiple action potentials. To achieve this, the early ion channel expression patterns described above change markedly. First and foremost, the density of Na^+ and K^+ channel expression increases by many fold. In rats, by ED21 the Na^+ current density was observed to increase to 200 pA/pF, with further increases to 400 pA/pF at P5 and 750 pA/pF at postnatal day (P)12 (Schmid and Guenther, 1998). This rapid increase in Na^+ current results in a decreased threshold for action potential firing, a greater action potential amplitude, and a more rapid action potential depolarization. This developmental stage also sees a decrease in the activation potential of Na^+ channels. In rats, the half activation potential continues to decreases from -15 mV at ED18 to -23 mV at ED21 to -34 mV at P5 and finally -40 mV at P12 (Schmid and Guenther, 1998). These changes in activation potential, combined with increased expression, decrease the firing threshold and make for a more rapid depolarization phase of the action potential. Simultaneous to this, the inactivation potential increases. In rats, the half activation potential increases from -50 mV at ED18 to -44 mV at ED21 to -38 mV at P5 (Schmid and Guenther, 1998). This also increases the rate of the depolarization phase since fewer channels will be in the inactive conformation at

resting membrane potentials.

K^+ currents also drastically change as the RGCs mature. Similar to the Na^+ channel expression pattern, the density of the delayed rectifier K^+ channels in rats steadily increases by nearly eightfold between ED19 and P32 (Reiff and Guenther, 1999). This increase in delayed rectifier K^+ current increases the rate of membrane depolarization which results in sharper, more rapid action potentials. In addition, the most significant change that occurs during the maturation of RGCs is the expression of new classes of K^+ channels. In cat RGCs a linear K^+ conductance is observed from ED40 onwards which is likely mediated by tandem-pore domain K^+ channels (Robinson and Wang, 1998; Skaliora *et al*, 1995). Since this conductance is present even at low membrane potentials, it shifts the resting membrane potential nearer to the reversal potential for K^+, a trait exhibited by mature RGCs. Furthermore, as RGCs reach maturity they also begin to express inward rectifier K^+ channels (Chen *et al*, 2004; Qu *et al*, 2009; Tian *et al*, 2003) which act to stabilize the membrane potential at this new lower level of approximately -60 mV in postnatal rats (Robinson and Wang, 1998).

The expression of high voltage activated (HVA) Ca^{2+} channels is perhaps the most critical development that must occur in order for RGCs to gain high frequency firing capability. This concept appears paradoxical at first glance since HVA Ca^{2+} channels mediate long duration inward currents that would normally broaden action potentials and suppress repolarization. However, in RGCs, HVA Ca^{2+} channels are coexpressed with Ca^{2+} activated K^+ channels (Henne and Jeserich, 2004; Rothe *et al*, 1999). This creates a paradigm in which a relatively

small inward current activates a much larger outward current that rapidly repolarizes the RGC. Indeed, Rothe *et al* identified HVA Ca^{2+} channel and Ca^{2+} activated K^{+} channel expression as the most critical ion channels needed for repetitive firing to occur in mice RGCs (Rothe *et al*, 1999). Furthermore, much like LVA Ca^{2+} channels, HVA Ca^{2+} channels are also important for a number of developmental processes.

Spontaneous Electrical Activity

Once RGCs become capable of generating action potentials, waves of spontaneous electrical activity (SEA) can be observed within the ganglion cell layer of the developing retina. Using multi-electrode arrays and calcium imaging, SEA is observed to occur concomitantly with dentritic outgrowth and arbourization within the inner plexiform layer (IPL). It is designated as spontaneous since it is generated in the absence of light stimulus and occurs prior to photoreceptor differentiation. These waves of SEA move at velocities between 100 and 500 m/s (this value varies across species and developmental time points), rates that are much slower than mature electrical activity. The waves have no propagation bias, meaning they can move in any direction across the retina, triggering RGC spiking and leaving Ca^{2+} transients in their wake. SEA is developmentally critical and has been implicated in a number of cellular processes including cell survival, synapatic organization in the optic tectum/superior colliculus and dentritic arbourization.

SEA in RGCs is categorized into three stages based on the time of occurrence and the mechanism of wave initiation and propagation. Stage I

commences just after dentritic outgrowth begins, prior to the formation of synapses in the IPL. Since this stage occurs prior to synaptic transmission to RGCs, it is therefore independent of neural input from other retinal cell types. Indeed, antagonists of acetylcholine, γ-aminobutyric acid (GABA), glutamate and glycine receptors do not effect the initiation or propagation of these early stage waves (Syed *et al*, 2004). However, Stage I SEA can be potentiated by the application of BayK8644, an L-type Ca^{2+} channel agonist (Singer *et al*, 2001) and can be interrupted by application of adenosine receptor antagonists and gap junction inhibitors (Singer *et al*, 2001; Syed *et al*, 2004). This evidence suggests that these waves are initiated by adenosine receptor activation via autocrine/paracrine signalling, and that they propagate along RGC plasma membranes in the form of Ca^{2+} influx through voltage-gated Ca^{2+} channels. Additionally, these waves propagate from RGC to RGC via gap junctions. It is also likely that GABA suppresses Stage I waves *in vivo* since application of $GABA_B$ receptor blockers increases wave frequency (Syed *et al*, 2004).

The function of Stage I SEA is not known. However, this adenosinic activity has been shown to increase concentrations of cyclic adenosine monophosphate (cAMP) via the activation of adenosine A_2 receptors (Stellwagen *et al*, 1999; Torborg and Feller, 2005). This results in activation of protein kinase A (PKA) and subsequent phosphorylation cAMP response element-binding (CREB) protein which has been shown to elicit a myriad of effects on a number of processes including cell survival, neurite outgrowth and ion channel expression (Socodato *et al*, 2011). Furthermore, the Ca^{2+} influx that accompanies Stage I

SEA also enhances these processes, since both cAMP and Ca^{2+} second messenger signal transduction cascades converge to activate CREB. Therefore, it is likely that the function of Stage I SEA is to prepare the RGC for high frequency action potential firing by facilitating proper neural connectivity (by promoting neurite outgrowth) and excitability (by promoting ion channel expression), and by enhancing cell survival mechanisms, protecting RGCs against the Ca^{2+} insult that accompanies repetitive firing.

Stage II SEA begins after the first rudimentary synapses are formed between RGCs and amacrine cells in the IPL. This stage is dependent on cholinergic input from star burst amacrine cells since application of nicotinic acetylcholine receptor antagonists disrupts this stage (Feller et al, 1996). However, that is not to say that adenosine is not still intimately involved in Stage II waves. During Stage II, adenosine agonists have been shown to increase wave frequency whereas adenosine antagonists decrease wave frequency (Stellwagen *et al*, 1999). Furthermore, when Stage II waves are disrupted by nicotinic receptor blockers, Stage I waves reemerge as the dominant electrical events (Syed *et al*, 2004). It appears that Stage II waves, much like their Stage I predecessors, propagate via gap junctions since inhibitors of gap junctions prevent their propagation (Firth *et al*, 2005; Torborg and Feller, 2005). However, Stage II SEA exhibits a refractory period and the rate of Stage II waves can be slowed by tetrodotoxin application (Stellwagen *et al*, 1999). This suggests that Na^{+} channels are involved in the propagation of these waves, but action potential firing is not necessary for their propagation or initiation.

The purpose of Stage II SEA is more completely understood than that of Stage I SEA. Numerous studies show that disrupting Stage II SEA by a variety of methods prevents the establishment of retinotopic maps in the superior colliculus and optic tectum of rodents and lower vertebrates respectively (Firth *et al*, 2005; Torborg and Feller, 2005). Furthermore, studies also show that these waves are necessary for the proper formation of ocular dominance columns in the lateral geniculate nucleus (LGN) of higher mammals (Torborg and Feller, 2005). This evidence suggests that Stage II SEA is involved in synaptogenesis and pruning of RGC axons. Studies tracking the propagation of waves across the retina show that the frequency and velocity of Stage II SEA is such that the probability of coincident action potential firing decays exponentially as the distance between RGCs is increased (Godfrey and Eglen, 2009; Torborg and Feller, 2005). This means that adjacent cells are much more likely to fire at the same time compared to distant cells. This provides a Hebbian mechanism by which adjacent synapses originating from adjacent retinal RGCs are potentiated, while adjacent synapses originating from distant RGCs are depressed and their axons are pruned.

Stage III is the final stage of SEA. It occurs at a later developmental time point when bipolar cells are born and form synapses with RGCs. It is therefore logical that Stage III SEA is driven by glutamatergic input from bipolar cells. Indeed, glutamate receptor antagonists block both the initiation (Zhou and Zhao, 2000) and propagation of Stage III SEA while adenosine receptor antagonists and nicotinic acetylcholine receptor antagonists are incapable of inhibiting SEA during this stage (Zhou and Zhao, 2000). However, the application of muscarinic

acetylcholine receptor antagonists has been shown to prevent wave initiation without affecting propagation (Zhou and Zhao, 2000). As in the other stages, Stage III propagation is mediated by gap junctions since genetic knockout of connexin 36 prevents stage III retinal waves (Torborg and Feller, 2005). This also suggests that Stage I and II SEA are propagated by gap junctions formed by different connexin proteins. Stage III SEA is modulated by both GABA and glycine. Application of GABA and glycine receptor antagonists increase wave frequency (Syed *et al*, 2004), which suggests that these neurotransmitter have the endogenous function of suppressing Stage III waves as RGCs reach maturity. This inference is supported by the fact that as development continues and retinal waves cease, the application of GABA and glycine receptor blockers restores SEA (Syed *et al*, 2004).

The function of Stage III SEA is not completely understood but it has been suggested that it is necessary for the segregation of ON and OFF synapses in the IPL (Firth *et al*, 2005). As RGC dendrites grow into the IPL, they form synapses throughout the thickness of this layer (Sernagor *et al*, 2001). However, as the retina matures these synapses are segregated into two mutually exclusive layers comprising ON and OFF RGC dendrites. This segregation is concomitant with Stage III SEA. Additionally, SEA results in increased intracellular Ca^{2+} which is necessary to stabilize RGC dendrites (Lohmann *et al*, 2002). Furthermore, metabotropic glutamate receptor (a receptor expressed exclusively by ON bipolar cells) antagonism blocks Stage III waves (Zhou and Zhao, 2000), suggesting that they originate primarily from the ON-centre retinal circuitry. This reveals

differences in SEA between ON and OFF RGCs which provides a possible mechanism for IPL synapse segregation by Stage III SEA.

IV: CELL LINES AS MODELS OF RETINAL GANGLION CELL PHYSIOLOGY

Background

There are many advantages of using a cell line to study RGC physiology. One of these advantages is self-propagation. Cell lines essentially provide an unlimited source of cells for experimentation, which is highly advantageous for electrophysiological studies since the patch clamp technique has a relatively low success rate even when applied by the most experienced technicians. Furthermore, using a cell line avoids many of the moral implications involved in *in vivo* experiments or the dissection of primary cells from an animal source. Most importantly, a cell line is essential for the study of avian RGCs since an antibody reactive with Thy-1 is required to create a RGC enriched primary culture by immunopanning. Currently, an avian Thy-1 antibody is not commercially available.

There are, however, some limitations of cell line models of RGCs. Foremost, like all neurons, RGCs are post-mitotic. This phenotype, by definition, precludes the creation of a cell line that perfectly represents the physiology of RGCs. However, if a cell line displays RGC characteristics such as proper transcription factor expression, neurofilament expression and robust ion channel expression, it can be argue that it is a valid model of RGCs. In this section, the development and physiology of the QNR/D and RGC-5 cell lines will be compared and contrasted in order to illustrate their suitability as models for RGCs.

The QNR/D Cell Line as a Model of Embryonic Retinal Ganglion Cells

The QNR/D cell line was established using a two-stage immortalization and cloning procedure. First, retinal cells from ED7 quail were infected with rous sarcoma virus (Pessac *et al*, 1983). This virus encodes v-Src, a constitutively active non-receptor tyrosine kinase (Roskoski Jr., 2004). This established an immortal but heterogeneous cell line whose neuronal characteristics varied from cell to cell. In order to create a homogeneous cell line, single cells from the original cell line were isolated by dilution cloning (Pessac *et al*, 1983). One of these clones, QNR/D exhibited robust neuronal characteristics, namely synaptobrevin expression, A2B5 antigen expression and action potential firing (Pessac *et al*, 1983). Furthermore, when QNR/D cells are reintroduced into the vitreous of ED9 chicks, they migrate and embed themselves in the ganglion cell layer of the retina (Trisler *et al*, 1996).

Another relevant phenotype of QNR/D cells is the expression of GH and GHR. The expression of GH and GHR in the developing retina of both mammals and avian species is well-established, and determining their role in these tissues is an important field in neuroretinal studies (discussed in section IV). Thus their expression is arguably necessary for a valid model of RGC physiology. The presence of both of these proteins has been demonstrated at the protein level by immunocytochemistry, western blot and enzyme-linked immunosorbent assay (ELISA) techniques, as well as at the messenger ribonucleic acid (mRNA) level by reverse transcription polymerase chain reaction (RT-PCR) (Sanders *et al*, 2010). Furthermore, the function of GH signalling in the QNR/D cell line appears

to parallel that of GH *in vivo* since GH knockdown by small interfering ribonucleic acid (siRNA) results in increased apoptosis of QNR/D cells (Sanders *et al*, 2010). Additionally, the discovery that growth hormone releasing hormone (GHRH) is expressed in both chick RGCs and QNR/D cells (Harvey *et al*, 2012) suggests local regulation of GH production and further validates the utility of the QNR/D cell line for GH studies. However, because the electrophysiological properties of these cells have not been assessed, their utility in non-GH studies remains in question.

The RGC-5 Cell Line as a Model of Retinal Ganglion Cells

RGC-5 cells are widely used as a cell line model of RGCs. In fact, a pubmed search reveals over 150 studies have been published in which RGC-5 cell were used in this capacity. However, a number of publications have cast aspersions on the validity of this model. These studies suggest that both RGC marker expression and electrophysiological properties of RGC-5 cells are uncharacteristic of RGCs. Furthermore, the reported species origin of this cell line has come under criticism. These inadequacies as a RGC model will be briefly described.

The expression of protein markers by RGC-5 cells is not characteristic of RGCs. When this cell line was first transformed it was reported these cells express Thy-1. Furthermore, Frassetto *et al* (2006) report the expression of Thy-1 in both undifferentiated and staurosporine differentiated RGC-5 cells. However, more recent publications provide conflicting accounts of the presence of Thy-1 in RGC-5 cells. Van Bergen *et al* (2009) did not observe Thy-1 expression in either

undifferentiated cells or cells differentiated by succinyl concanavalin A. Additionally, these same authors reported an absence of neurofilament protein expression, another marker of RGCs, in RGC-5 cells (Van Bergen *et al*, 2009).

Electrical properties of RGC-5 cells are not characteristic of RGCs. No voltage-gated channels are expressed in undifferentiated RGC-5 cells (Moorhouse *et al*, 2004). Furthermore, these cells express a number of non-voltage-gated channels that are not typical of RGCs. For example, RGC-5 cells express un-gated inwardly rectifying K^+ channels that are not found in mature RGCs or in RGC precursors at any time during their development (Moorhouse *et al*, 2004). RGC-5 cells also express Cl^- channels and Gd^{3+} insensitive stretch-gated channels that are not found in mature RGCs (Moorhouse *et al*, 2004). However, a large outward K^+ current could be elicited by staurosporine-induced differentiation of RGC-5 cells, although no inward currents were observed (Frassetto *et al*, 2006).

Perhaps the greatest limitation of the RGC-5 cell line is the current controversy over its species of origin. Krishnamoorthy *et al* (2001) reported that this cell line was created by the transformation of PD1 rat retinal cells with the ψ2 E1A virus. These transformed cells were subsequently cloned to isolate a cell line possessing a RGC phenotype. However, a number of publications report that this cell line is derived from the mouse, not the rat (Van Bergen *et al*, 2009; Wood *et al*, 2010). Van Bergen *et al* obtained the genomic DNA sequence of the Thy-1 gene and the mitochondrial DNA sequence of the tRNA-phe gene in RGC-5 cells and they found that both sequences matched the DNA sequences of these genes in *Mus musculus* and not in *Rattus norvegicus*. These observations are extremely

curious and cast doubt on the reported origins of this cell line and its validity as an RGC model.

V. GROWTH HORMONE EXPRESSION AND ACTIVITY IN THE AVIAN NEURORETINA

Background

GH is a 22kDa protein that is classically viewed as an endocrine hormone produced by the somatotroph cells of the anterior pituitary. Once secreted into the general circulation, GH binds to GHR and directly, or through the activity of insulin-like growth factors (IGFs), regulates cellular proliferation, metabolism and somatic growth. Although this may be GH's primary endocrine role postnatally, it is also present in many extra-pituitary sites where it has local autocrine/paracrine functions (Harvey and Hull, 2003).

Growth Hormone in Neural Tissues

Many of the extra-pituitary sites of GH expression are within the CNS. In fact, GH is expressed within the developing nervous system well before the differentiation of the pituitary somatotrophs. In the chick embryo, GH and GHR immunoreactivity is present in all major divisions of the brain as early as ED 3 (Harvey *et al*, 2001). It is also present in the spinal cord, optic and otic vesicles at this time. By ED 14 however, GH expression is restricted to a number of specialized CNS sites. These include the cerebral cortex, cerebellum and choroid plexus (Harvey *et al*, 2001). Furthermore, in the mature brain GH and GHR immunoreactivity have been observed in the cortex, hippocampus, striatum, olfactory bulbs and cerebellum of mammals (Harvey, 2010; Harvey and Hull, 2003) as well as in the hypothalamus, hippocampus and septal areas of avian species (Harvey 2010; Harvey and Hull, 2003).

In early development, GH acts as a growth and differentiation factor,

promoting cell proliferation in a wide range of tissues. Indeed, several studies have demonstrated GH's mitogenic effect on neuronal precursor cells. This is evident in GH deficient (GHD) mice, which exhibit reduced cerebral and cerebellar mass (Noguchi *et al*, 1985) because of retarded neuronal growth and reduced neuron number (Noguchi, 1996). Furthermore, endogenous autocrine/paracrine GH is required for neurosphere growth *in vitro*, since GHR knockout ($GHR^{-/-}$) neurospheres must be rescued by other growth factors (McLenachan *et al*, 2008). Additionally, exogenous GH has been shown to enhance the proliferation of wildtype neurospheres (McLenachan *et al*, 2008), neuronal hybrid cell lines (Lyuh *et al*, 2007) and primary human neural stem cells (Pathipati *et al*, 2011).

GH has also been demonstrated to promote the differentiation of neuronal precursor cells into functional neurons. Ajo *et al* (2007) showed marked increases in the expression of neuronal markers beta-tubulin and nestin, as well as increased neuritogenesis upon application of exogenous GH to ED14 and ED17 cortical cells. This suggests GH promoted neuronal differentiation in these cells. Furthermore, it has been demonstrated that exogenous GH application increases neuritogenesis in Stat5 knockout mice in a concentration dependent fashion (Byts *et al*, 2008). This, combined with unpublished data from our lab showing increased neurite outgrowth upon the application of recombinant GH, indicates GH signalling induces neurite outgrowth and neuronal differentiation. Also, when applied to primary human neural stem cells, GH increased cell migration, a pivotal step for neuritogenesis in radial glia precursors (Pathipati *et al*, 2011).

It has also been suggested that GH may act as a modulator of neurotransmission in the mature CNS. Studies have shown that exogenous administration of GH resulted in decreased levels of homovanillic acid, a dopamine metabolite, in the cerebrospinal fluid of human patients with GHD. This suggests a decrease in dopaminergic signalling (Burman *et al*, 1996). This effect also was observed in the hypothalamus of a number of species (Johansson *et al*, 2005) and is associated with negative feedback regulation of GH secretion (Johansson *et al*, 2005).

GH also has been shown to modulate neurotransmission in the hippocampus, and as such may affect long-term potentiation (LTP) and the formation of memory. In fact, an increase in GH expression within the hippocampus has been observed during learning processes (Zearfoss *et al*, 2008). Currently, new research is beginning to shed light on the molecular mechanisms of GH activity in this region. The Nyberg group has demonstrated that subcutaneous GH injections up-regulate the transcription of mRNA encoding the NR2B subunit of the N-methyl-D-aspartic acid (NMDA) receptor (Le Greves *et al*, 2002). This suggests GH promotes LTP since the expression of the NR2B subunit is associated with LTP while the expression of the NR2A subunit is associated with long term depression (LTD) (Le Greves *et al*, 2005; Le Greves *et al*, 2002). Additionally, GH has been shown to promote EPSPs mediated by both NMDA and 2-amino-3-(5-methyl-3-oxo-1,2-oxazol-4-yl) propanoic acid (AMPA) receptors (Mahmoud and Grover, 2006). This effect occurred acutely (within minutes of GH application) and was dependent upon both phosphatidylinositol 3'-

kinase (PI3K) and mitogen activated protein kinase (MAPK) mediated signal transduction (Mahmoud and Grover, 2006). Further, studies by Zearfoss *et al.* showed that enhancement of EPSPs was also dependent on mRNA polyadenylation since cordycepin, an inhibitor of polyadenylation, prevented GH enhancement of LTP (Zearfoss *et al*, 2008).

Growth Hormone in the Neuroretina

Another neural site of GH production is the developing neuroretina. In the chick, GH, as well as GHR, are produced by the RGCs as early as ED4 (Baudet *et al*, 2007), well before the onset of pituitary GH production. This indicates local expression. Furthermore, the GH present within the developing retina consists of many different isoforms. One such isoform is 15-kDa GH. This GH is translated from mRNA identical to that of pituitary GH. However, retinal GH is rapidly cleaved after translation resulting in the 15-kDa moiety that is predominant in the retina (Harvey *et al*, 2007). This protein is secreted into the intraocular cavity where it binds the opticin proteoglycan and is thereby concentrated in the vitreous humour (Sanders *et al*, 2003). Also present in the developing chick retina is small chicken GH (scGH). This protein is translated from a novel truncated mRNA. This GH isoform is not present in the vitreous as it lacks a secretion signal sequence (Baudet *et al*, 2007). This suggests scGH signaling via an intracrine mechanism within the RGC itself.

This GH expression pattern is concomitant with the wave of apoptotic cell death that occurs in RGCs from ED 6 to ED 8 (Sanders *et al*, 2005). This suggests a possible role for GH in regulating these apoptotic processes. Indeed, there is a

wealth of evidence that GH has anti-apoptotic effects within RGCs. GH has been shown to promote cell survival of embryonic chick RGCs *in ovo* (Sanders *et al*, 2005) and in primary culture (Sanders *et al*, 2008; Sanders *et al*, 2006). Specifically, the administration of GH antiserum resulted in increased cleavage of caspase-3 (Sanders *et al*, 2006) and caspase-9 (Sanders *et al*, 2008) and subsequently increased apoptosis (Sanders *et al*, 2008; Sanders *et al*, 2006). This neuroprotective effect of GH is mediated, at least partially, by the PI3K/Akt kinase pathway since the addition of Wortmannin (an inhibitor of Akt phosphorylation) abrogated the anti-apoptotic effect of GH (Sanders *et al*, 2006). Furthermore, GH administration to these cells has been shown to reduce the transcription of the pro-apoptotic genes caspase-3 and apoptosis inducing factor (Harvey *et al*, 2006).

The 15-kDa isoform of GH is also present within the nerve fibres of the optic nerve, optic chiasm and optic tract from ED5 to ED8, a time frame that coincides with the development of these structures (Baudet *et al*, 2007). Furthermore, this protein is present in the retinorecipient regions of the optic tectum as early as ED4, prior to RGC synaptogenesis (Baudet *et al*, 2007). This expression suggests a role for GH in axonal outgrowth and guidance in the developing visual system. This hypothesis is supported by the fact that GH enhances axonal outgrowth in primary RGC cultures (Baudet *et al*, 2009).

References:

1. Adler R. A model of retinal cell differentiation in the chick embryo. *Progress in Retinal and Eye Research*, 19:529–57, 2000.

2. Ajo R., Cacicedo L., Navarro C. and Sanchez-Franco F. Growth Hormone Action on Proliferation and Differentiation of Cerebral Cortical Cells from Fetal Rat. *Endocrinology* 144(3):1086–1097, 2007.

3. Alatzoglou K.S., Kelberman D. and Dattani M.T. The role of SOX proteins in normal pituitary development. *Journal of Endocrinology*, 200:245–258, 2009.

4. Anchan R.M., Reh T.A., Angello J., Balliet A. and Walker M. EGF and TGF-alpha stimulate retinal neuroepithelial cell proliferation in vitro. *Neuron*, 6:923–36, 1991.

5. Atkinson-Leadbeater K. and McFarlane S. Extrinsic factors as multi-functional regulators of retinal ganglion cell morphogenesis. *Developmental Neurobiology*, E-publication ahead of print, 2011.

6. Austin C.P., Feldman D.E., Ida J.A. Jr. and Cepko C.L. Vertebrate retinal ganglion cells are selected from competent progenitors by the action of notch. *Development*, 121:3637–50, 1995.

7. Bailey T.J., El-Hodiri H., Zhang L., Shah R., Mathers P.H. and Jamrich M. Regulation of vertebrate eye development by rx genes. *International Journal of Developmental Biology*, 48:761–70, 2004.

8. Baudet M.L., Hassanali Z., Sawicki G., List E.O., Kopchick J.J. and Harvey S. Growth hormone action in the developing neural retina: A proteomic analysis. *Proteomics* 8: 389–401, 2008.

9. Baudet M.L., Martin B.T., Hassanali Z., Parker E., Sanders E.J. and Harvey S. Expression, Translation, and Localization of a Novel, Small Growth Hormone Variant. *Endocrinology* 148: 103-115, 2007.

10. Baudet M.L., Rattray D. and Harvey S. Growth Hormone and its Receptor in Projection Neurons of the Chick Visual System: Retinofugal and Tectobulbar Tracts. *Neuroscience* 148: 151–163, 2007.

11. Baudet M.L., Rattray D., Martin B.T., and Harvey S. Growth Hormone Promotes Axon Growth in the Developing Nervous System. *Endocrinology* 150: 2758–2766, 2009.

12. Bean B.P. The action potential in mammalian central neurons. *Nature*,

8:451–65, 2007.

13. Bonnefort X., Lacampagne A., Sanchez-Hormigo A., Fino E., Creff A., Mathieu M.N., Smallwood S., Carmignac D., Fortanaud P., Travo P., Alonso G., Courtois-Coutry N., Pincus S.M., Robinson I.C.A.F. and Mollard P. Revealing the large-scale network organization of growth hormone-secreting cells. *Proceedings of the Nation Academy of Science*, 102: 16880 –16885, 2005.

14. Burman P., Hetta J, Wide L., Mansson J.E., Ekman R. and Karlsson F.A. Growth hormone treatment affects brain neurotransmitters and thyroxine. *Clinical Endocrinology* 44: 319-324, 1996.

15. Byts N., Samoylenko A., Fasshauer T., Ivanisevic M., Hennighausen L., Ehrenreich H. and Siren A.L. Essential role for Stat5 in the neurotrophic but not in the neuroprotective effect of erythropoietin. *Cell Death and Diff.* 15: 783-792, 2008.

16. Callaway E.M. Structure and function of parallel pathways in the primate early visual system. Journal of Physiology, 566: 13–19, 2005.

17. Catsicas M., Bonness V., Becker D. and Mobbs P. Spontaneous Ca^{2+} transients and their transmission in the developing chick retina. *Current Biology*, 8:283–6, 1998.

18. Chen L., Yu Y.C., Zhao J.W. and Yang X.L. Inwardly rectifying potassium channels in rat retinal ganglion cells. *European Journal of Neuroscience*, 20:956–64, 2004.

19. Chen L.F., Yin Z.Q. Chen S. and Chen Z.S. Differentiation and production of action potentials by embryonic rat retina stem cells in vitro. *Investigative Ophthalmology and Visual Science*, 49:5144–50, 2008.

20. Clark B.D., Kurth-Nelson Z.L. and Newman E.A. Adenosine-evoked hyperpolarization of retinal ganglion cells is mediated by g-protein-coupled inwardly rectifying K^+ and small conductance Ca^{2+}-activated K^+ channel activation. *Journal of Neuroscience*, 29:11237–45, 2009.

21. de Melo J., Du G., Fonseca M., Gillespie L.A., Turk W.J., Rubenstein J.L.R. and Eisenstat D.D. Dlx1 and Dlx2 function is necessary for terminal differentiation and survival of late-born retinal ganglion cells in the developing mouse retina. *Development*, 132:311–22, 2005.

22. de Melo J., Qiu X., Du G., Cristante L., and Eisenstat D.D. Dlx1, Dlx2, Pax6, Brn3b, and Chx10 homeobox gene expression defines the retinal ganglion and inner nuclear layers of the developing and adult mouse

retina. *The Journal of Comparative Neurology*, 461:187–204, 2003.

23. de Melo J., Zhou Q.P., Zhang Q., Zhang S., Fonseca M., Wigle J.T., and Eisenstat D.D. Dlx2 homeobox gene transcriptional regulation of trkB neurotrophin receptor expression during mouse retinal development. *Nucleic Acids Research*, 36:872–84, 2008.

24. Deiner M.S., Kennedy T.E., Fazeli A., Serafini T., Tessier-Lavigne M. and Sretavan D.W. Netrin-1 and DCC mediate axon guidance locally at the optic disc: loss of function leads to optic nerve hypoplasia. *Neuron*, 19:575–89, 1997.

25. Do M. T. H. and Yau K.W. Intrinsically photosensitive retinal ganglion cells. *Physiology Reviews*, 90:1547–81, 2010.

26. Doh S.T., Hao H., Loh S.C., Patel T., Tawil H.Y., Chen D.K., Pashkova A., Shen A., Wang H. and Cai, L. Analysis of retinal cell development in chick embryo by immunohistochemistry and in ovo electroporation techniques. *BMC Developmental Biology*, 10:8, 2010.

27. Eiraku M., Takata N., Ishibashi H., Kawada M., Sakakura E., Okuda S., Sekiguchi K., Adachi T. and Sasai Y. Self-organizing optic-cup morphogenesis in three-dimensional culture. *Nature*, 472:51–6, 2011.

28. Farah M.H. Neurogenesis and cell death in the ganglion cell layer of vertebrate retina. *Brain Research Reviews*, 52:264–74, 2006.

29. Feller M.B., Wellis D.P., Stellwagen D., Werblin F.S. and Shatz C.J. Requirement for cholinergic synaptic transmission in the propagation of spontaneous retinal waves. *Science*, 272:1182–7, 1996.

30. Firth S.I., Wang C.T. and Feller M.B. Retinal waves: mechanisms and function in visual system development. *Cell Calcium*, 37:425–32 5, 2005.

31. Fischer A.J. and Bongini R. Turning müller glia into neural progenitors in the retina. *Molecular Neurobiology*, 42:199–209, 2010.

32. Fjell J., Dib-Hajj S., Fried K., Black J.A. and Waxman S.G. Differential expression of sodium channel genes in retinal ganglion cells. *Brain Research Molecular Brain Research*, 50:197–204, 1997.

33. Flores-Morales A., Greenhalgh C.J., Norstedt G. and Rico-Bautista E. Negative Regulation of Growth Hormone Receptor Signaling. *Molecular Endocrinology* 20: 241-253, 2006.

34. Fohlmeister J.F., Cohen E.D. and Newman E.A. Mechanisms and

distribution of ion channels in retinal ganglion cells: using temperature as an independent variable. *Journal of Neurophysiology*, 103:1357–74, 2010.

35. Franze K., Grosche J., Skatchkov S.N., Schinkinger S., Foja C., Schild D., Uckermann O., Travis K., Reichenbach A., and Guck J. Muller cells are living optical fibers in the vertebrate retina. *Proceedings of the National Academy of Science USA*, 104:8287–92, 2007.

36. Frassetto L.J., Schieve C.R., Lieven C.J., Utter A.A., Jones M.V., Agarwal N. and Levin L.A. Kinase-Dependent Differentiation of a Retinal Ganglion Cell Precursor. *Investigative Ophthalmology and Visual Science*, 47: 427–438, 2006.

37. Furukawa T., Mukherjee S., Bao Z.Z., Morrow E.M. and Cepko C.L. rax, Hes1, and notch1 promote the formation of Müller glia by postnatal retinal progenitor cells. *Neuron*, 26:383–94, 2000.

38. Godfrey K.B. and Eglen S.J. Theoretical models of spontaneous activity generation and propagation in the developing retina. *Molecular Biosystems*, 5:1527–35, 2009.

39. Harvey S. Extrapituitary growth hormone. *Endocrinology* 38: 335–359, 2010.

40. Harvey S. and Hull K. Neural Growth Hormone: An Update. *Journal of Molecular Neuroscience* 20: 1-13, 2003.

41. Harvey S., Baudet M.L. and Sanders E.J. Growth hormone and cell survival in the neural retina: caspase dependence and independence. *Neuroreport* 17: 1715-1718, 2006.

42. Harvey S., Johnson C.D.M. and Sanders E.J. Growth hormone in neural tissues of the chick embryo. *Journal of Endocrinology* 169: 487–498, 2001.

43. Harvey S., Kakebeeke M. and Sanders E.J. Growth Hormone Localization in the Neural Retina and Retinal Pigmented Epithelium of Embryonic Chicks. *Journal of Molecular Neuroscience* 22: 139–145, 2004.

44. Harvey S., Kakebeeke M., Murphy A.E. and Sanders E.J. Growth hormone in the nervous system: autocrineor paracrine roles in retinal function? *Canadian Journal of Physiology and Pharmacology* 81: 371–384, 2003.

45. Harvey S., Lin W., Gliterman D., El-Abry N., Qiang W. and Sanders E.J. Release of retinal growth hormone in the chick embryo: Local regulation? *General and Comparative Endocrinology*, 2012.

46. Harvey S., Martin B.T., Baudet M.L., Davis P., Sauve Y., Sanders E.J. Growth hormone in the visual system: comparative endocrinology. *General and Comparative Endocrinology*. 153: 124–131, 2007.

47. Henne J. and Jeserich G. Maturation of spiking activity in trout retinal ganglion cells coincides with upregulation of K_v3.1- and BK-related potassium channels. *Journal of Neuroscience Research*, 75:44–54, 2004.

48. Höltje M., Brunk I., Grosse J., Beyer E., Veh R.W., Bergmann M., Grosse G. and Ahnert-Hilger G. Differential distribution of voltage-gated potassium channels K_v 1.1-K_v1.6 in the rat retina during development. *Journal of Neuroscience Research*, 85:19–33, 2007.

49. Huang S.J. and Robinson D.W. Activation and inactivation properties of voltage-gated calcium currents in developing cat retinal ganglion cells. *Neuroscience*, 85:239–47, 1998.

50. Hutcheson D.A. and Vetter M.L. The bHLH factors Xath5 and XneuroD can upregulate the expression of Xbrn3d, a pou-homeodomain transcription factor. *Developmental Biology*, 232:327–38, 2001.

51. Ito C., Im W.B., Takagi H., Takahashi M., Tsuzuki K., Liou S.Y. and Kunihara M. U-92032, a T-type calcium channel blocker and antioxidant, reduces neuronal ischemic injuries. European *Journal of Pharmacology* 257: 203-210, 1994.

52. James J., Das A.V., Rahnenführer J. and Ahmad I. Cellular and molecular characterization of early and late retinal stem cells/progenitors: differential regulation of proliferation and context dependent role of notch signaling. *Journal of Neurobiology*, 61:359–76, 2004.

53. Johansson V., Winberg S. and Bjornsson B.T. Growth hormone-induced stimulation of swimming and feeding behaviour of rainbow trout is abolished by the D1 dopamine antagonist SCH23390. *General and Comparative Endocrinology*, 141: 58-65, 2005.

54. Kaplan E. and Benardete E. The dynamics of primate retinal ganglion cells. *Progress in Brain Research*, 134:17–34, 2001.

55. Krishnamoorthy R.R., Agarwal P., Prasanna G., Vopat K., Lambert W., Sheedlo H.J., Pang I.H., Shade D., Wordinger R.J., Yorio T., Clark A.F. and Agarwal N. Characterisation of a transformed rat retinal ganglion cell line. *Molecular Brain Research*, 86: 1–12, 2001.

56. Koeberle P.D., Wang Y. and Schlichter L.C. K_v1.1 and K_v1.3 channels

contribute to the degeneration of retinal ganglion cells after optic nerve transection in vivo. *Cell Death and Differentiation*, 17:134–44, 2010.

57. Lanning N.J. and Carter-Su C. Recent advances in growth hormone signalling. *Reviews in Endocrine and Metabolic Disorders* 7: 225-235, 2006.

58. Le Greves M., Le Greves P. and Nyberg F. Age-related effects of IGF-1 on the NMDA-, GH- and IGF-1-receptor mRNA transcripts in the rat hippocampus. *Brain Research Bulletin.* 65: 369-374, 2005.

59. Le Greves M., Steensland P., Le Greve P. and Nyberg F. Growth hormone induces age-dependent alteration in the expression of hippocampal growth hormone receptor and N-methyl-D-aspartate receptor subunits gene transcripts in male rats. *Proceedings of the National Academy of Science* 99: 7119-7123, 2002.

60. Le Greves M., Zhou Q., Berg M., Le Greves P., Fholenhag, Meyerson B. and Nyberg F. Growth hormone replacement in hypophysectomized rats affects spatial performance and hippocampal levels of NMDA receptor subunit and PSD-95 gene transcript levels. *Experimental Brain Research* 173: 267-273, 2006.

61. Lea W.R. and Harvey S. Growth Hormone (GH) suppression of catecholine turnover in the chicken hypothalamus: implications for GH autoregulation. *Journal of Endocrinology*, 193: 245–251, 1993.

62. Lilley S. and Robbins J. The rat retinal ganglion cell in culture: an accessible CNS neurone. *Journal of Pharmacology and Toxicology Methods*, 51:209–20, 2005.

63. Lin B., Wang S.W. and Masland R.H. Retinal ganglion cell type, size, and spacing can be specified independent of homotypic dendritic contacts. *Neuron*, 43:475–85, 2004.

64. Lin Y.P., Ouchi Y., Satoh S. and Watanabe S. Sox2 plays a role in the induction of amacrine and müller glial cells in mouse retinal progenitor cells. *Investigative Ophthalmology and Visual Science*, 50:68–74, 2009.

65. Ling L. and Lobie P.E. RhoA/Rock Activation by Growth Hormone Abrogates p300/Histone Deacetylase 6 Repression of Stat5-mediated Transcription. *Journal of Biological Chemistry* 279: 32737-32750, 2004.

66. Lipton S.A. and Tauck D.L. Voltage-dependent conductances of solitary ganglion cells dissociated from the rat retina. *Journal of Physiology*, 385:361–91, 1987.

67. Liu W., Lagutin O., Swindell E., Jamrich M., and Oliver G. Neuroretina specification in mouse embryos requires six3-mediated suppression of wnt8b in the anterior neural plate. *Journal of Clinical Investigation*, 120:3568–77, 2010.

68. Livesey F.J. and Cepko C.L. Vertebrate neural cell-fate determination: lessons from the retina. *Nature Reviews Neuroscience*, 2:109–18, 2001.

69. Lohmann C., Myhr K.L. and Wong R.O.L. Transmitter-evoked local calcium release stabilizes developing dendrites. *Nature*, 418:177–81, 2002.

70. Lyuh E., Kim H.J., Kim M., Lee J.K., Park K.S., Yoo K.Y., Lee K.W. and Ahn Y.O. Dose-specific or dose-dependent effect of growth hormone treatment on the proliferation and differentiation of cultured neuronal cells. *Growth Hormone and IGF Research* 17: 315-322, 2007.

71. Mahmoud G.S. and Grover L.M. Growth Hormone Enhances Excitatory Synaptic Transmission in Area CA1 of Rat Hippocampus. *Journal of Neurophysiology* 95: 2962-2974, 2006.

72. Marquardt T. and Gruss P. Generating neuronal diversity in the retina: one for nearly all. *Trends in Neuroscience*, 25:32–8, 2002.

73. Martinez-Morales J.R., Del Bene F., Nica G., Hammerschmidt M., Bovolenta P. and Wittbrodt J. Differentiation of the vertebrate retina is coordinated by an FGF signaling center. *Developmental Cell*, 8:565–74, 2005.

74. McLenachan S., Lum M.G., Waters M.J. and Turnley A.M. Growth hormone promotes proliferation of adult neurosphere cultures. *Growth Hormone and IGF Research* XXX: XXX-XXX, 2008.

75. Mehta V. and Sernagor E. Early neural activity and dendritic growth in turtle retinal ganglion cells. *European Journal of Neuroscience*, 24:773–86, 2006.

76. Moody, W. J., and Bosma, M. M. Ion channel development, spontaneous activity, and activity-dependent development in nerve and muscle cells. *Physiology Reviews*, 85: 883–941, 2005.

77. Moorhouse A.J., Li S., Vickery R.M. Hill M.A. and Morley J.W. A patch-clamp investigation of membrane currents in a novel mammalian retinal ganglion cell line. *Brain Research*, 1003: 205–208, 2004.

78. Mu X., Fu X., Beremand P.D., Thomas T.L. and Klein W.H. Gene

regulation logic in retinal ganglion cell development: Isl1 defines a critical branch distinct from but overlapping with pou4f2. *Proceedings of the National Academy of Science*, 105: 6942–7, 2008.

79. Mu X. and Klein W.H. A gene regulatory hierarchy for retinal ganglion cell specification and differentiation. *Cell and Developmental Biology*, 15:115–123, 2004.

80. Noguchi T. Effects of growth hormone on cerebral development: morphological studies. *Hormone Research* 45: 5-17, 1996.

81. Noguchi T., Sugiasaki T. and Tsukada Y. Microcephalic cerebrum with hypomyelination in the growth hormone-deficient mouse. *Neurochemical Research* 10:1097-1106, 1985.

82. Oliver G., Mailhos A., Wehr R., Copeland N.G., Jenkins N.A. and Gruss P. Six3, a murine homologue of the sine oculis gene, demarcates the most anterior border of the developing neural plate and is expressed during eye development. *Development*, 121:4045–4055, 1995.

83. Ohsawa R. and Kageyama R. Regulation of retinal cell fate specification by multiple transcription factors. *Brain Research*, 1192:90–8, 2008.

84. Pan L., Deng M., Xie X. and Gan L. Isl1 and Brn3b co-regulate the differentiation of murine retinal ganglion cells. *Development*, 135:1981–90, 2008.

85. Pathipati P., Gorba T., Sheepens A., Goffin V., Sun Y. and Fraser M. Growth hormone and prolactin regulate human neural stem cell regenerative activity. *Neuroscience* 190: 409 – 427, 2011.

86. Pessac B., Girard A., Romey G, Crisanti P., Lorinet A.M. and Calothy G. A neural clone derived from a Rous sarcoma virus-tranformed quail embryo neuroretina established culture. *Nature*, 302: 616–618, 1983.

87. Pinto L.H. and Klumpp D.J. Localization of potassium channels in the retina. *Progress in Retinal and Eye Research*, 17:207–30, 1998.

88. Poggi L., Zolessi F.R. and Harris W.A. Time-lapse analysis of retinal differentiation. *Current Opinion in Cell Biology*, 17:676–81, 2005.

89. Pollock N.S., Ferguson S.C.D. and McFarlane S. Expression of voltage-dependent potassium channels in the developing visual system of xenopus laevis. *Journal of Comparative Neurology*, 452:381–91, 2002.

90. Qiu F., Jiang H. and Xiang M. A comprehensive negative regulatory

program controlled by Brn3b to ensure ganglion cell specification from multipotential retinal precursors. *Journal of Neuroscience*, 28:3392–403, 2008.

91. Qu J. Mulo I. and Myhr K.L. The development of $K_v4.2$ expression in the retina. *Neuroscience Letters*, 464:209–13, 2009.

92. Qu J. and Myhr K.L. The development of intrinsic excitability in mouse retinal ganglion cells. *Developmental Neurobiology*, 68:1196–212, 2008.

93. Qu J. and Myhr K.L. The morphology and intrinsic excitability of developing mouse retinal ganglion cells. *PLoS One*, 6:e21777, 2011.

94. Rapaport D.H. and Dorsky R.I. Inductive competence, its significance in retinal cell fate determination and a role for delta-notch signaling. *Seminars in Cell and Developmental Biology*, 9:241–7, 1998.

95. Reiff D.F. and Guenther E. Developmental changes in voltage-activated potassium currents of rat retinal ganglion cells. *Neuroscience*, 92:1103–17, 1999.

96. Robinson D.W. and Wang G.Y. Development of intrinsic membrane properties in mammalian retinal ganglion cells. *Seminars in Cell and Developmental Biology*, 9:301–10, 1998.

97. Roskoski Jr. R. Src protein–tyrosine kinase structure and regulation. *Biochemical and Biophysical Research Communications*, 324: 1155–1164, 2004.

98. Rothe T., Bähring R., Carroll P. and Grantyn R. Repetitive firing deficits and reduced sodium current density in retinal ganglion cells developing in the absence of BDNF. *Journal of Neurobiology*, 40:407–19, 1999.

99. Rothe T., Jüttner R., Bähring R. and Grantyn R. Ion conductances related to development of repetitive firing in mouse retinal ganglion neurons in situ. *Journal of Neurobiology*, 38:191–206, 1999.

100. Sanders E.J., Lin W.L.., Parker E. and Harvey S. Growth hormone expression and neuroprotective activity in a quail neural retina cell line. *General and Comparative Endocrinology*, 165: 111–119, 2010.

101. Sanders E.J., Parker E., Aramburo C. and Harvey S. Retinal growth hormone is an anti-apoptotic factor in embryonic retinal ganglion cell differentiation. *Experimental Eye Research* 81: 551–560, 2005.

102. Sanders E.J., Parker E. and Harvey S. Growth hormone-mediated survival of embryonic retinal ganglion cells: Signaling mechanisms. *General and Comparative Endocrinology,* 156: 613-621, 2008.

103. Sanders E.J., Parker E. and Harvey S. Retinal ganglion cell survival in development: Mechanisms of retinal growth hormone action. *Experimental Eye Research,* 83:1205–1214, 2006.

104. Sanders E.J., Walter M.A., Parker E., Aramburo C. and Harvey S. Opticin Binds Retinal Growth Hormone in the Embryonic Vitreous *Investigative Ophthalmology & Visual Scienc*e, 44: 5404–5409, 2003.

105. Schmid S. and Guenther E. Developmental regulation of voltage-activated Na^+ and Ca^{2+} currents in rat retinal ganglion cells. *NeuroReport*, 7:677–681, 1996.

106. Schmid S. and Guenther E. Alterations in channel density and kinetic properties of the sodium current in retinal ganglion cells of the rat during in vivo differentiation. *Neuroscience*, 85:249–58, 1998.

107. Schmid S. and Guenther E. Voltage-activated calcium currents in rat retinal ganglion cells in situ: changes during prenatal and postnatal development. *Journal of Neuroscience*, 19:3486–94, 1999.

108. Scott H.J., Stebbing M.J., Walters C.E., McLenachan S., Ransome M.I., Nichols N.R. and Turnley A.M. Differential effects of SOCS2 on neuronal differentiation and morphology. *Brain Research* 1067: 138-145., 2006.

109. Sernagor E., Eglen S.J. and Wong R.O. Development of retinal ganglion cell structure and function. *Progress in Retinal and Eye Research*, 20:139–74, 2001.

110. Scheepens A., Sirimanne E., Beiharz E., Breier B.H., Waters M.J., Gluckman P.D., Williams C.E. Alterations in the neural growth hormone axis following hypoxic-ischemic brain injury. *Molecular Brain Research* 68: 88–100, 1999.

111. Shin D.H., Lee E., Kim J.W., Kwon B.S., Jung M.K., Jee Y.H., Kim J., Bae S. and Chang Y.P. Protective effect of growth hormone on neuronal apoptosis after hypoxia– ischemia in the neonatal rat brain. *Neuroscience Letters*. 354: 64–68, 2004.

112. Silva A.O., Ercole C.E. and McLoon S.C. Regulation of ganglion cell production by Notch signaling during retinal development. *Journal of Neurobiology*, 54:511–24, 2003.

113. Singer J.H., Mirotznik R.R. and Feller M.B. Potentiation of L-type calcium channels reveals nonsynaptic mechanisms that correlate spontaneous activity in the developing mammalian retina. *Journal of Neuroscience*, 21:8514–22, 2001.

114. Skaliora I., Robinson D.W., Scobey R.P. and Chalupa L.M. Properties of K^+ conductances in cat retinal ganglion cells during the period of activity-mediated refinements in retinofugal pathways. *European Journal of Neuroscience*, 7:1558–68, 1995.

115. Socodato R., Brito R., Calaza K.C. and Paes-de Carvalho R. Developmental regulation of neuronal survival by adenosine in the in vitro and in vivo avian retina depends on a shift of signaling pathways leading to CREB phosphorylation of depohosphoryation. *Journal of Neurochemistry*, 116:227–239, 2011.

116. Stellwagen D., Shatz C.J. and Feller M.B. Dynamics of retinal waves are controlled by cyclic amp. *Neuron*, 24:673–85, 1999.

117. Syed M.M., Lee S., Zheng J. and Zhou Z.J. Stage-dependent dynamics and modulation of spontaneous waves in the developing rabbit retina. *Journal of Physiology*, 560,Pt 2:533–49, 2004.

118. Taranova O.V., Magness S.T., Fagan B.M., Wu Y., Surzenko N., Hutton S.R. and Pevny L.H. Sox2 is a dose-dependent regulator of retinal neural progenitor competence. *Genes and Development*, 20(9):1187–202, 2006.

119. Tetreault N., Champagne M.P. and Bernier G. The LIM homeobox transcription factor Lhx2 is required to specify the retina field and synergistically cooperates with Pax6 for Six6 trans-activation. *Developmental Biology*, 327: 541–550, 2009.

120. Tian M., Chen L., Xie J.X., Yang X.L. and Zhao J.W. Expression patterns of inwardly rectifying potassium channel subunits in rat retina. *Neuroscience Letters*, 345:9–12, 2003.

121. Torborg C.L. and Feller M.B. Spontaneous patterned retinal activity and the refinement of retinal projections. *Progress in Neurobiology*, 76:213–235, 2005.

122. Trisler D., Rutin J. and Pessac B. Retinal engineering: Engrafted neural cell lines locate in appropriate layer. *Proceedings of the National Academy of Science*, 93: 6269-6274, 1996.

123. Turnley A.M., Faux C.H., Rietze R.L., Coonan J.R. and Bartlett P.F. Suppressor of cytokine signaling 2 regulates neuronal differentiation by

inhibiting growth hormone signaling. *Nature Neuroscience*, 5: 1155-1162, 2002.

124. Van Bergen N.J., Wood J.P., Chidlow G., Trounce I.A., Casson R.J., Ju W.K., Weinreb R.N. and Crowston J. Re-characterisation of the RGC-5 retinal ganglion cell line. *Investigative Ophthalmology and Visual Science*, 50:4267–4272, 2009.

125. Van Wart A. and Matthews G. Expression of sodium channels $Na_v1.2$ and nav1.6 during postnatal development of the retina. *Neuroscience Letters*, 403:315–7, 2006.

126. Waid D. and McLoon S. Ganglion cells influence the fate of dividing retinal cells in culture. *Development*, 125:1059–1066, 1998.

127. Wallace V.A. Proliferative and cell fate effects of hedgehog signaling in the vertebrate retina. *Brain Research*, 1192:61–75, 2008.

128. Wang S.W., Mu X., Bowers W.J., Kim D.S., Plas D.J., Crair M.C., Federoff H.J., Gan L. and Klein W.H. Brn3b/Brn3c double knockout mice reveal an unsuspected role for Brn3c in retinal ganglion cell axon outgrowth. *Development*, 129:467–77, 2002.

129. Wong R.O., Chernjavsky A., Smith S.J. and Shatz C.J. Early functional neural networks in the developing retina. *Nature*, 374:716-8, 1995.

130. Wong W.T., Sanes J.R. and Wong R.O. Developmentally regulated spontaneous activity in the embryonic chick retina. *Journal of Neuroscience*, 18:8839-52, 1998.

131. Wood J.P.M., Chidlow G., Tran T., Crowston J.G. and Casson R.J. A Comparison of Differentiation Protocols for RGC-5 Cells. *Investigative Ophthalmology and Visual Science*, 51: 3774–3783, 2010.

132. Zearfoss N.R., Alarcon J.M., Trifilieff P., Kandel E. and Richter JD. A Molecular Circuit Composed of CPEB-1 and c-Jun Controls Growth Hormone-Mediated Synaptic Plasticity in the Mouse Hippocampus. *Journal of Neuroscience* 28: 8502-8509, 2008.

133. Zhang S.S.M., Wei J.Y., Li C., Barnstable C.J. and Fu X.Y. Expression and activation of stat proteins during mouse retina development. *Experimental Eye Research*, 76:421–31, 2003.

134. Zhou Z.J. and Zhao D. Coordinated transitions in neurotransmitter systems for the initiation and propagation of spontaneous retinal waves. *Journal of Neuroscience*, 20:6570–7, 2000.

CHAPTER TWO

MATERIALS AND METHODS

Cell Culture

QNR/D cell cultures were initiated from cryogenic stocks provided by American Type Culture Collection (ATCC). Frozen stocks were thawed in a 40^{o}C water bath and immediately diluted in 10 mL of Dulbecco's modified Eagle's medium (DMEM) (Gibco, catalog# 11995065, Burlington, ON, Canada, Grand Island, NY, USA). This diluted suspension was then centrifuged at 100 *g* for 5 minutes. The supernatant containing the cryogenic medium was removed and the cell pellet was resuspended in 2 mL of fresh DMEM supplemented with 10% fetal bovine serum (FBS) (Gibco, catalog# 12483020, Burlington, ON, Canada, Grand Island, NY, USA), and 1% antibiotic/antimycotic solution (Gibco, catalog# 15240062, Burlington, ON, Canada, Grand Island, NY, USA) to discourage microbial contamination. The final concentration of antimicrobial agents in the medium was 100 μg/mL of penicillin G, 100 μg/mL of Streptomycin sulphate and 0.25 μg/mL amphotericin B. This 2 mL cell suspension was then placed in a 35 mm petri dish (Sarsted, catalog# 83.1800, Montreal, QC, Canada, Numbrecht, Germany) and incubated at 40^{o}C in humidified air composed of 5% CO_2 and 95% atmospheric air. Once the initial culture had reached 80% confluence it was subcultured at a 1:3 ratio using a cell dissociation solution containing 0.05% trypsin and 0.53mM ethylenediaminetetraacetic acid (EDTA) (Gibco, catalog# 25300-054, Burlington, ON, Canada, Grand Island, NY, USA).

QNR/D cultures were maintained on 25 cm^2 tissue culture flasks (Corning, catalog# 430168, Corning, NY, USA) and incubated under the same conditions as previously described. The cell culture medium was changed every two to three

days. Once the cell cultures had proliferated to 80% confluence, they were subcultured at a 1:3 ratio using the same trypsin and EDTA cell dissociation solution. All of these techniques correspond to the instructions on the ATCC website except for the incubation temperature. The incubator temperature was set to 40^{o}C instead of ATCC recommended 38.5-39^{o}C since virtually no proliferation was observed empirically at temperatures below 39^{o}C. For experimentation, QNR/D cells were plated upon coverslips inserted into the wells of 24-well plates and incubated in normal culture medium for 24 hours to allow for cell adhesion before experiments were commenced.

Immunocytochemistry

QNR/D cells were plated at a concentration of 2 x 10^{5} cells/mL on 15mm round coverslips inserted into 24 well plates. Cells were incubated under cell culture conditions for 24 hours to allow for cell adhesion to the coverslips before experimentation proceeded. Culture medium was aspirated and cells were washed 3 times for 5 minutes with sterile phosphate buffered saline (PBS). Cell cultures where then fixed with paraformaldehyde for 30 minutes at room temperature. After fixation, cells were permeabilized with 0.4% Triton X-100 in PBS for 15 minutes. 10% normal goat serum (NGS) was then added to block non-specific antibody binding. The cells were then incubated with primary antibodies overnight at 4^{o}C, after which secondary antibodies were incubated for 1 hour at room temperature in the dark. Alexa Fluor 488 conjugated goat anti-mouse IgG (Invitrogen, Catalog# A-11001, Burlington, ON, Canada, Grand Island, NY, USA) and Alexa Fluor 488 conjugated goat anti-rabbit (Invitrogen, Catalog# A-

11008, Burlington, ON, Canada, Grand Island, NY, USA) secondary antibodies were used at a 1:100 dilution. See Table 1 for a list of primary antibodies used. Cultures were washed three times for five minutes with sterile PBS between each step except for the blocking to primary antibody transition.

Specimens were mounted in *Prolong* Gold antifade with 4'-6-diamidino-2-phenylindol (DAPI) (Invitrogen, catalog# P36930, Burlington, ON, Canada, Grand Island, NY, USA) on microscope slides. Negative controls were produced by replacing the primary antibody with normal serum of the same species as the primary antibody. Immunofluorescence was detected and photographed using a Zeiss LSM710 confocal microscope under 400x magnification.

Electrophysiology

Electrophysiological data were collected using the patch clamp apparatus. Micropipettes were produced from capillary tubes using a two-stage electrode puller (Narishige, Tokyo, Japan) and fire-polished using a wire resistor microforge (Narishige, Tokyo, Japan). Silver chloride coated silver wires were used as electrodes. During recordings cells were bathed in an extracellular solution whose pH was titrated to 7.4 with hydrochloric acid and whose osmolarity was adjusted to 270 mOsmol in order to obtain high resistance seals. Cells were dialysed with an intracellular solution whose pH was titrated to 7.4 with sodium hydroxide and whose osmolarity was adjusted to 265 mOsmol to reduce the intracellular osmotic pressure that would be exerted due to the lower osmolarity of the extracellular solution. For Ca^{2+} current recordings barium was used as a charge carrier instead of calcium due to its higher conductance through

L-type calcium channels and to prevent current rundown caused by calcium-dependent inactivation of L-type calcium channels. (Refer to Table 2 and Table 3 for detailed description of bath solutions.) Cells were viewed under an inverted phase contrast microscope (Nikon, Melville, NY, USA) and the micropipette was controlled using a hydraulic micromanipulator (Nikon, Melville, NY, USA). The electrical activity of cells was analysed under the whole cell configuration. Recordings were done upon an air-supported platform in order to dampen disruptive floor vibration. All recordings were conducted at room temperature. Membrane potentials were clamped by an Axon instruments amplifier, while the Axopatch 7.0 program was used to program and control the voltage step protocols as well as record the current across the cell membranes.

Whole Cell Voltage Clamp Current Recording

The ionic currents were recorded from QNR/D cells one day after plating on glass coverslips (day 0) to determine current expression. Cells with round perikarya and smooth membranes were selected for recording. These cells were patch clamped in the whole cell configuration and the voltage was stepped at 10 mV intervals from holding potentials of -80mV and -40mV. The currents produced by a series of 16 voltage steps and 12 voltage steps (for -80mV and -40mV holding potentials respectively) were recorded and analyzed. Currents at the -40mV holding potential were then subtracted from currents at -80mV holding potential to separate the Ca^{2+} currents conducted by LVA Ca^{2+} channels (T-type) from that of HVA Ca^{2+} channels (L-type, N-type, P/Q-type and R-type) and to separate the K^{+} currents conducted by A-type K^{+} channels from that of delayed

rectifier K^+ channels. Capacitive transients (whose integral represents the charge displacement caused by the voltage step) were also recorded in order to calculate the membrane capacitance. Calcium currents were then compared to the membrane capacitance in order to normalize the current magnitudes to cell surface area. Statistical differences in results were determined by repeated measures analysis of variance (rANOVA) using SPSS software (IBM, Armonk, New York USA). Statistical differences between current-voltage curves were calculated by a Huynh-Feldt posttest since Mauchly's Test indicated sphericity violation. Results with a level of significance below 0.05 ($P<0.05$) were considered significant.

Growth Hormone Treatment

Cells in the experimental group were cultured in complete culture medium (DMEM with 10% FBS and 1% antibiotic/antimycotic solution) supplemented with recombinant avian GH at a concentration of 10^{-6} M. This concentration was chosen because 10^{-6} M is the near the physiological concentration of ocular GH in the developing retina (Baudet *et al* unpublished data) and of most neurotransmitters within the synaptic cleft. Furthermore, this concentration yielded significant results in *in vitro* studies by Sanders *et al*. Cells in the negative control group were incubated in normal culture medium supplemented only with the GH administration vehicle (0.01 M bicarbonate solution). The GH containing medium and the control medium were changed every 24 hours for the duration of the experiments.

Table 1: List of Primary Antibodies Used for Immunocytochemistry Experiments

Name	Antigen	Immunogen	Clonality	Species Raised In	Dilution
3A10	Neurofilament associated antigen	Chick nervous tissue	Monoclonal	Mouse	1:50
39.4D5	Islet-1 homeobox	C-terminal portion of rat Islet-1	Monoclonal	Mouse	1:10
40E-C	Vimentin	homogenized adult canary brain	Monoclonal	Mouse	1:100
cGH	GH	Chicken GH	Polyclonal	Rabbit	1:500
cGHR	GHR	Chicken GHR	Polyclonal	Rabbit	1:500
RA4	Chick RGC associated antigen		Monoclonal	Mouse	1:100
Q¢PN	Quail cell associated antigen	Quail embryonic wingbud zone of polarizing activity	Monoclonal	Mouse	1:100

Table 2: Composition of Solutions for Calcium Current Recording

Solute	**Extracellular Bath Solute Concentrations (mM)**	**Intracellular Dialysing Fluid Solute Concentrations (mM)**
Adenosine Triphosphate Sodium Salt (ATP-N_2)	0	2.0
Barium Chloride ($BaCl_2$)	20	0
Caesium Chloride (CsCl)	5.0	130
Cyclic Adenosine monophosphate (cAMP)	0	0.25
EGTA	0	10
Glucose	20	5
HEPES	20	20
Magnesium Chloride ($MgCl_2$)	0	5.0
Potassium Chloride (KCl)	5.0	0
Tris	105	0

Table 3: Composition of Solutions for Sodium and Potassium Current Recording

Solute	**Extracellular Bath Solute Concentrations (mM)**	**Intracellular Dialysing Fluid Solute Concentrations (mM)**
Adenosine Triphosphate Sodium Salt (ATP-Na_2)	0	4.0
Calcium Chloride ($CaCl_2$)	1.8	1.0
EGTA	0	11
Glucose	10	5
HEPES	10	10
Magnesium Chloride ($MgCl_2$)	1.2	2.0
Potassium Chloride (KCl)	5.4	130
Sodium Chloride (NaCl)	140	0

CHAPTER THREE

RESULTS

I. IMMUNOCYTOCHEMISTRY

The expression of a number of proteins was analyzed by immunocytochemistry. These experiments were done to corroborate the identity of the cell line under investigation and to confirm the presence of GH signalling activity within that cell line.

To confirm that the cells under investigation were of embryonic quail origin, they were incubated with Q¢ PN monoclonal antibody. This antibody was designed to discriminate between quail cells and cells originating from other species (Selleck and Bronner-Fraser, 1995). The immunoreactivity observed in QNR/D cells was limited to the nuclei as evidenced by the colocalization of the DNA stain DAPI. The observed immunoreactivity was absent when the antibody was replaced with normal mouse serum (Figure 1).

To confirm that the QNR/D cell line was of RGC lineage, antibodies recognizing RGC-specific transcription factors were applied. First, QNR/D cells were incubated with 39.4D5 monoclonal antibody. This antibody has been shown to bind the RGC-specific transcription factor Islet-1 homeobox when incubated with embryonic chick retinae (Pimentel *et al*, 2000). When applied to QNR/D cell line, immunoreactivity was observed. The distribution of this immunoreactivity was both cytoplasmic and nuclear but with higher staining intensity present in the nucleus. This staining was absent when this antibody was replaced with normal mouse serum (Figure 2). QNR/D cells were also treated with another RGC-specific monoclonal antibody, R4A (McLoon and Barnes, 1989). Upon incubation with R4A, immunoreactivity was observed in a punctate distribution throughout

the cell cytoplasm. This staining was also absent when normal mouse serum replaced the monoclonal antibody in the protocol (Figure 3).

The expression of intermediate filament proteins was also assessed by immunocytochemistry. Since the expression of these cytoskeletal proteins changes during RGC differentiation, their expression pattern indicates the maturity of the cell. Developing RGCs express the type III intermediate filament vimentin and upon differentiation the RGC cytoskeletal composition changes to include the Type IV intermediate filament neurofilaments (Alvarez-Buylla and Nottebohm, 1988; Pollerberg *et al*, 1995). To determine vimentin expression the monoclonal antibody 40E-C was used because this antibody was designed to recognize vimentin in differentiating avian radial glia (Alvarez-Buylla *et al*, 1987). When QNR/D cells were incubated with 40E-C, immunoreactivity was observed in a filamentous configuration that was specifically dense within radial processes. This immunoreactivity was absent when 40E-C antibody was replaced with normal mouse serum (Figure 4). To determine neurofilament expression the monoclonal antibody 3A10 was used because this antibody recognizes neurofilaments in embryonic chick neural tissues (Serafini *et al*, 1996). When QNR/D cells were incubated with 3A10, immunoreactivity was observed in a punctate distribution throughout the cytoplasm. This immunoreactivity was absent when 3A10 antibody was replaced with normal mouse serum (Figure 5).

To confirm the presence of GH and GHR, anit-GH and anti-GHR antiserum was applied to QNR/D cells. GH immunoreactivity was present in a punctate distribution throughout the cytoplasm and nucleus of QNR/D cells. This

staining is absent in control cells incubated with normal rabbit serum (Figure 6). GHR immunoreactivity was also present within the cytoplasm and the nuclei of QNR/D cells. Again, this staining was absent in control cells incubated with normal rabbit serum (Figure 7).

II. ELECTROPHYSIOLOGY

The electrophysiological properties of QNR/D cells were investigated using the patch clamp technique. Experiments were conducted in whole-cell configuration under both current clamp and voltage clamp conditions. Electrical responses were measured 24 hours after plating. Also, to investigate the effect of GH on these electrophysiological properties, electrical responses were measured after 1 hour, 24 hours and 72 hours of exposure to GH. When recording passive electrical responses, action potentials and K^+ currents, cells were bathed in physiological solutions while Ca^{2+} currents were recorded in a Na^+-free environment (see Materials and Methods section for solution composition).

Passive Electrical Responses

One of the electrophysiological properties that was measured was input resistance. 24 hours after plating the average input resistance of QNR/D cells was 2.8 GΩ ± 0.6 GΩ. From cell to cell the input resistance ranged from 0.379 GΩ to 5.12 GΩ. The input resistance did not change with GH treatment of 1 hour, 24 hours, or 72 hours. At each of these time points the average input resistance was within error of both control and baseline levels (Figure 18).

The other passive electrical response investigated in QNR/D cells was the ability to generate action potentials. Cells were bathed with a physiological extracellular solution and patch clamped in whole-cell configuration under current clamp conditions. The membrane potential was adjusted to -80 mV in order to relieve any channel inactivation that may occur at the physiological membrane potential. Current injections of up to 700 pA did not generate voltage spikes

(Figure 8-A). Additionally, QNR/D cells were bathed with a physiological extracellular solution and patch clamped in whole-cell configuration under current voltage clamp conditions in order to record Na^+ currents. No Na^+ currents were observed when cells were subject to increasing voltage steps from a -80 mV holding potential to a final membrane potential of 80 mV (Figure 8-C).

Previous studies have stated that this cell line will generate action potentials in response to small injections of current after 4 days in culture. Furthermore, the authors report that these action potentials can be inhibited with the Na^+ channel blocker tetrodotoxin. (Pessac *et al*, 1983) My findings disagree with this claim since action potentials could not be generated at any time point ranging from 24 hours after plating to an entire week without subculturing and no Na^+ currents were observed under voltage clamp conditions at any time during experimentation. If action potentials were to occur, a substantial Na^+ current would be required to generate them.

As a positive control, action potentials and Na^+ currents were recorded from differentiated N1E-115 murine neuroblastoma cells. These cells were exposed to 2% dimethyl sulfoxide (DMSO) for 6 days in order to induce robust ion channel expression and spiking activity as described by Kimhi *et al* (1976). After this treatment, cells were bathed with a physiological extracellular solution and patch clamped in whole-cell configuration under current clamp conditions. Voltage spikes similar to those observed by Moolenaar and Spector (Moolenaar and Spector, 1978) were provoked by current injections as small as 100 pA (Figure 8-B). Furthermore, when differentiated N1E-115 cells were bathed with a

physiological extracellular solution and patch clamped in whole-cell configuration under current voltage clamp conditions large Na^+ currents were activated by voltages steps as small as 30 mV from a holding potential of -80 mV (Figure 8-D).

Calcium Currents

Ca^{2+} currents were recorded from cells bathed in a Na^+-free solution and patch clamped in whole cell voltage clamp configurations. 24 hours after plating, QNR/D cells exhibited Ca^{2+} currents resembling T-type currents observed in other preparations. These currents activated at low voltages (approximately -60 mV) and were transient in duration due to rapid channel inactivation (Figure 9, Figure 13). They also exhibited large tail currents typical of T-type Ca^{2+} channels (Figure 9). To further define these characteristics, current magnitude was measured in response to increasing holding potentials. The fraction of the total current generated from each holding potential was plotted as a function of that holding potential to generate an inactivation curve. This inactivation curve is described by the Boltzmann Function,

$$I = I_{max} / \left[1 + \exp\left((V_{mid} - V)/V_c\right)\right]$$

where: I is the faction of maximum current,

I_{max} is the maximum current,

V is the holding potential,

V_{mid} is the holding potential at which half-maximal current is observed and

V_c is the voltage required to change I e-fold

From this equation the value of V_{mid} for this current was determined to be -35 mV with a standard error of 0.6 mV and V_c was determined to be 7.5 mV with a standard error of 0.5 mV (Figure 15, Table 4). These values are typical of T-type Ca^{2+} currents measured in retinal cells (Pan, 2000).

To confirm the identity of these currents, a number of pharmacological antagonists were applied to the extracellular environment by perfusion. Ca^{2+} current was completely abolished by the application of 5 μM mibefradil, a selective T-type Ca^{2+} channel antagonist (Figure 10, Figure 11). This inhibition was nearly instantaneous and was partially reversible by perfusion with fresh bathing solution (Figure 10). This current was unaffected by the application of 10 μM nifedipine, a L-type Ca^{2+} channel antagonist.

The magnitude of this current did not significantly change with GH treatment. After 1 hour, 24 hours and 72 hours T-type current density was within error of both control and baseline levels (Figure 19). Furthermore, no additional current types emerged upon GH treatment.

As a positive control, Ca^{2+} currents were recorded from the N1E-115 cell line. These cells also expresses predominantly T-type Ca^{2+} current but can be differentiated by exposure to 2% DMSO to express L-type currents as well. After 48 hours of GH treatment, the T-type current density in these cells was significantly reduced in comparison to untreated controls ($P<0.05$) (Figure 20). Furthermore, after differentiation by DMSO exposure, N1E-115 cells exhibited significant L-type currents. These currents are characterized by activation at

higher voltages (Figure 14), a lack of inactivation and small tail currents (Figure 12).

Potassium Currents

K^+ currents were recorded from cells bathed in a physiological solution and patch clamped in whole cell voltage clamp configuration. 24 hours after plating, QNR/D cells exhibited two distinct K^+ currents. One of these currents exhibited low activation threshold (approximately -10 mV), transient duration due to rapid inactivation as well as outward rectification (Figure 16-A, Figure 17). Furthermore, this current could be completely abolished by increasing the holding potential to -40 mV. The fact that this current is inactivated by elevated holding potentials indicates that A-type K^+ channels conduct this current. Furthermore, this property of inactivation at higher holding potentials allowed for the separation of this current from other K^+ currents that were present. The second current that was observed activated at higher thresholds (approximately 20 mV), was sustained in duration and exhibited outward rectification (Figure 16-B, Figure 17). This current was not affected by increasing the holding potential to -40 mV nor was it affected by the absence of Ca^{2+} ions in the bath. These observations suggest that this is the delayed rectifier K^+ current.

Treatment of QNR/D cells with GH had no effect on the magnitude of either of these current types. The density of both of these currents remained within error of the currents recorded from untreated control cells (Figures 21, 22 and 23).

Figure 1: Quail Nuclear Marker Immunoreactivity in QNR/D Cells A) QNR/D cells labelled with Q¢PN, a nuclear quail cell marking antibody (green) (400x) B) QNR/D cells labelled with Q¢PN (green) and nuclei labelled with the DNA stain DAPI (blue) (400x) C) QNR/D cells incubated with normal mouse serum and nuclei labelled with the DNA stain DAPI (blue)

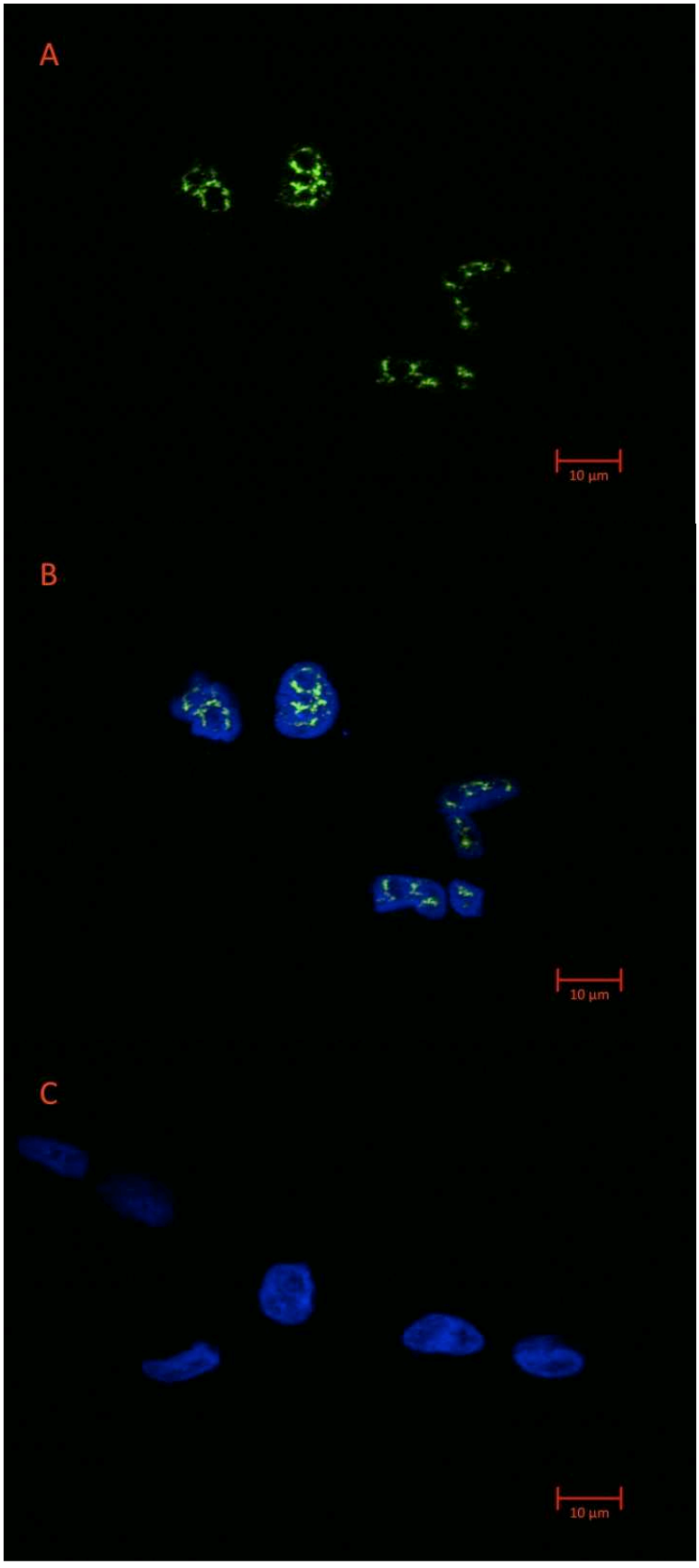
A
10 µm
B
10 µm
C
10 µm

Figure 2: Islet-1 Homeobox Immunoreactivity in QNR/D Cells A) QNR/D cells labelled with 39.4D5, an islet-1 binding antibody (green) (400x) B) QNR/D cells labelled with 39.4D5 (green) and nuclei labelled with the DNA stain DAPI (blue) (400x) C) QNR/D cells incubated with normal mouse serum and nuclei labelled with the DNA stain DAPI (blue)

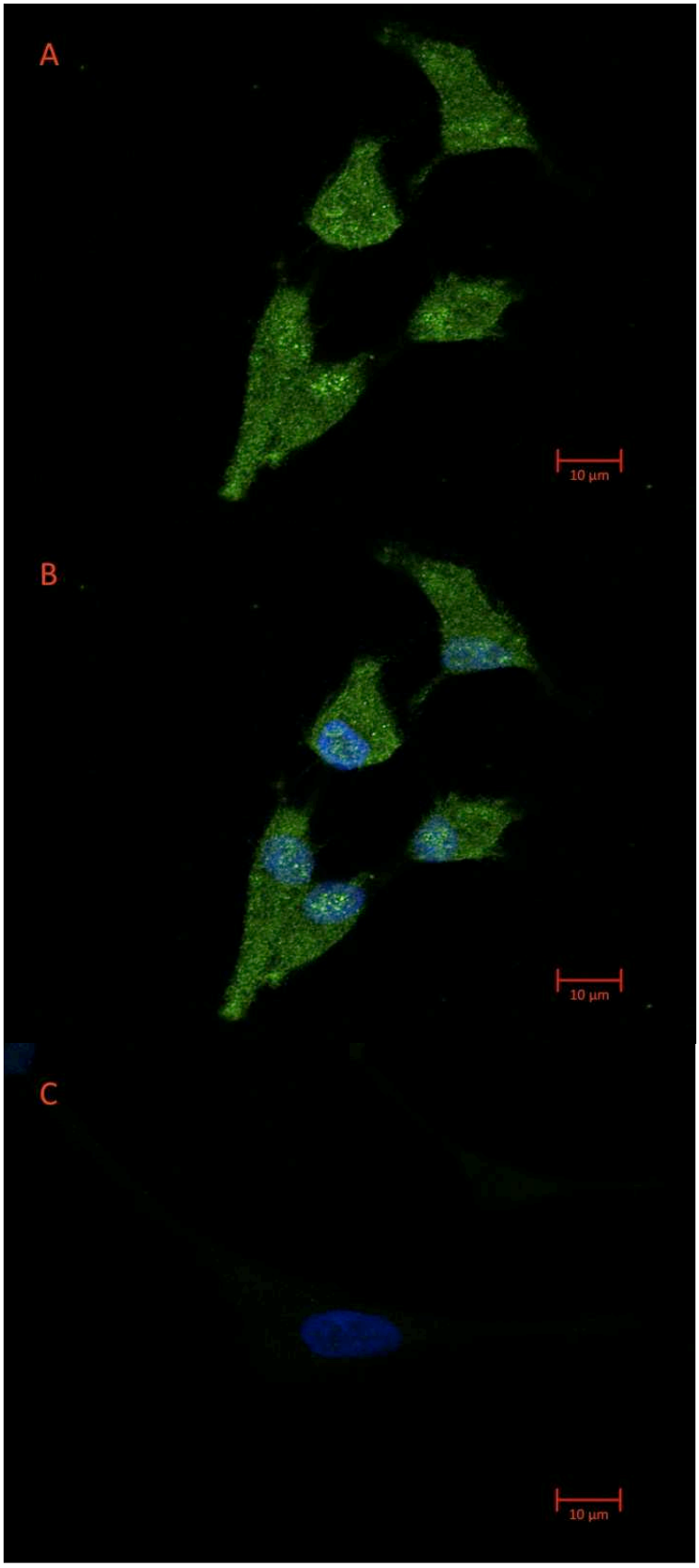
A
10 µm
B
10 µm
C
10 µm

Figure 3: Avian Retinal Ganglion Cell Marker Immunoreactivity in QNR/D Cells A) QNR/D cells labelled with R4A, a retinal ganglion cell marker antibody (green) (400x) B) QNR/D cells labelled with R4A (green) and nuclei labelled with the DNA stain DAPI (blue)(400x) C) QNR/D cells incubated with normal mouse serum and nuclei labelled with the DNA stain DAPI (blue)

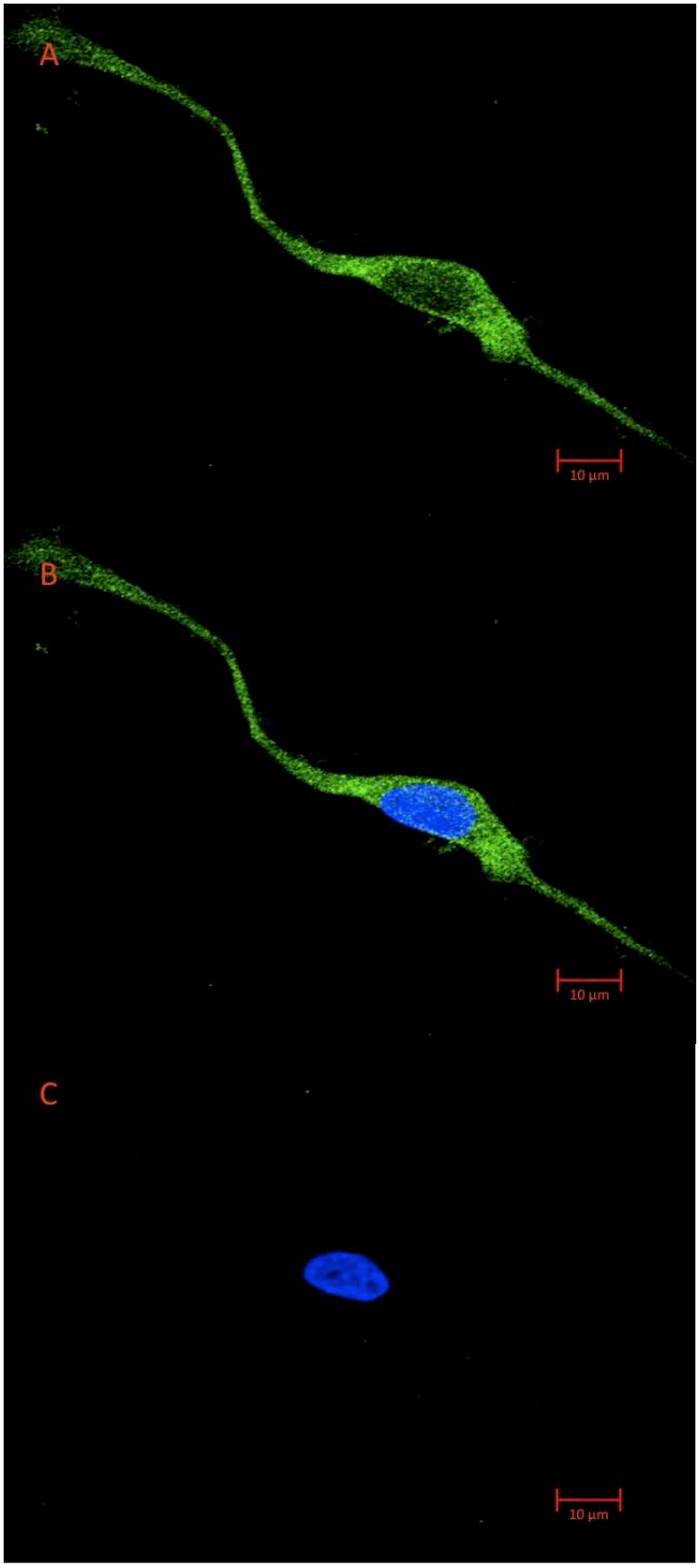
A
10 µm
B
10 µm
C
10 µm

Figure 4: Vimentin Immunoreactivity in QNR/D Cells A) QNR/D cells labelled with 40E-C a vimentin binding antibody (400x Alexafluor 488) and B) QNR/D cells labelled with 40E-C (green) and nuclei labelled with the DNA stain DAPI (blue) (400x) C) QNR/D cells incubated with normal mouse serum and nuclei labelled with the DNA stain DAPI (blue)

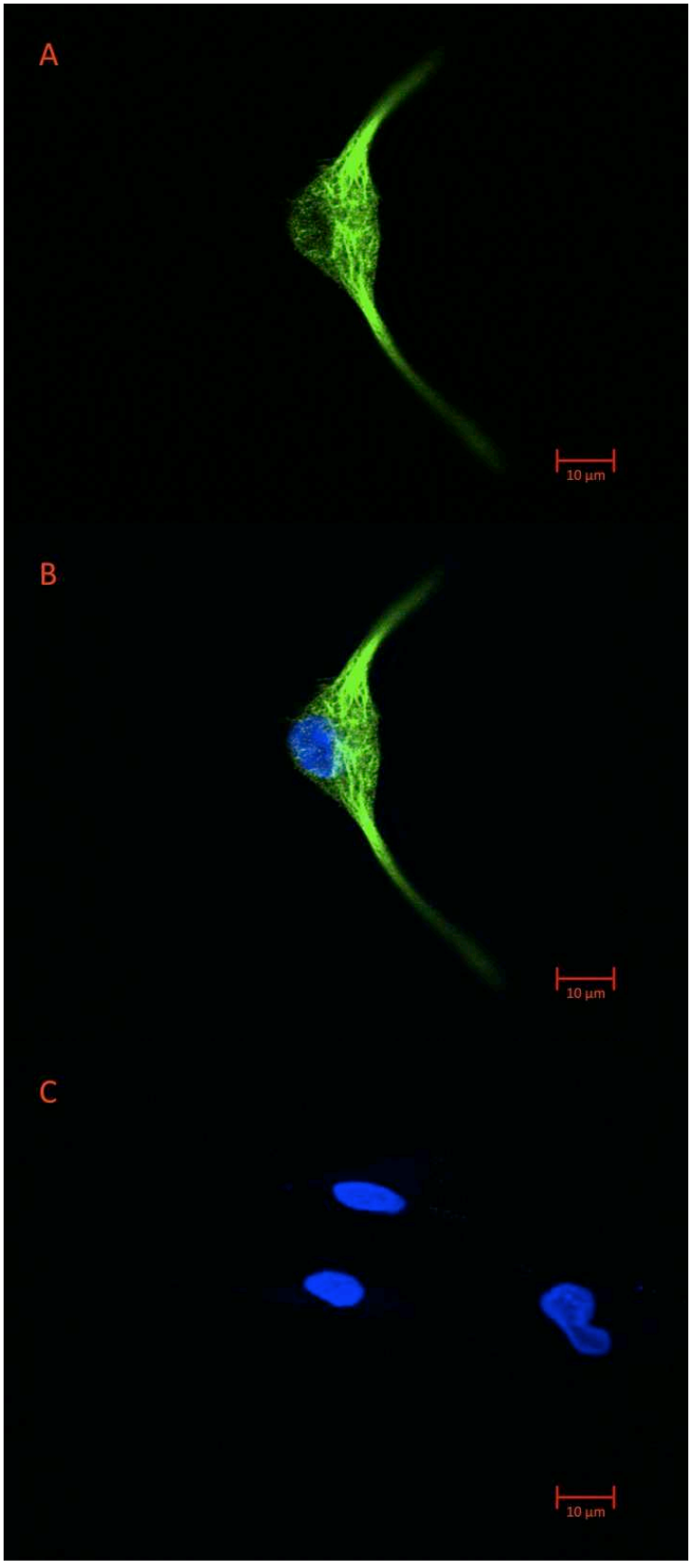
A
10 µm
B
10 µm
C
10 µm

Figure 5: Neurofilament Immunoreactivity in QNR/D Cells A) QNR/D cells labelled with 3A10 a neurofilament binding antibody (400x Alexafluor 488) and B) QNR/D cells labelled with 3A10 (green) and nuclei labelled with the DNA stain DAPI (blue) (400x) C) QNR/D cells incubated with normal mouse serum and nuclei labelled with the DNA stain DAPI (blue)

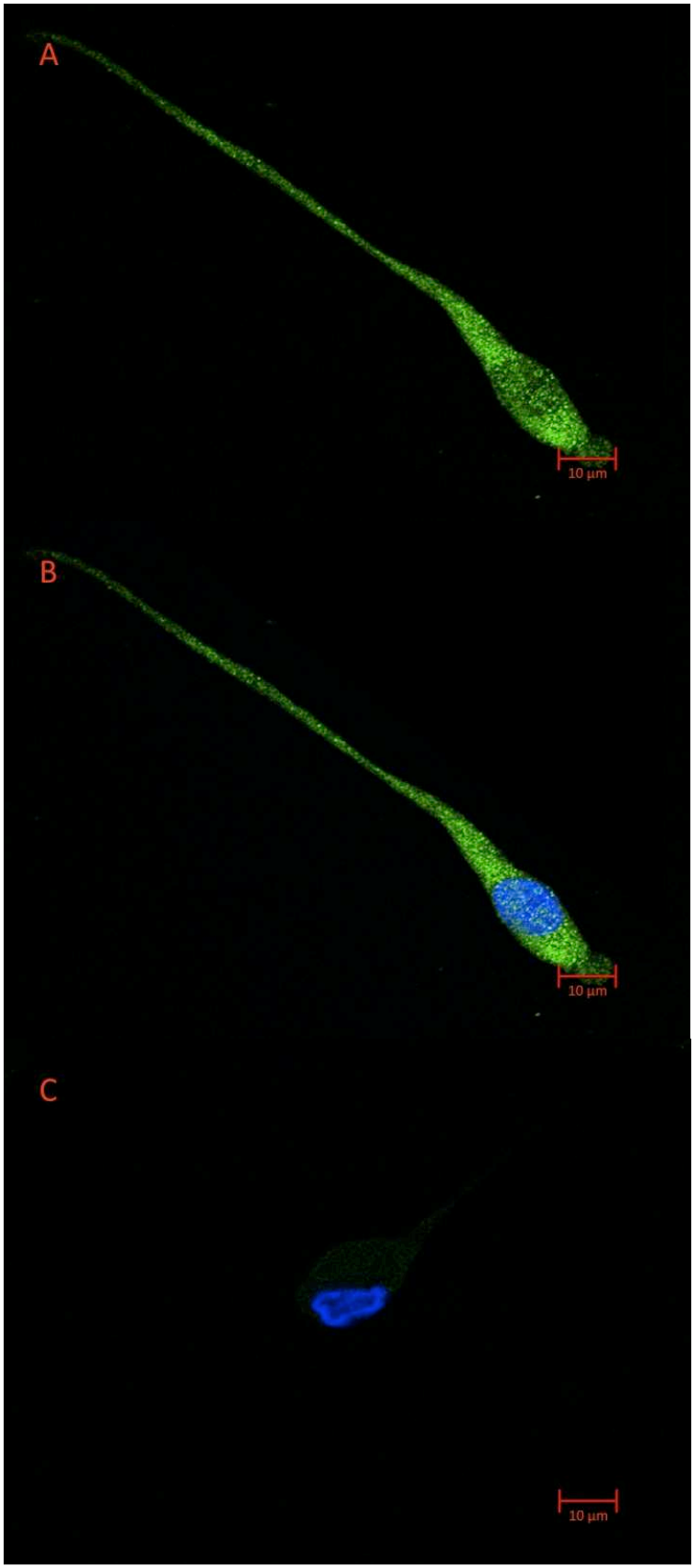
A
10 µm
B
10 µm
C
10 µm

Figure 6: Growth Hormone Immunoreactivity in QNR/D Cells A) QNR/D cells labelled with anti-cGH (green) (400x) and B) QNR/D cells labelled with anti-cGH (green) and nuclei labelled with the DNA stain DAPI (blue) (400x) C) QNR/D cells incubated with normal rabbit serum and nuclei labelled with the DNA stain DAPI (blue)

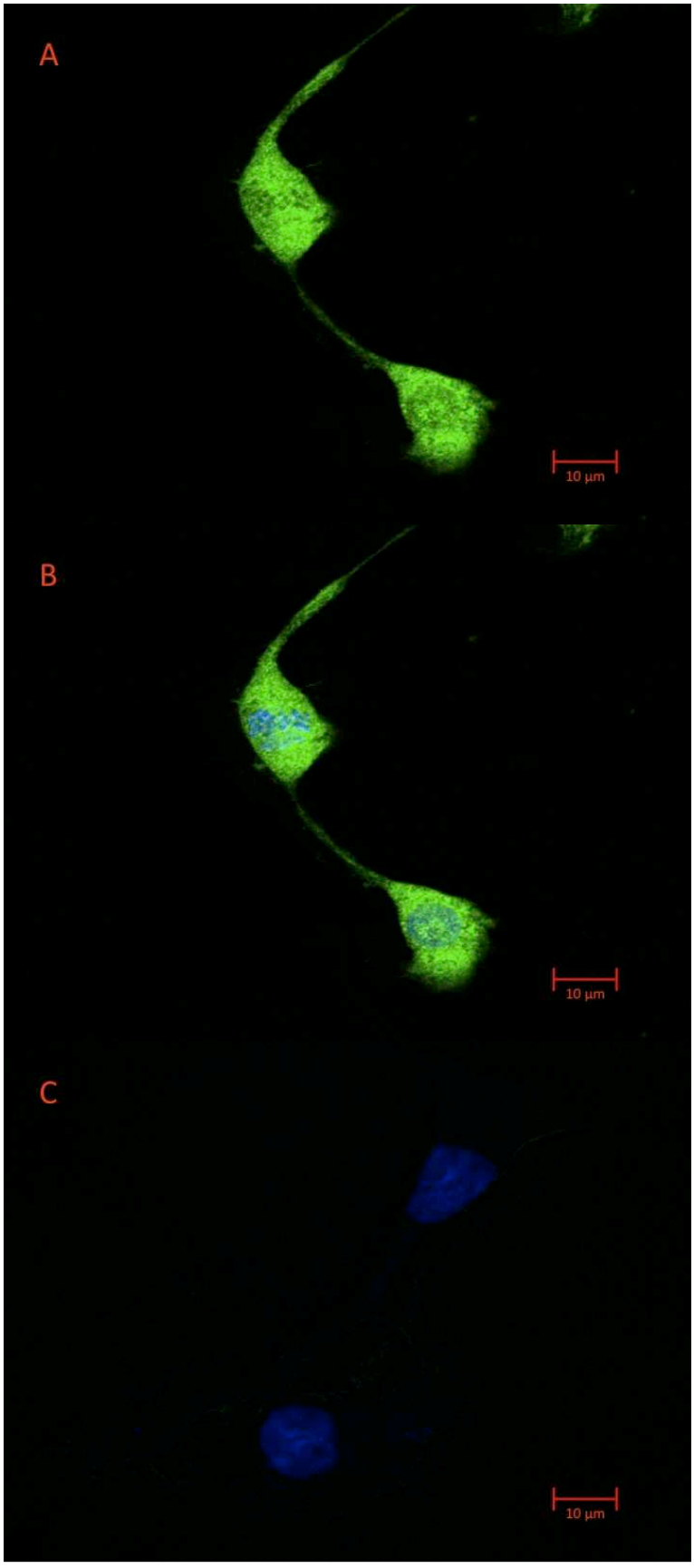
A
10 µm
B
10 µm
C
10 µm

Figure 7: Growth Hormone Receptor Immunoreactivity in QNR/D Cells A) QNR/D cells labelled with anti-cGHR (green) (400x) and B) QNR/D cells labelled with anti-cGHR (green) and nuclei labelled with the DNA stain DAPI (blue) (400x) C) QNR/D cells incubated with normal rabbit serum and nuclei labelled with the DNA stain DAPI (blue)

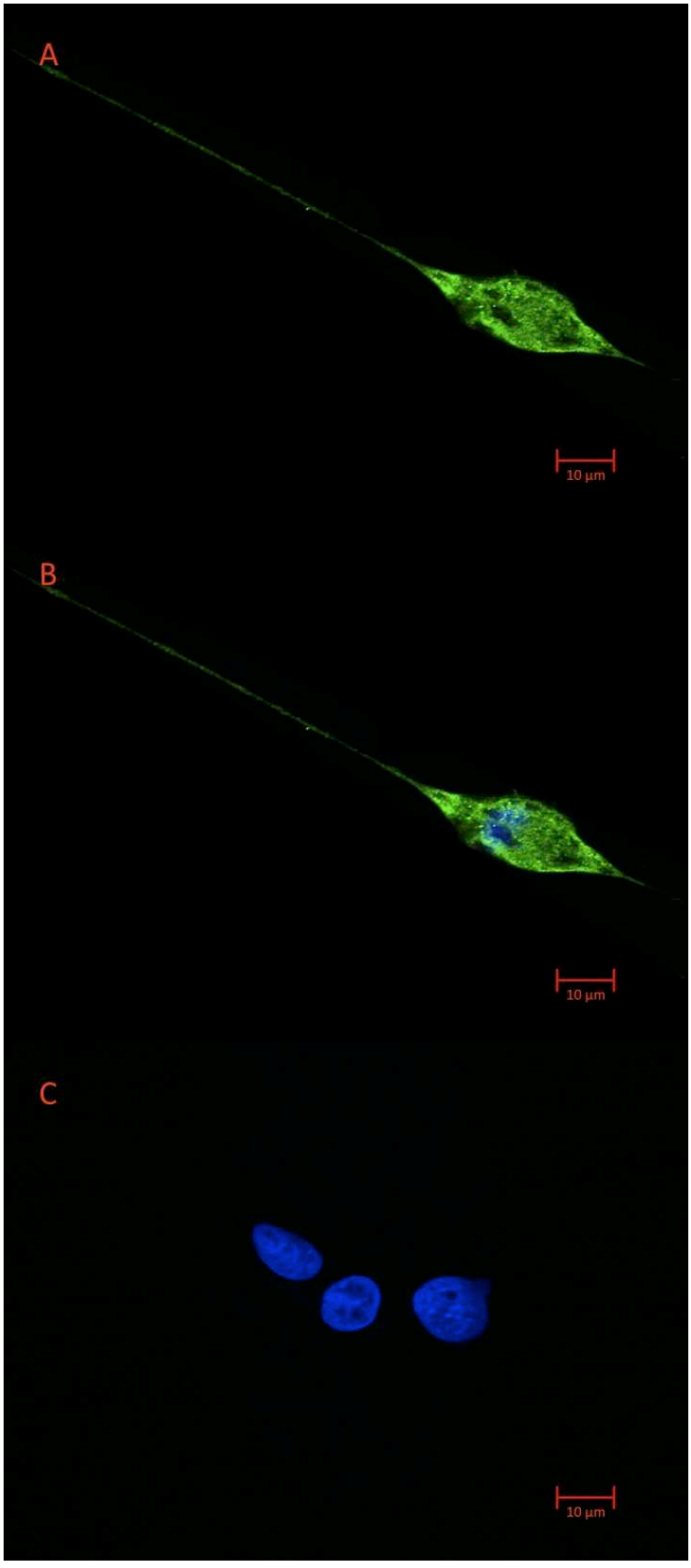
A
10 µm
B
10 µm
C
10 µm

Figure 8: Action potentials in QNR/D Cells A) No action potentials were generated when current was injected into QNR/D cells after 24 hours in culture. Cells were bathed in a physiological solution and patch clamped in current clamp configuration. The membrane potential was adjusted to -80 mV and current was injected in 20 ms pulses with magnitudes ranging from 50 pA to 700 pA in 50 pA increments as depicted by the stimulus waveform inset. X-axis scale units are ms, Y-axis scale units are mV. As evident from the smooth and steady increase in membrane potential, no action potentials were generated. B) Spiking properties were recorded from N1E-115 cells after 6 days of DMSO exposure. Cells were bathed in a physiological solution and patch clamped in current clamp configuration. Current injections were applied to the resting membrane potential (approximately -40 mV) in 100 ms pulses with magnitudes ranging from 100 pA to 500 pA in 100 pA increments as depicted by the stimulus waveform inset. X-axis scale units are ms, Y-axis scale units are mV. C) No Na+ currents were observed when QNR/D cells after 24 hours in culture. Cells were bathed in a physiological solution and patch clamped in whole cell voltage clamp configuration. The inward current observed is clearly a result of Ca^{2+} channel activation as evidenced by the long current duration, small current amplitude and large tail currents. The membrane potential was held at -80 mV and stepped to 80 mV in 10 mV increments with the visible current traces depicting steps to -70 mV, -40 mV, -30 mV, -20 mV, and 10 mV. X-axis scale units are ms, Y-axis scale units are pA. D) Na^{+} currents were recorded from N1E-115 cells after 6 days of DMSO exposure. Cells were bathed in a physiological solution and patch clamped in whole cell voltage clamp configuration. The membrane potential was held at -80 mV and stepped to 80 mV in 10 mV increments with the visible current traces depicting steps to -70 mV, -30 mV, -20 mV, -10 mV and 20 mV. X-axis scale units are ms, Y-axis scale units are pA. The inward current observed is clearly produced by Na^{+} channel activation as evidenced by the rapid current inactivation and large current amplitude.

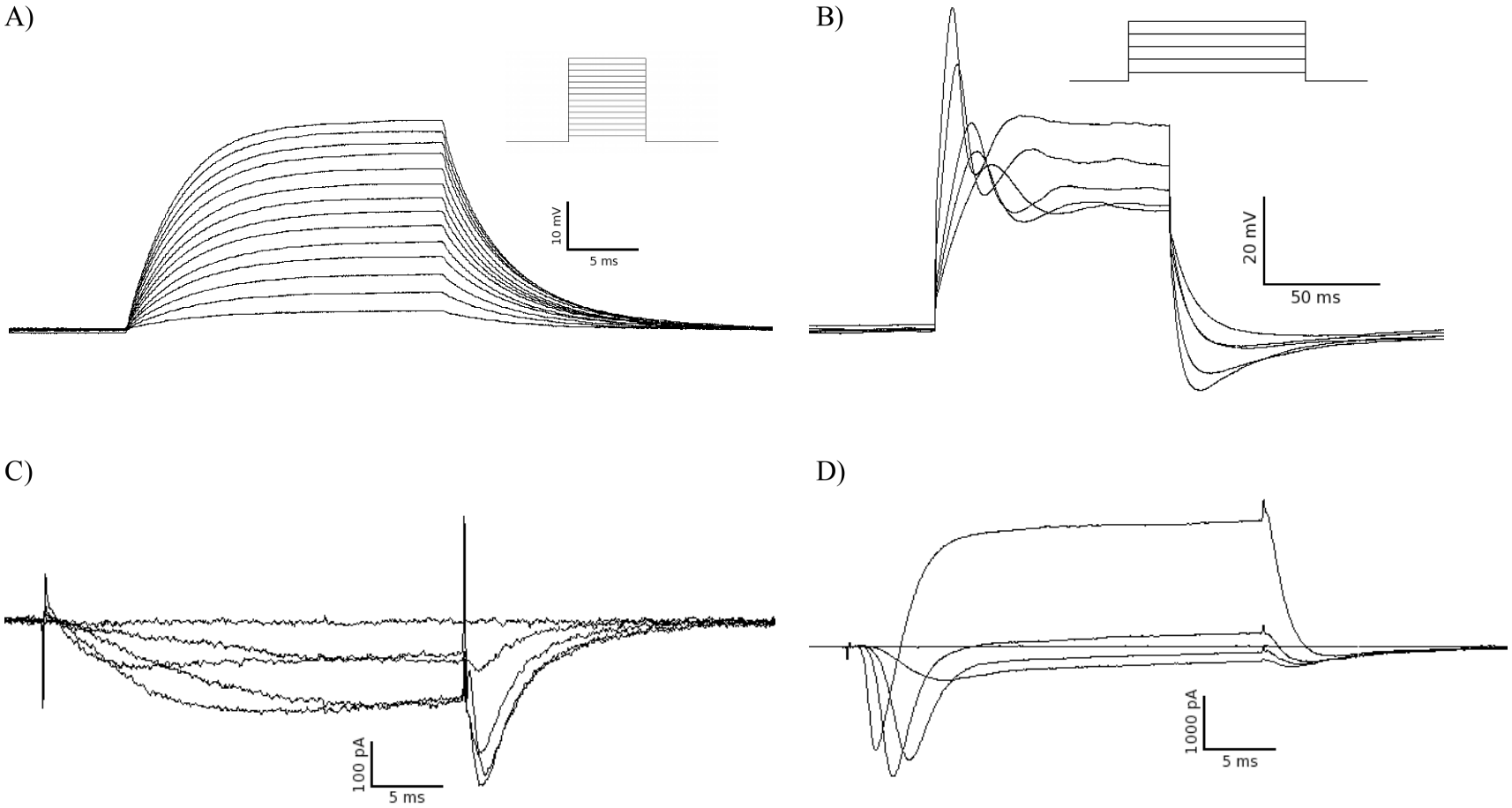
A)
10 mV
5 ms
B)
20 mV
50 ms
C)
100 pA
5 ms
D)
1000 pA
5 ms

Figure 9. Calcium Currents in QNR/D Cells Ca^{2+} currents were recorded from QNR/D cells 24 hours after plating. Cells were bathed in Na^{+}-free solution and patch clamped in whole cell voltage clamp configuration. The membrane potential was held at -80 mV and stepped to 80 mV in 10 mV increments. X-axis scale units are ms, Y-axis scale units are pA. A) Voltage steps to -70 mV, -20 mV, 0 mV, 20 mV and 40 mV visible. Note the transient current duration. B) 30 ms voltage step to -10 mV visible with expanded X-axis scale. Note the large tail current.

A)

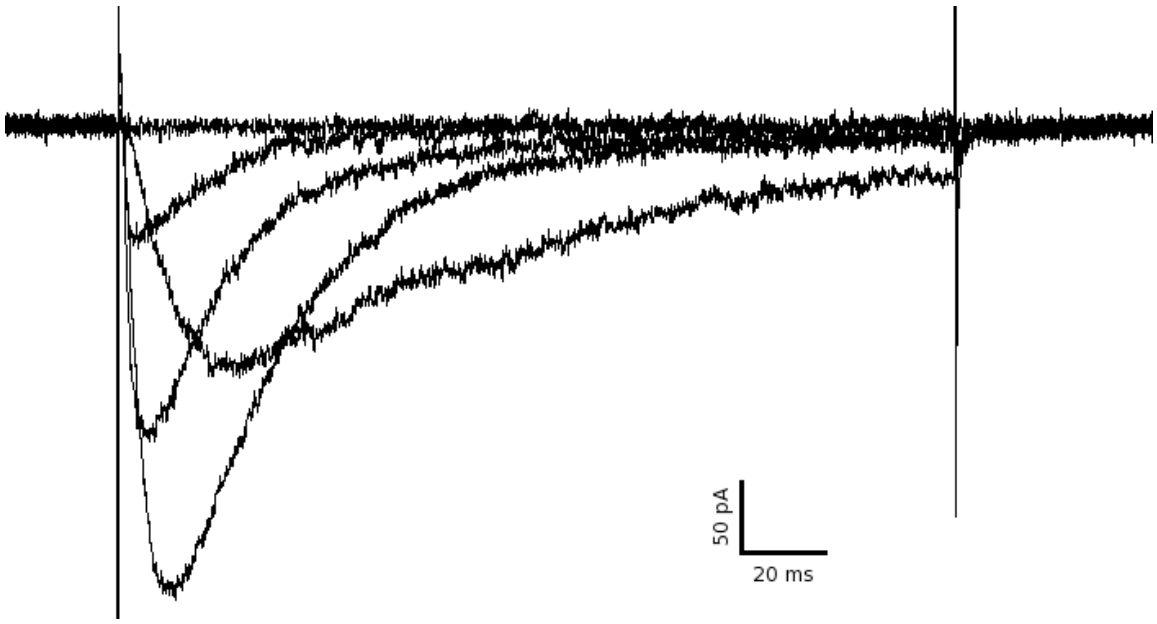

B)

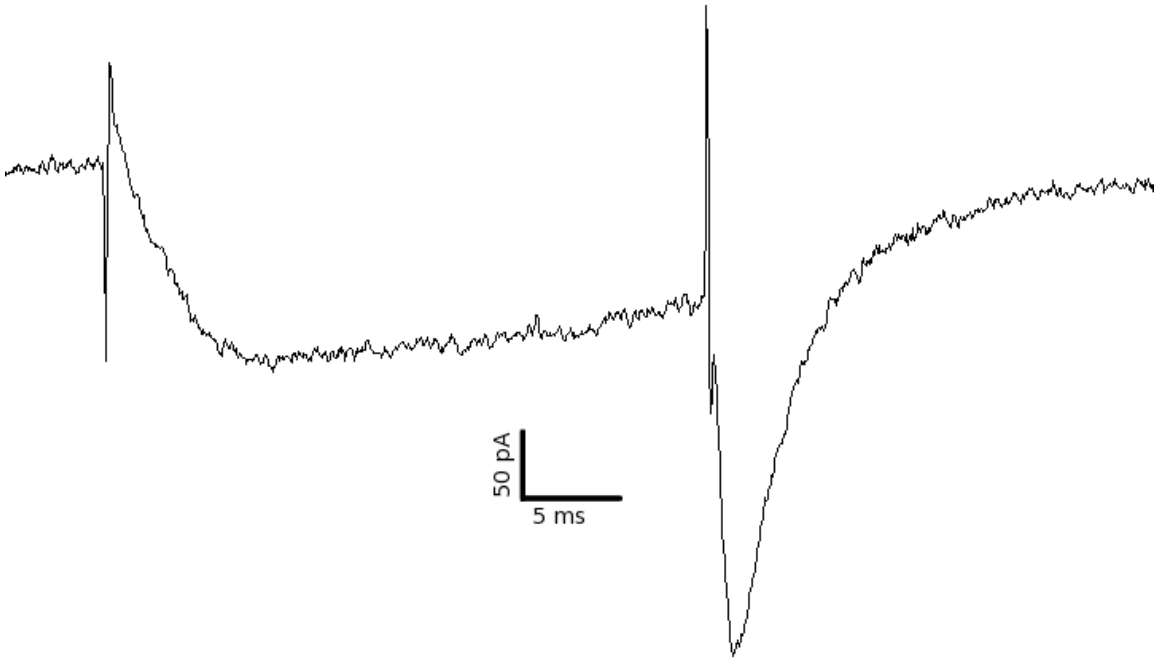

Figure 10. The Effect of 5 μM Mibefradil on Calcium Currents in QNR/D Cells T-type specific Ca^{2+} channel antagonist Mibefradil was used to block T-type current in QNR/D cells. Ca^{2+} currents were recorded from QNR/D cells 24 hours after plating. Cells were bathed in Na^{+}-free solution and patch clamped in whole cell voltage clamp configuration. The membrane potential was held at -80 mV and stepped to 80 mV in 10 mV increments. X-axis scale units are ms, Y-axis scale units are pA. A) -80 mV to 0 mV step prior to Mibefradil perfusion. B) -80 mV to 0 mV step after Mibefradil perfusion. Note: the total abolishment of current. C) -80 mV to 0 mV step after Mibefradil washout. Note: the current only partial recovers from Mibefradil block.

A)

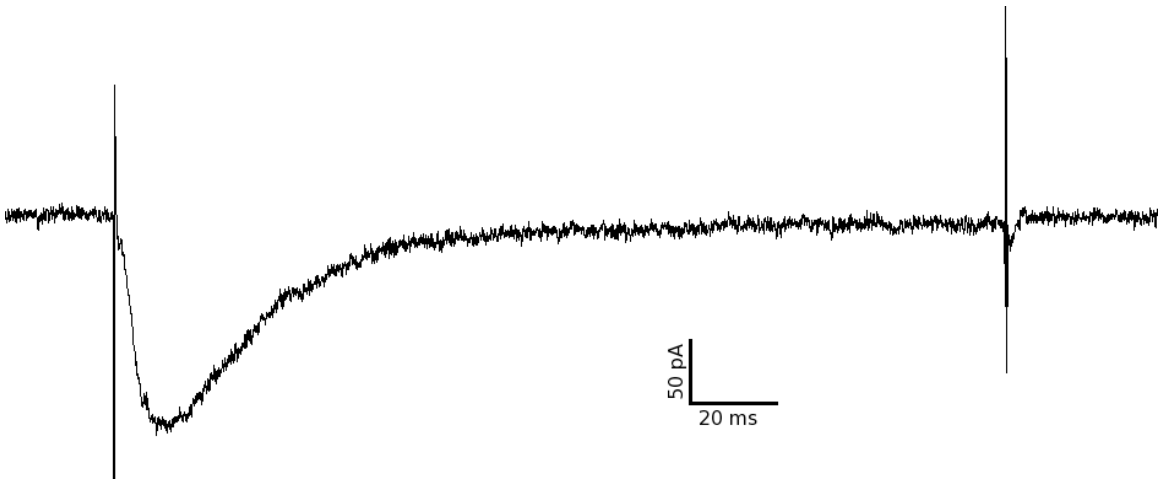

B)

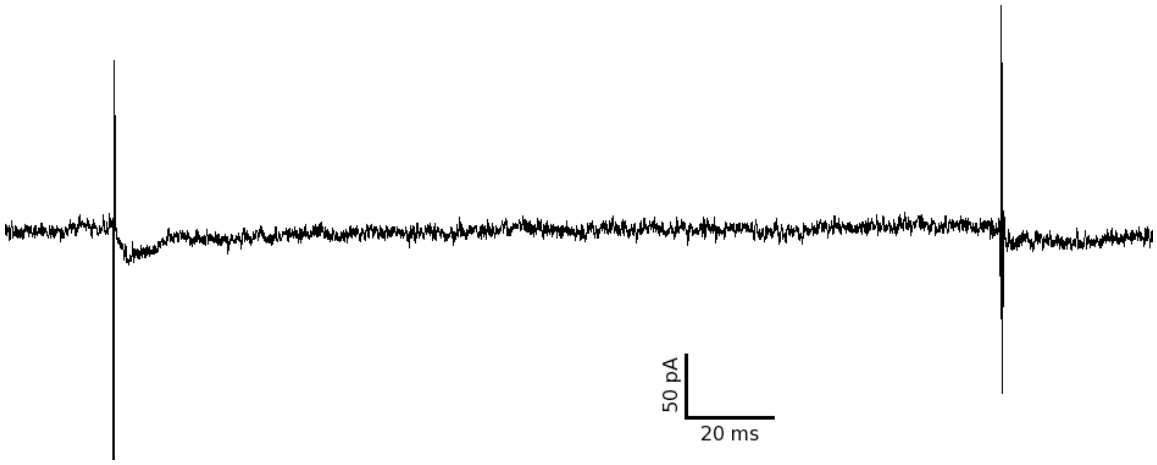

C)

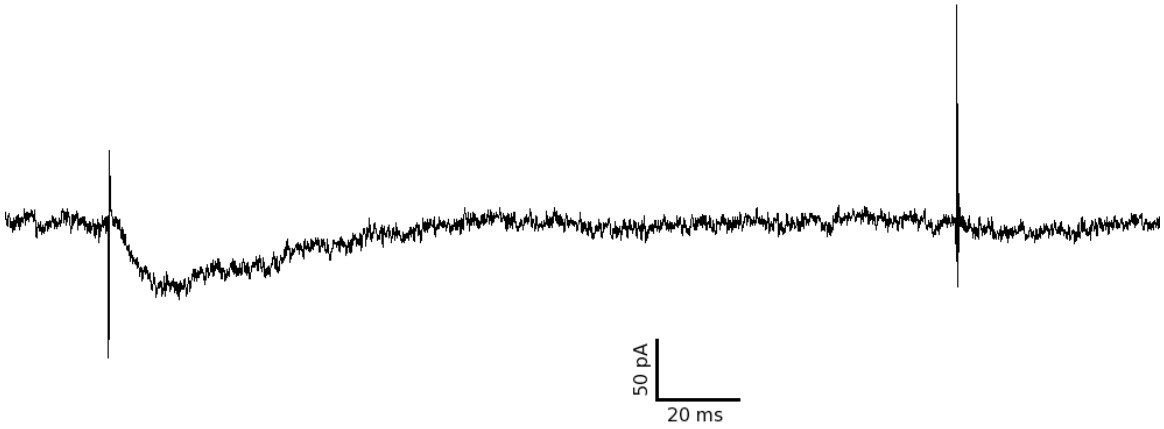

Figure 11: The Effect of Mibefradil Perfusion on Calcium Currents in QNR/D Cells This chart illustrates the relationship between voltage and Ca^{2+} current density prior to (blue line) and after (red line) the perfusion of 5 μM mibefradil, a selective T-type Ca^{2+} channel antagonist. Each data point represents the average current density recorded from 5 cells.

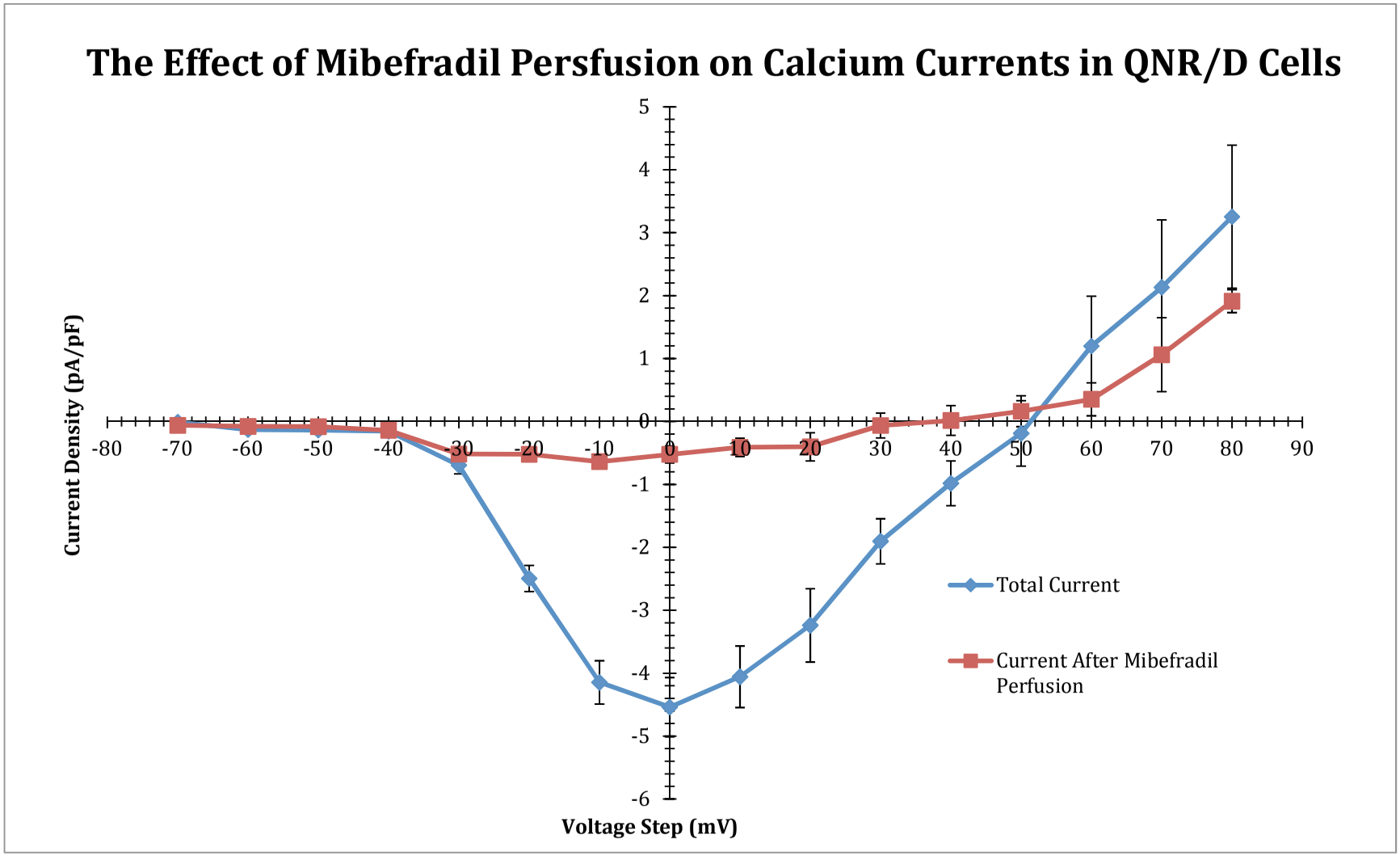
The Effect of Mibefradil Persfusion on Calcium Currents in QNR/D Cells
Current Density (pA/pF)
Voltage Step (mV)
5
4
3
2
1
0
-1
-2
-3
-4
-5
-6
-80
-70
-60
-50
-40
-30
-20
-10
0
10
20
30
40
50
60
70
80
90
Total Current
Current After Mibefradil Perfusion

Figure 12: L-type Calcium Currents in N1E-115 Cells Ca^{2+} currents were recorded from N1E-115 cells after 6 days of DMSO exposure. Cells were bathed in a Na^{+}-free solution and patch clamped in whole cell voltage clamp configuration. The membrane potential was held at -40 mV in order to inactivate any T-type Ca^{2+} channels that may be present and stepped to 80 mV in 10 mV increments. X-axis scale units are ms, Y-axis scale units are pA. A) Voltage steps to -10 mV, 0 mV, 10 mV and 20 mV visible. B) Voltage step to 20 mV visible. Note the sustained current duration and small tail currents.

A)

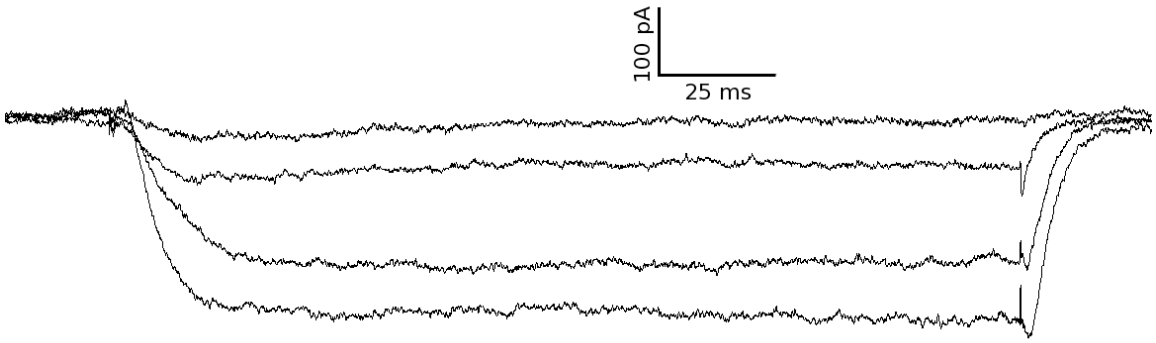

B)

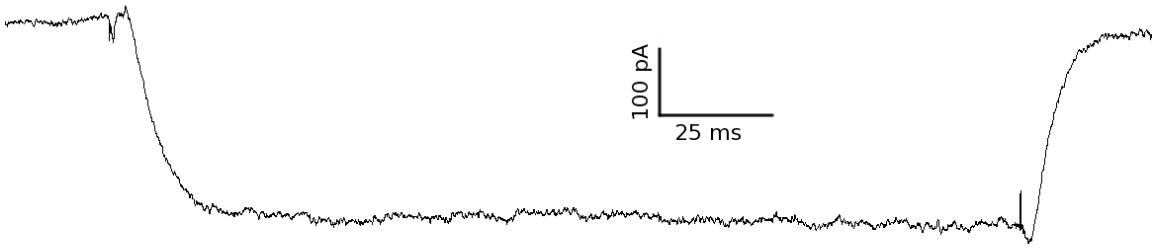

Figure 13: T-type Calcium Current in QNR/D Cells 24 Hours After Plating
This chart illustrates the relationship between voltage and T-type Ca^{2+} current density recorded from QNR/D cells 24 hours after plating. Each data point represents the average current density recorded from 12 cells. Current density is calculated by dividing the total current by the cell capacitance. A peak current density of -4.13 pA/pF with a standard error of 0.67 pA/pF occurred at a membrane potential of 0 mV.

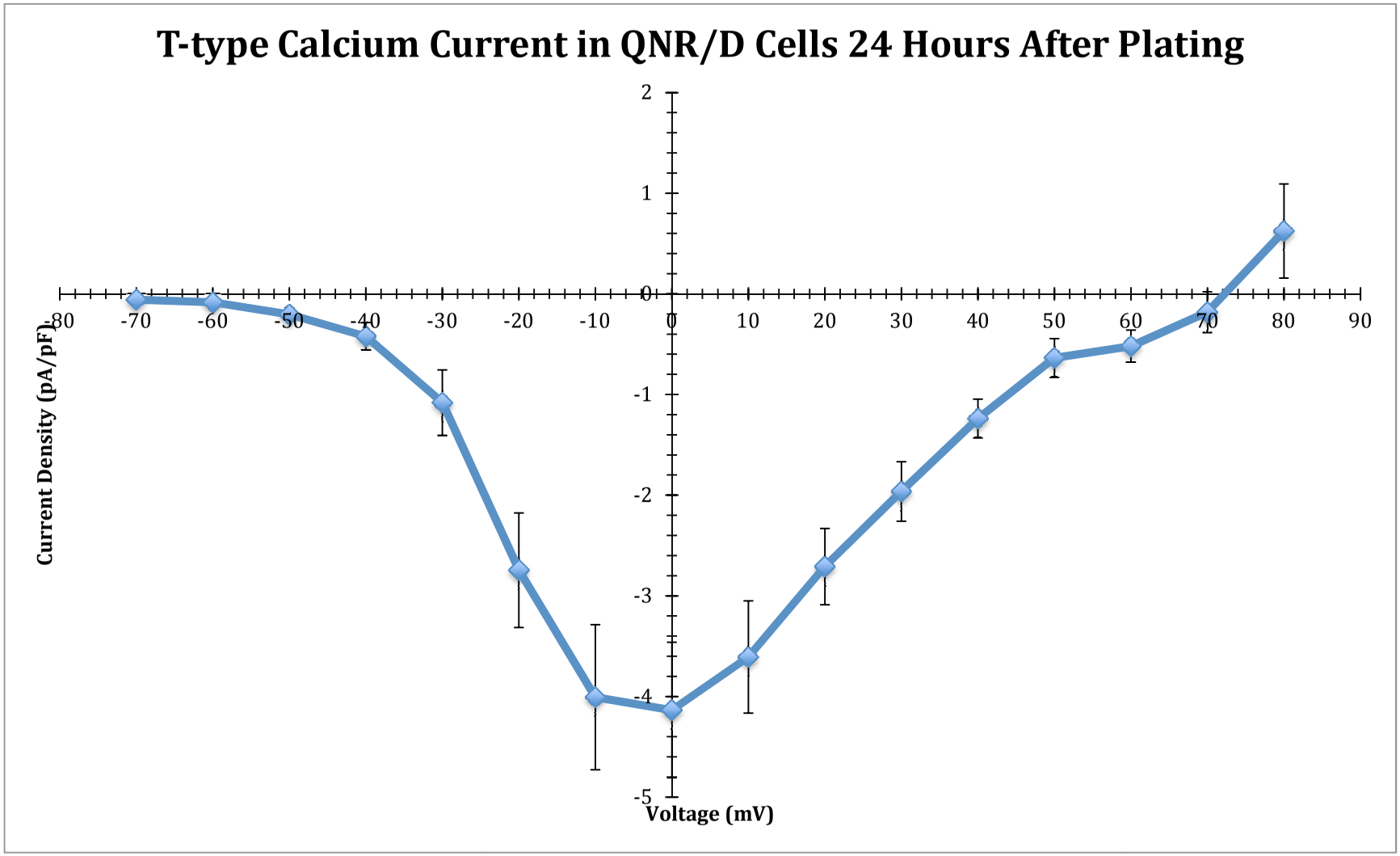
T-type Calcium Current in QNR/D Cells 24 Hours After Plating
Current Density (pA/pF)
Voltage (mV)
2
1
0
-1
-2
-3
-4
-5
-80
-70
-60
-50
-40
-30
-20
-10
0
10
20
30
40
50
60
70
80
90

Figure 14: Calcium Currents in N1E-115 Cells After 6 Days of DMSO Exposure This chart illustrates the relationship between voltage and Ca^{2+} current density recorded from N1E-115 cells after 6 days of DMSO exposure. The total Ca^{2+} (blue line), the T-type current (red line) and the L-type current (green line) are depicted in the chart. Each data point represents the average current density recorded from 5 cells. Shifting the holding potential to -40 mV, a potential that inactivates all T-type channels, isolated the L-type current. The T-type current was then calculated by subtracting the L-type current from the total current. Each data point represents the average current density recorded from 5 cells. Current density is calculated by dividing the total current by the cell capacitance. T-type current activation occurred at -50 mV and peak T-type current was achieved at -20 mV. In contrast, L-type current activation occurred at -20 mV and peak L-type current was achieved at 20 mV.

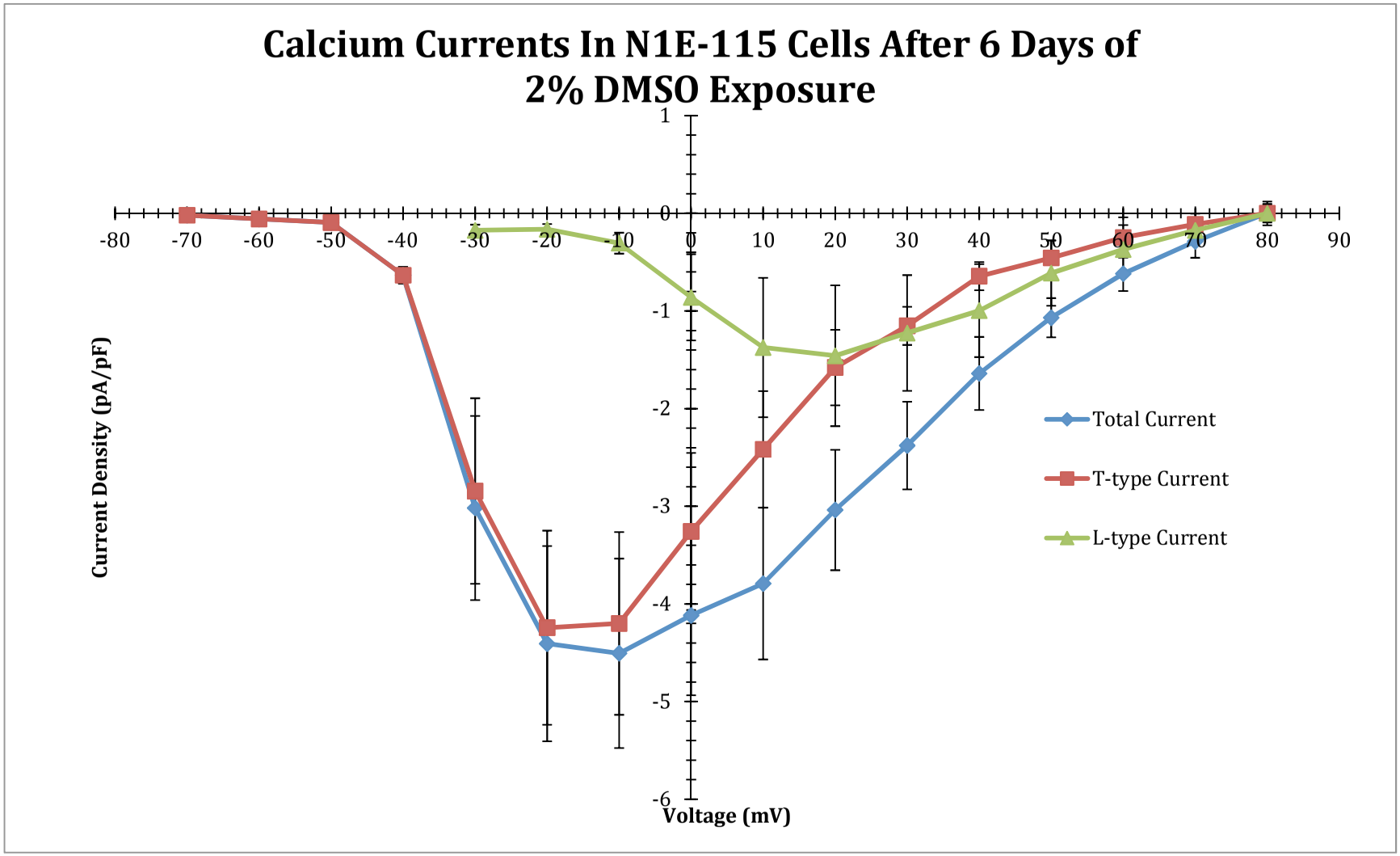
Calcium Currents In N1E-115 Cells After 6 Days of 2% DMSO Exposure
Current Density (pA/pF)
Voltage (mV)
1
0
-1
-2
-3
-4
-5
-6
-80
-70
-60
-50
-40
-30
-20
-10
0
10
20
30
40
50
60
70
80
90
Total Current
T-type Current
L-type Current

Figure 15: Steady State Inactivation of Voltage-gated Calcium Channels Expressed in QNR/D Cells This chart illustrates the fraction of the total current generated from increasing holding potentials. Each data point represents the fraction of total current density recorded from 5 cells 24 hours after plating. The curve generated by the data points (blue line) can be described by the Boltzmann function (red line),

$$I = I_{max} / [1 + \exp((V_{mid} - V)/V_c)]$$

where: I is the faction of maximum current,

I_{max} is the maximum current,

V is the holding potential,

V_{mid} is the holding potential at which half-maximal current is observed and

V_c is the voltage required to change I e-fold

The values for each of these coefficients are presented in Table 4.

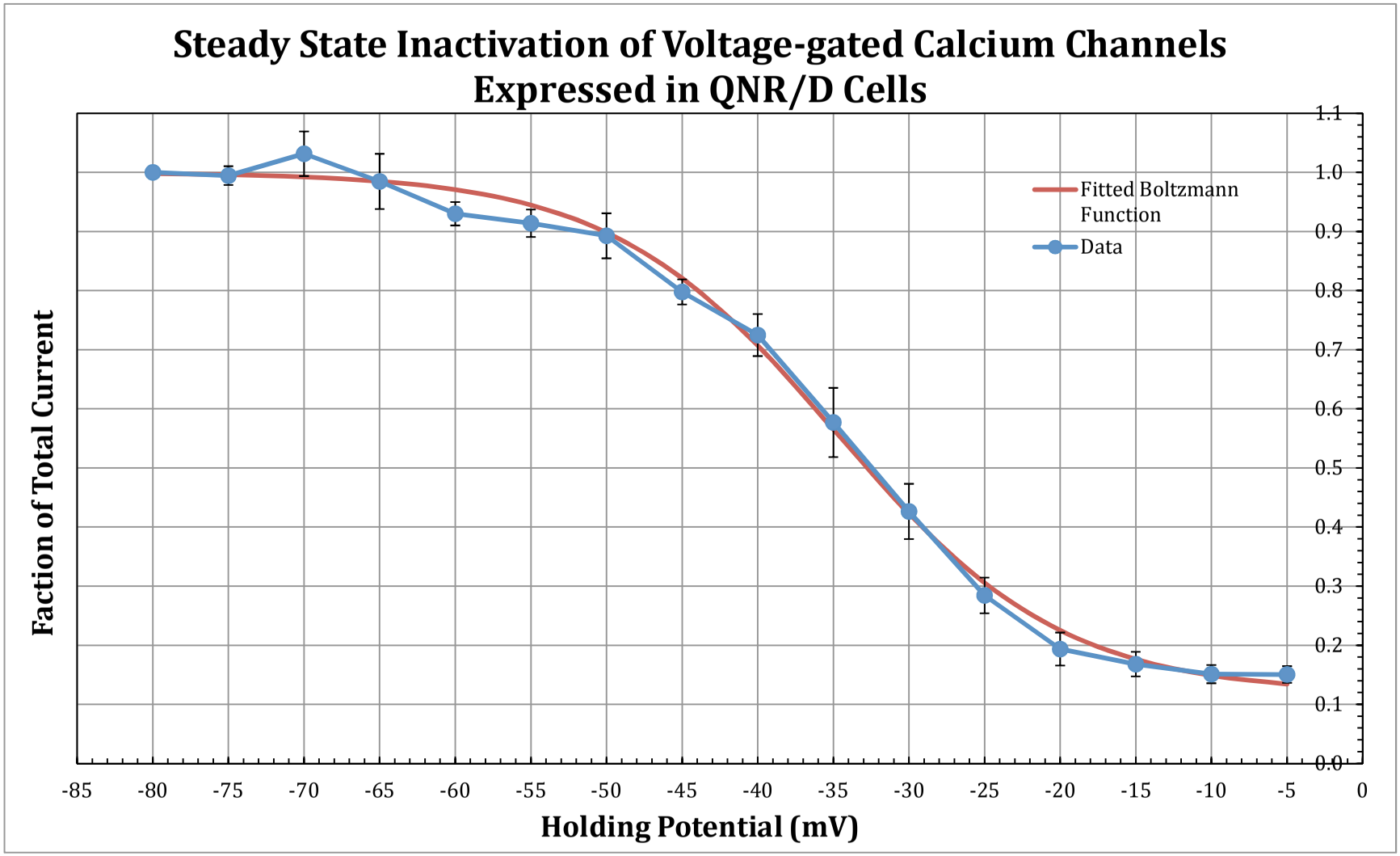
Steady State Inactivation of Voltage-gated Calcium Channels Expressed in QNR/D Cells
Faction of Total Current
Holding Potential (mV)
Fitted Boltzmann Function
Data
1.1
1.0
0.9
0.8
0.7
0.6
0.5
0.4
0.3
0.2
0.1
0.0
-85
-80
-75
-70
-65
-60
-55
-50
-45
-40
-35
-30
-25
-20
-15
-10
-5
0

Figure 16: Potassium Currents in QNR/D Cells K^+ currents were recorded from QNR/D cells 24 hours after plating. Cells were bathed in a physiological solution and patch clamped in whole cell voltage clamp configuration. X-axis scale units are ms, Y-axis scale units are pA. A) The membrane potential was held at -80 mV and stepped to 80 mV in 10 mV increments. Voltage steps to -30 mV, 30 mV, 40 mV, 50 mV, 60 mV, 70 mV and 80 mV visible. Note the transient duration of the current. B) The membrane potential was held at -40 mV and stepped to 80 mV in 10 mV increments. Voltage steps to -30 mV, 30 mV, 40 mV, 50 mV, 60 mV, 70 mV and 80 mV visible. Note the sustained duration of the current.

A)

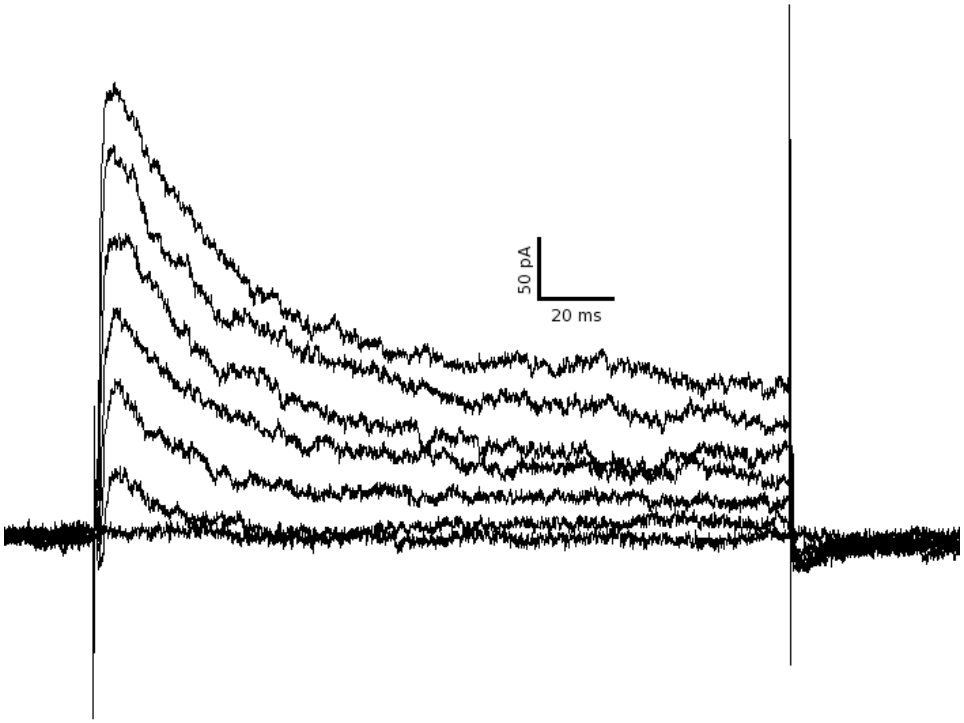

B)

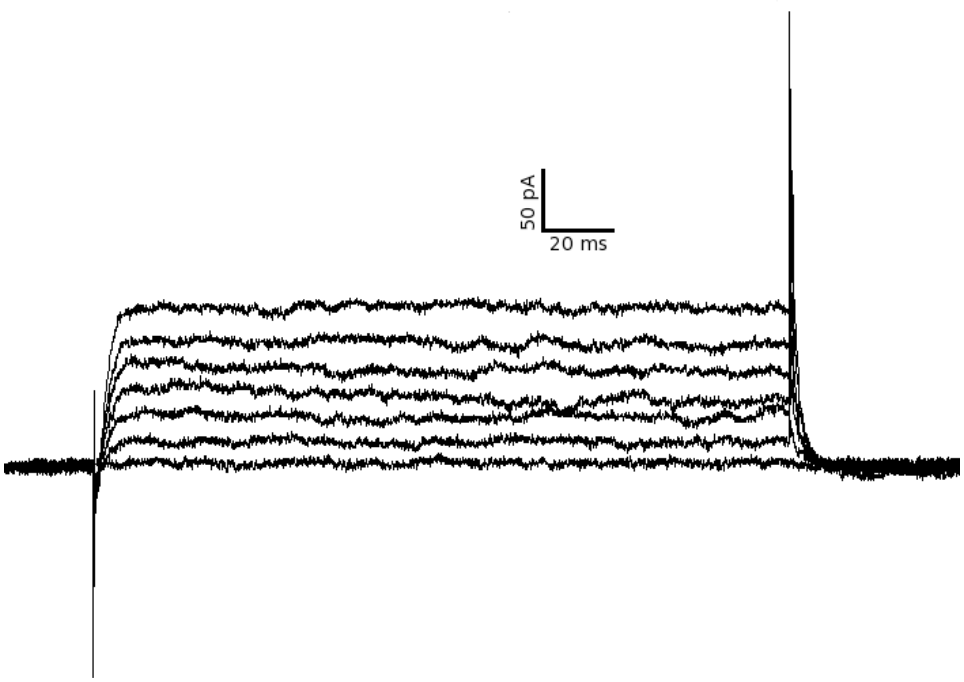

Figure 17: Potassium Currents in QNR/D Cells 24 Hours After Plating This chart illustrates the relationship between voltage and K^+ current density recorded from QNR/D cells 24 hours after plating. The total K^+ (blue line), the delayed rectifier current (green line) and the A-type current (red line) are depicted in the chart. The delayed rectifier current was isolated by shifting the holding potential to -40 mV, a potential that inactivates all A-type channels. The A-type current was then calculated by subtracting the delayed rectifier current from the total current. Each data point represents the average current density recorded from 8 cells. Current density is calculated by dividing the total current by the cell capacitance. A peak total current density of 5.94 pA/pF with a standard error of 1.37 pA/pF occurred at a membrane potential of 80 mV. A peak delayed rectifier current density of 1.17 pA/pF with a standard error of 0.78 pA/pF occurred at a membrane potential of 80 mV. A peak A-type current density of 4.77 pA/pF with a standard error of 1.05 pA/pF occurred at a membrane potential of 80 mV.

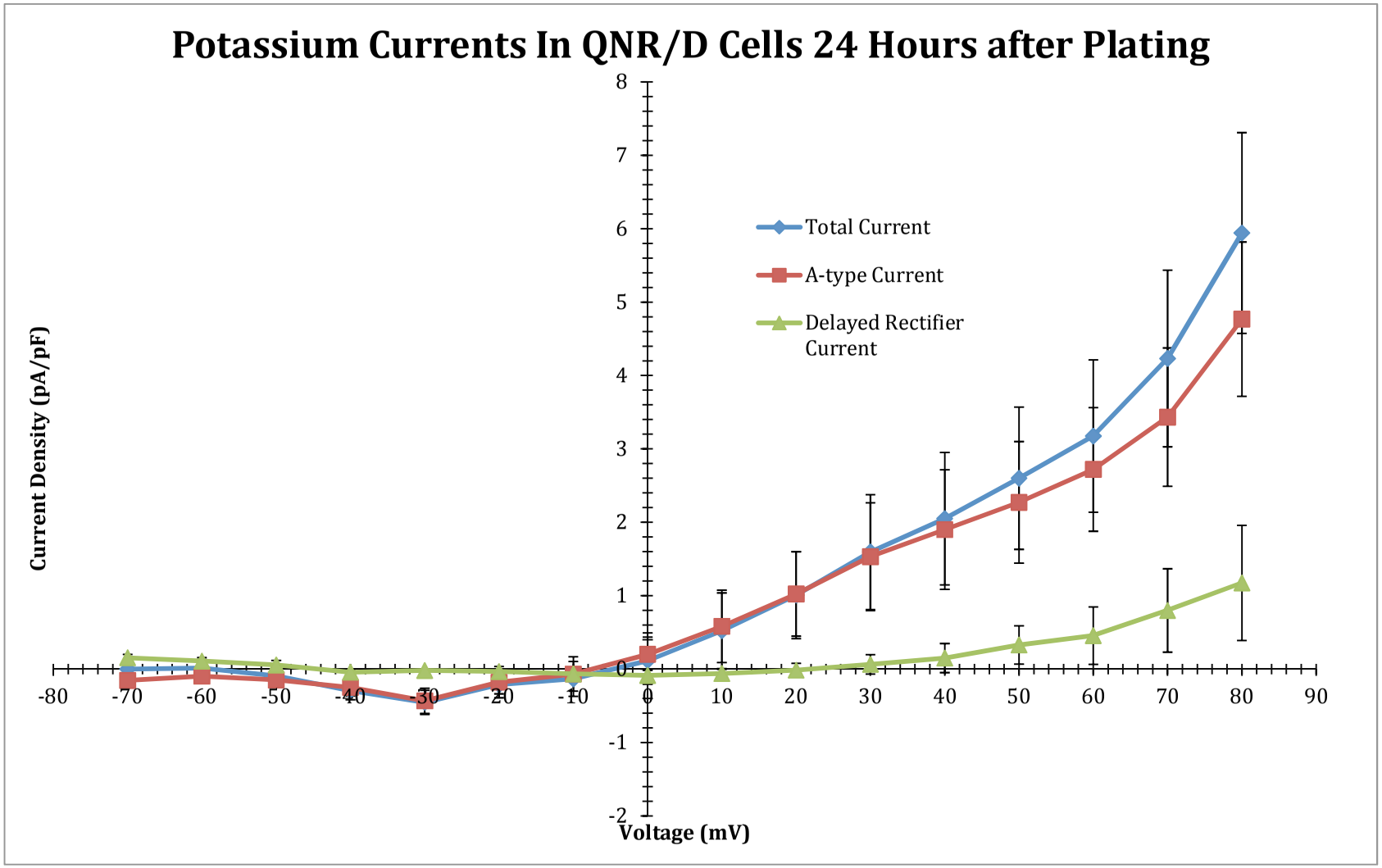
Potassium Currents In QNR/D Cells 24 Hours after Plating
Total Current
A-type Current
Delayed Rectifier Current
Current Density (pA/pF)
Voltage (mV)
8
7
6
5
4
3
2
1
0
-1
-2
-80
-70
-60
-50
-40
-30
-20
-10
0
10
20
30
40
50
60
70
80
90

Figure 18: Input Resistance Measured in QNR/D Cells in Response to Growth Hormone Treatment The data was generated by taking the mean input resistance of 8 cells for each time point. Baseline input resistance of QNR/D cells was measured to be 2.83 GΩ with a standard error of 0.612 GΩ. At each of these time points the average input resistance of GH treated cells was within error of both control and baseline levels.

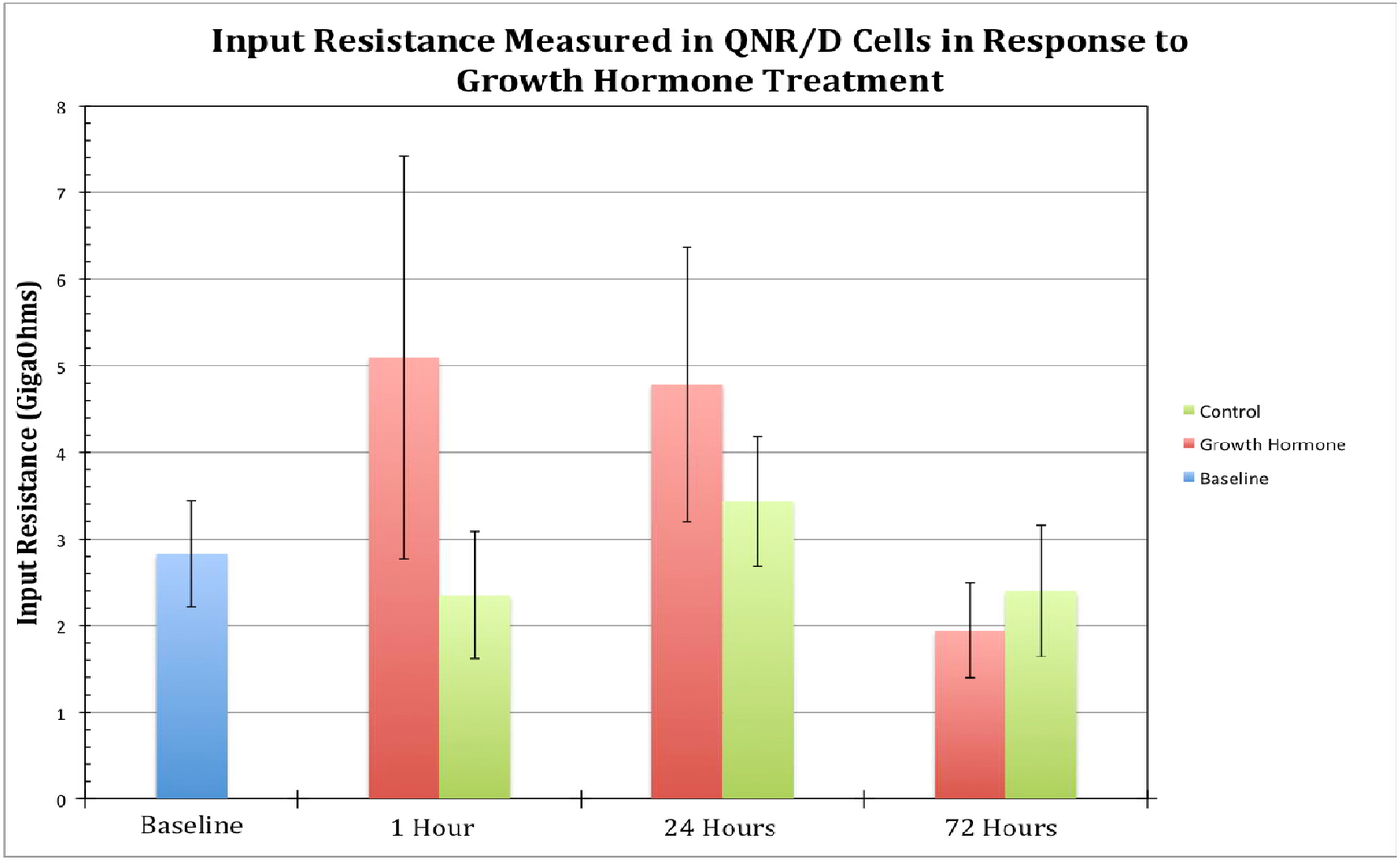
Input Resistance Measured in QNR/D Cells in Response to Growth Hormone Treatment
Input Resistance (GigaOhms)
0
1
2
3
4
5
6
7
8
Baseline
1 Hour
24 Hours
72 Hours
Control
Growth Hormone
Baseline

Figure 19: The Peak T-type Current Densities Recorded from QNR/D Cells in Response to Growth Hormone Treatment The data was generated by taking the mean peak T-type Ca^{2+} current recorded from 12 cells for each time point. Baseline peak T-type current of QNR/D cells was measured to be -4.13 pA/pF with a standard error of 0.67 pA/pF. At each of these time points the average peak T-type Ca^{2+} current recorded from GH treated cells was within error of both control and baseline levels.

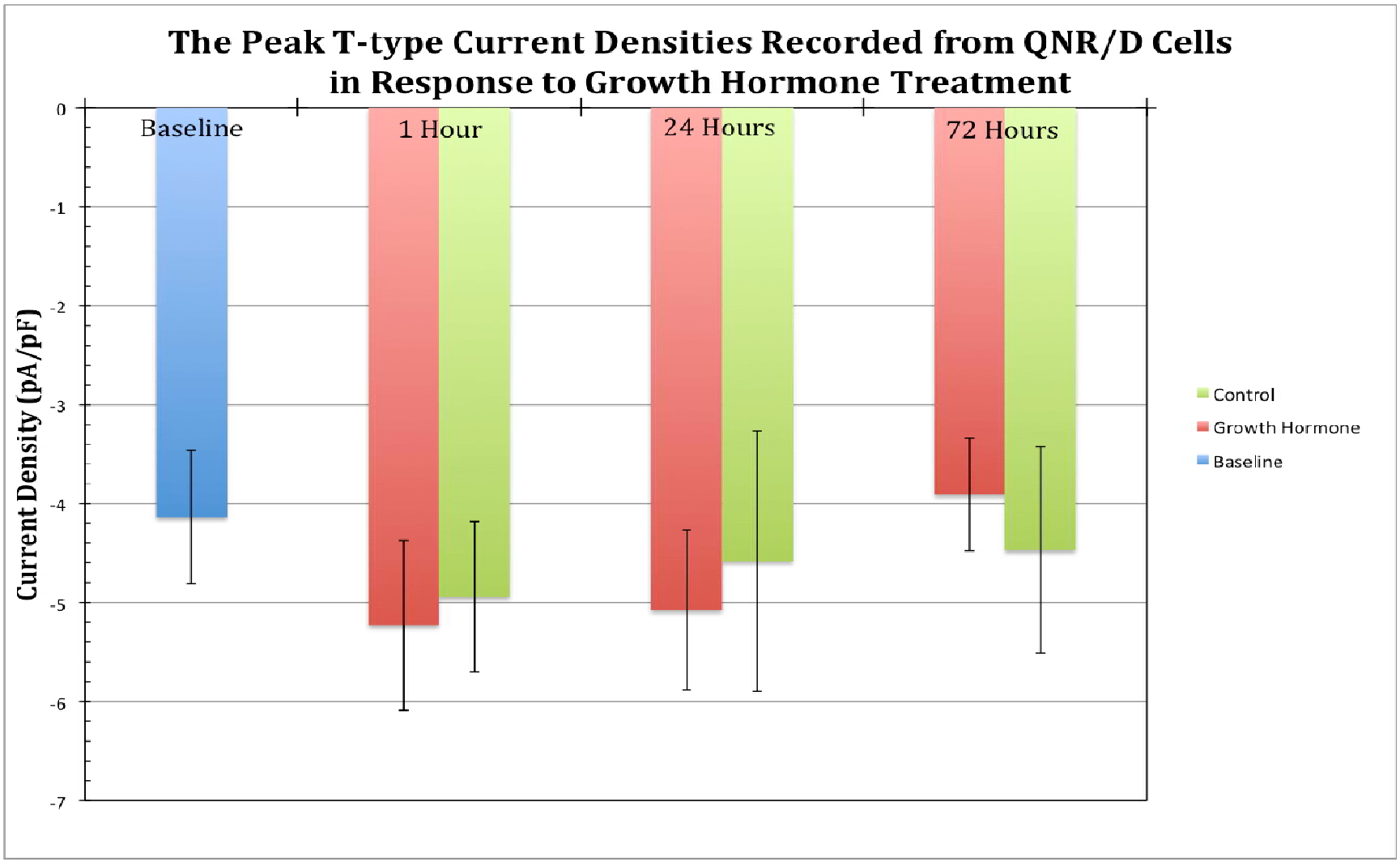
The Peak T-type Current Densities Recorded from QNR/D Cells in Response to Growth Hormone Treatment
Current Density (pA/pF)
0
-1
-2
-3
-4
-5
-6
-7
Baseline
1 Hour
24 Hours
72 Hours
Control
Growth Hormone
Baseline

Figure 20: The T-type Current Density in N1E-115 Neuroblastoma Cells After 48 Hours of Growth Hormone Treatment This chart illustrates the current voltage relationship of T-type Ca^{2+} in N1E-115 cells after 48 hours of GH treatment. The T-type Ca^{2+} current in GH treated cells (blue line) the T-type Ca^{2+} current in untreated control cells (red line) are depicted in the chart. The T-type Ca^{2+} current was isolated by shifting the holding potential to -40 mV, a potential that inactivates T-type Ca^{2+} channels in N1E-115 cells and subtracting the current at this holding potential from the total at the -80 mV holding potential. Each data point represents the average current density recorded from 12 cells. Current density is calculated by dividing the total current by the cell capacitance. A peak current density of -5.0 pA/pF with a standard error of 0.76 pA/pF occurred at a membrane potential of -10 mV in GH treated cells. A peak current density of -6.7 pA/pF with a standard error of 0.67 pA/pF occurred at a membrane potential of -20 mV in untreated control cells. The statistical significance of the difference between these curves was calculated to be 0.046 ($P<0.05$) by ANOVA with repeated measures.

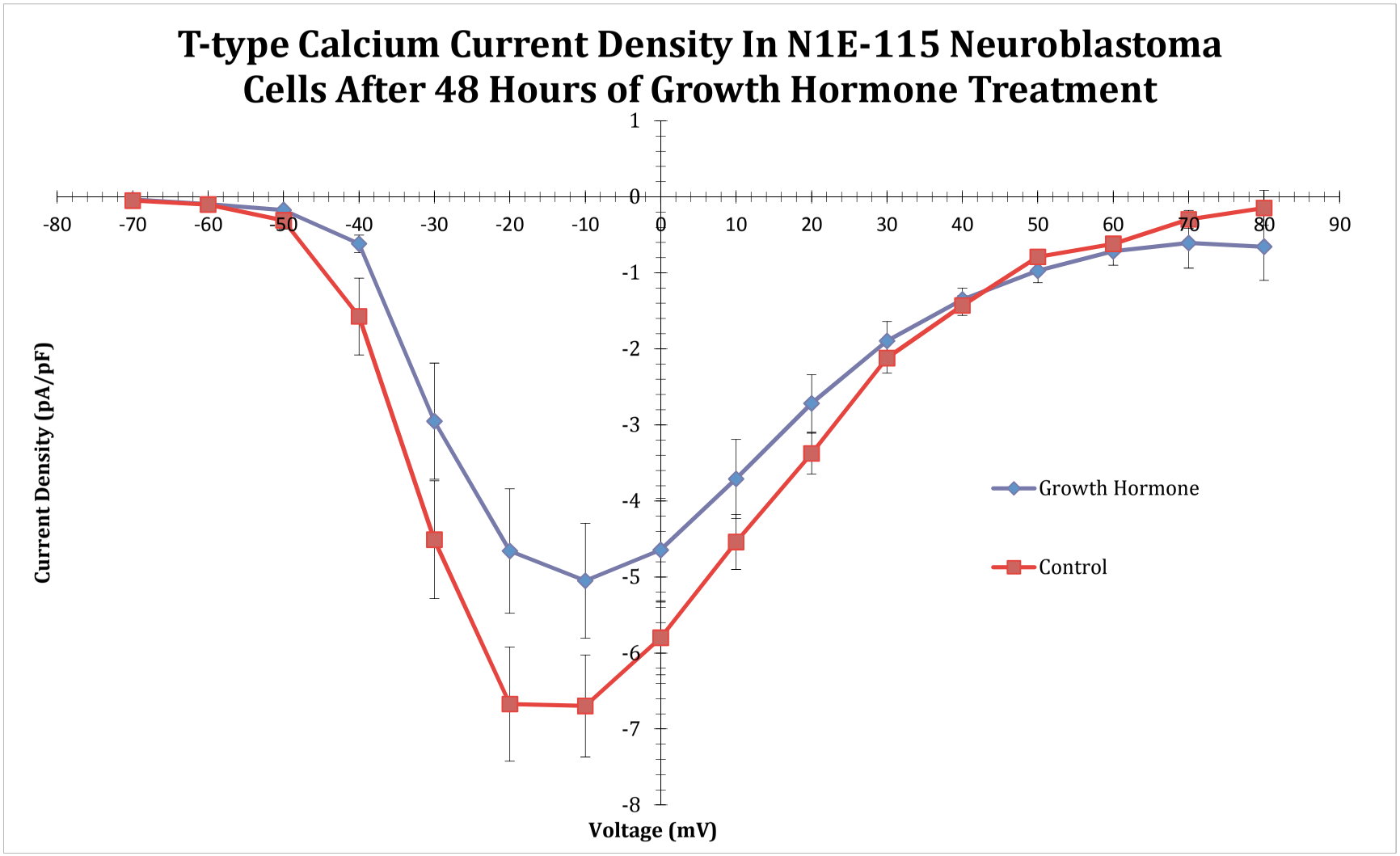
T-type Calcium Current Density In N1E-115 Neuroblastoma Cells After 48 Hours of Growth Hormone Treatment
Current Density (pA/pF)
Voltage (mV)
1
0
-1
-2
-3
-4
-5
-6
-7
-8
-80
-70
-60
-50
-40
-30
-20
-10
0
10
20
30
40
50
60
70
80
90
Growth Hormone
Control

Figure 21: The Peak Total Potassium Current Densities Recorded from QNR/D Cells in Response to Growth Hormone Treatment The data was generated by taking the mean peak total K^+ current recorded from 8 cells for each time point. Baseline peak total current of QNR/D cells was measured to be 5.94 pA/pF with a standard error of 1.37 pA/pF. At each of these time points the average peak total current recorded from GH treated cells was within error of both control and baseline levels.

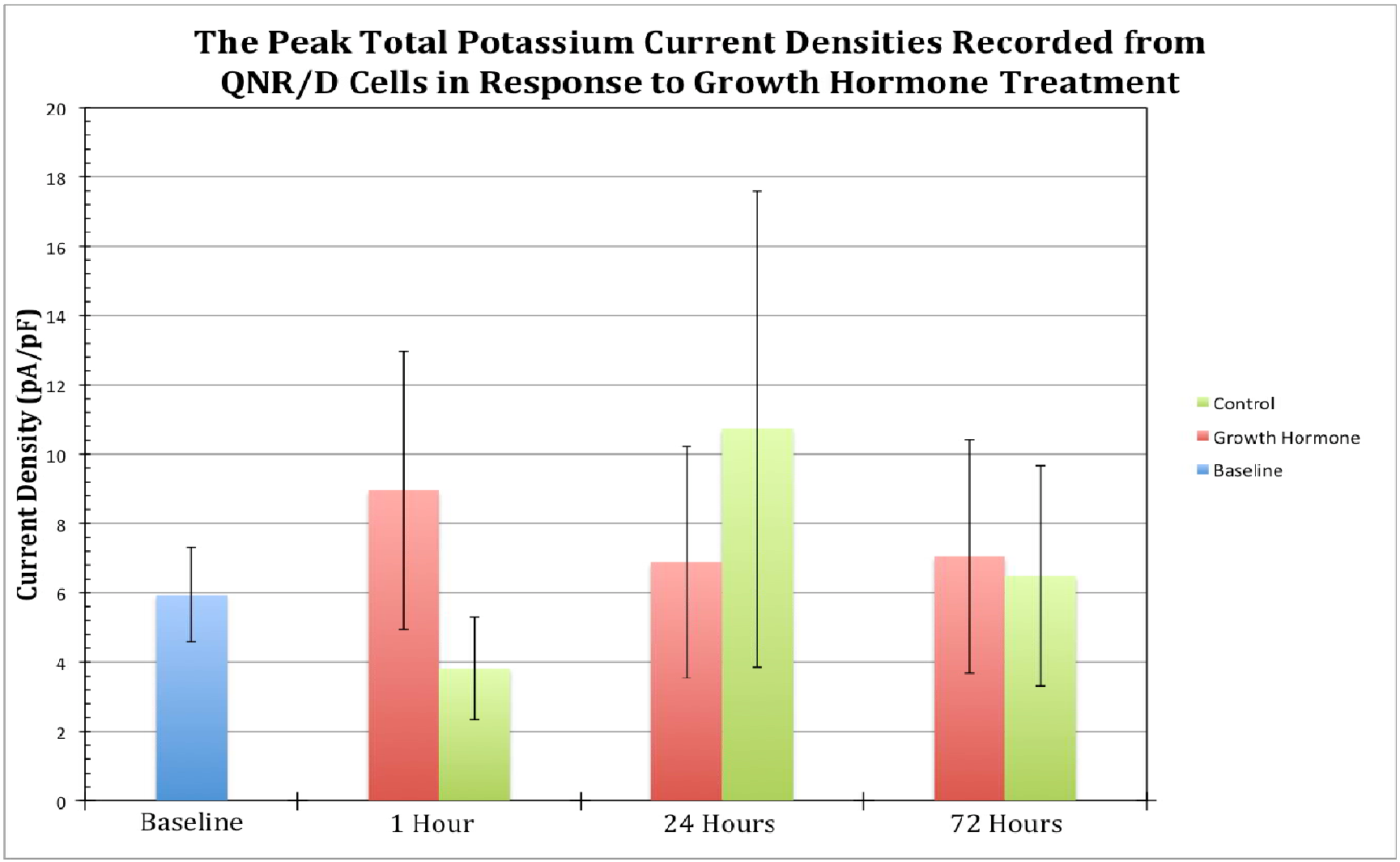
The Peak Total Potassium Current Densities Recorded from QNR/D Cells in Response to Growth Hormone Treatment
Current Density (pA/pF)
20
18
16
14
12
10
8
6
4
2
0
Baseline
1 Hour
24 Hours
72 Hours
Control
Growth Hormone
Baseline

Figure 22: The Peak A-type Potassium Current Densities Recorded from QNR/D Cells in Response to Growth Hormone Treatment The data was generated by taking the mean peak A-type K^+ current recorded from 8 cells for each time point. Baseline peak total current of QNR/D cells was measured to be 4.77 pA/pF with a standard error of 1.05 pA/pF. At each of these time points the average peak total current recorded from GH treated cells was within error of control levels.

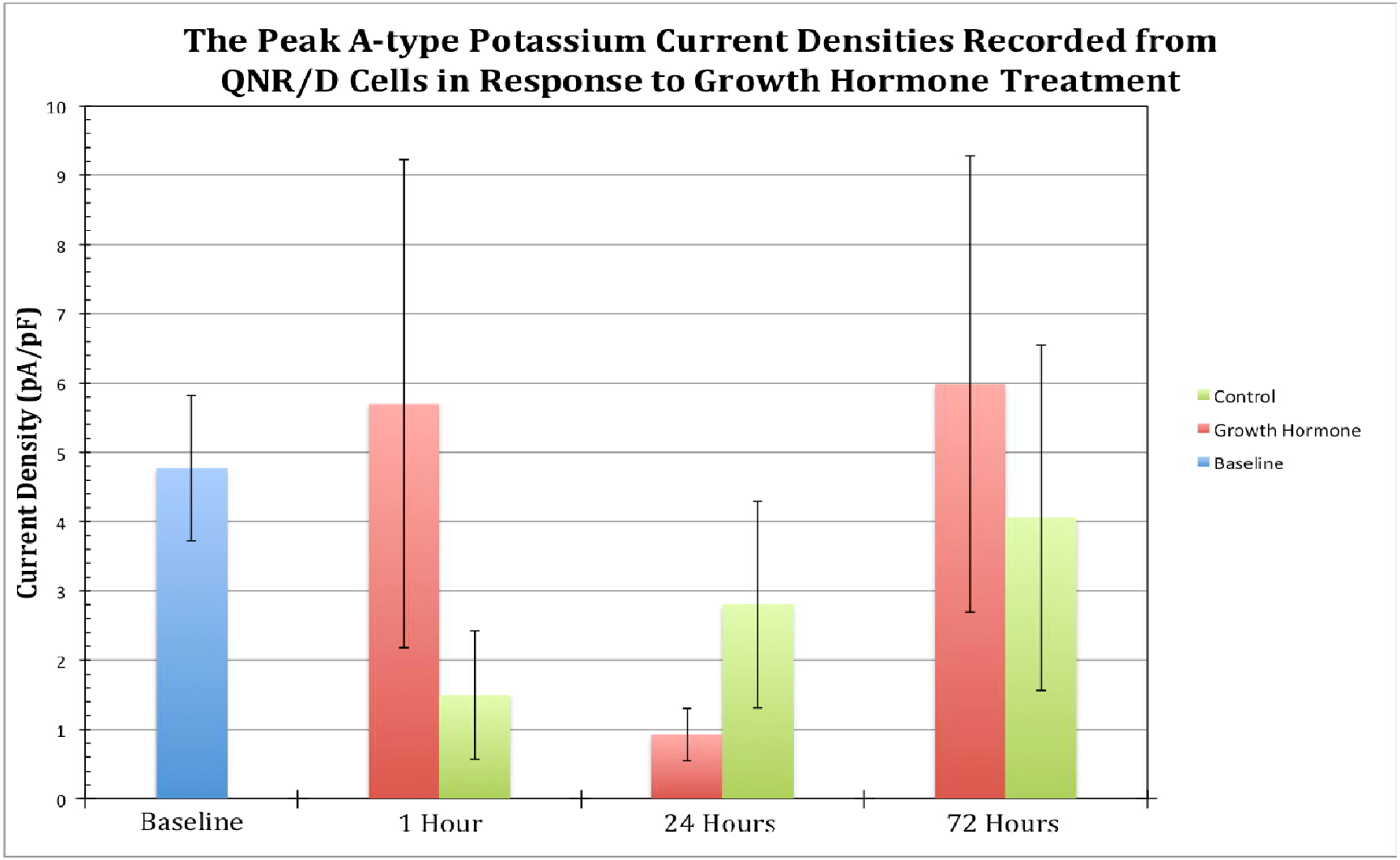
The Peak A-type Potassium Current Densities Recorded from QNR/D Cells in Response to Growth Hormone Treatment
Current Density (pA/pF)
10
9
8
7
6
5
4
3
2
1
0
Baseline
1 Hour
24 Hours
72 Hours
Control
Growth Hormone
Baseline

Figure 23: The Peak Delayed Rectifier Potassium Current Densities Recorded from QNR/D Cells in Response to GH Treatment The data was generated by taking the mean peak delayed rectifier K^+ current recorded from 8 cells for each time point. Baseline peak delayed rectifier current of QNR/D cells was measured to be 1.17 pA/pF with a standard error of 0.78 pA/pF. At each of these time points the average peak total current recorded from GH treated cells was within error of control levels.

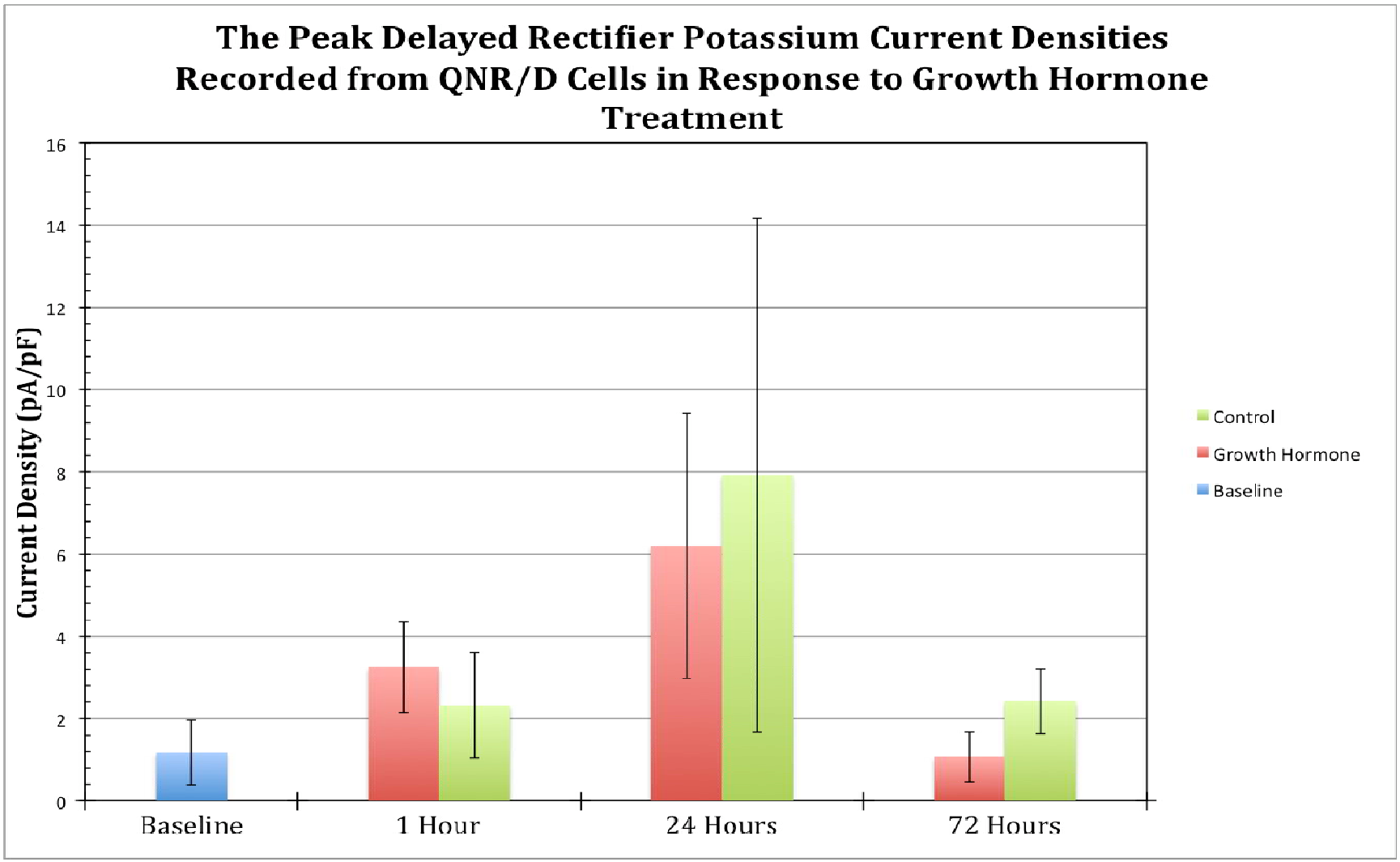
The Peak Delayed Rectifier Potassium Current Densities Recorded from QNR/D Cells in Response to Growth Hormone Treatment
Current Density (pA/pF)
16
14
12
10
8
6
4
2
0
Baseline
1 Hour
24 Hours
72 Hours
Control
Growth Hormone
Baseline

Table 4: The Coefficient Values of the Boltzmann Function Presented in Figure 15

Function Fitted	I_{max}	S.E.M.	V_{mid}	S.E.M.	V_c	S.E.M.	Correlation
Boltzmann Function: $I = I_{max} / [1 + \exp((V_{mid} - V)/V_c)]$ where: I is the faction of maximum current, I_{max} is the maximum current, V is the holding potential, V_{mid} is the holding potential at which half-maximal current is observed and V_c is the voltage required to change I e-fold	0.881985	0.02346	-34.786	0.57015	7.4730	0.52660	0.971741

References

1. Alvarez-Buylla A., Buskirk D.R. and Nottebohm F. Monoclonal antibody reveals radial glia in adult brain. *Journal of Comparative Neurology*. 264:159-170, 1987.

2. Alvarez-Buylla A., and Nottebohm F. Migration of Young Neurons in Adult Avian Brain. *Nature*, 335:353-354, 1988.

3. Hernandez-Sanchez C., Lopez-Carranza A., Alarcon C., De La Rosa E.J., and De Pablo F. Autocrine/paracrine Role of Insulin-Related Growth Factors in Neurogenesis: Local Expression and Effects on Cell Proliferation and Differentiation in Retina. *Proceeding of the National Academy of Science*, 92:9834-9838, 1995.

4. Jensen A.M. and Wallace V.A. Expression of Sonic Hedgehog and its Putative Role as a Precursor Cell Mitogen in the Developing Mouse Retina. *Development*, 124:363-371, 1997.

5. Kimhi Y., Palfrey C., Spector I., Barak Y. and Littauer U.Z. Maturation of neuroblastoma cells in the presence of dimethylsulfoxide. *Proceedings of the National Academy of Science*, 73:462–466, 1976.

6. McLoon S.C. and Barnes R.B. Early Differentiation of Retinal Ganglion Cells: An Axonal Protein Expressed by Premigratory and Migrating Retinal Ganglion Cells. *The Journal of Neuroscience*, 4:1424-1432, 1989.

7. Moolenaar W.H. and Spector I. Ionic currents in cultured mouse neuroblastoma cells under voltage-clamp conditions. *Journal of Physiology*, 278:265–286, 1978.

8. Pan Z.H. Differential Expression of High- and Two Types of Low-Voltage–Activated Calcium Currents in Rod and Cone Bipolar Cells of the Rat Retina. *Journal of Neurophysiology*, 83:513-527, 2000.

9. Pessac B., Girard A., Romey G., Crisanti P., Lorinet A.M. and Calothy G. A Neuronal Clone Derived From a Rous Sarcoma virus-transformed Quail Embryo Neuroretina Established Culture. *Nature*, 302:616-618, 1983.

10. Pimentel B., Sanz B., Varela-Nieto I., Rapp U.R., De Pablo F., and de la Rosa E.J. c-Raf Regulates Cell Survival and Retinal Ganglion Cell Morphogenesis during Neurogenesis. *The Journal of Neuroscience*, 20:3254–3262, 2000.

11. Pollerberg G.E., Kuschel C. and Zenke. Generation of Cell Lines from Embryonic Quail Retina Capable of Mature Neuronal Differentiation.

Journal of Neuroscience Research, 41:427–442, 1995.

12. Selleck A.J. and Bronner-Fraser M. Origins of the Avian Neural Crest: the Role of Neural Plate-Epidermal Interactions. *Development*, 121:525-538, 1995.

13. Serafini T., Colamarino S.A., Leonardo E.D., Wang H., Beddington R., Skarnes W.C. and Tessier-Lavigne M. Netrin-1 is required for commissural axon guidance in the developing vertebrate nervous system. *Cell*, 87: 1001–1014, 1996.

CHAPTER FOUR

GENERAL DISCUSSION AND CONCLUSIONS

Expression of Retinal Ganglion Cell Markers in QNR/D Cells

In these studies, QNR/D cells were explored as a possible avian RGC model. Their suitability is validated by the expression of RGC markers by these cells. The expression of a number of RGC markers was assessed by immunocytochemistry. These markers not only confirm the identity of the QNR/D cell line as derived from a quail RGC precursor but also indicate the level of developmental maturity of these cells. First and foremost, QNR/D cells are immunoreactive with Q¢PN antibody. This unequivocally establishes QNR/D cells as a quail derived cell line. This is an important determination in light of the current controversy surrounding the species origin of the RGC-5 cell line (Van Bergen *et al*, 2009). Furthermore, the strictly nuclear distribution of Q¢PN staining is as expected and establishes the credibility of the technique used for immunocytochemistry experiments.

The QNR/D cells were also immunoreactive for the R4A antigen. The R4A antibody recognizes RGC precursor cells immediately after their final cell division (Mcloon and Barnes, 1989) and as they migrate to the vitreal surface of the developing retina. Indeed, the creators of this antibody have described its antigen as "the earliest ganglion cell characteristic to develop yet reported" (Mcloon and Barnes, 1989). This suggests the R4A antibody recognizes RGC competent precursors. Furthermore, as RGCs mature the distribution of R4A immunoreactivity become restricted to RGC axons in the nerve fibre layer. In QNR/D cells, R4A immunoreactivity was present throughout the cytoplasm and

was not restricted to QNR/D neurites. This observation suggests that these cells are not mature or fully differentiated.

The expression of the Isl-1 transcription factor was also assessed by immunocytochemistry. This transcription factor is first expressed in RGC precursors at the specificity stage of their differentiation (Pan *et al*, 2008). In QNR/D cells Isl-1 immunoreactivity was present in both the cytoplasm and nucleus with especially intense staining in the nucleus. This distribution is as expected since Isl-1 transcription factor is produced in the cytoplasm and then transported and concentrated in the nucleus where it fulfills its physiological role. Furthermore, this is the same distribution observed when Isl-1 staining is performed on immunopanned chick RGCs (Sanders *et al*, 2009).

The expression of intermediate filaments in QNR/D cells was also investigated by immunocytochemistry. Vimentin distribution was clearly of a filamentous nature, showing that indeed it is functioning in a cytoskeletal capacity. Neurofilament protein expression however was not present in a filamentous distribution, suggesting that these proteins are being translated but not assembled into the cytoskeleton. These intermediate filament expression patterns suggest that QNR/D cells, though not fully differentiated RGCs, are primed for if not in the process of complete differentiation. Intermediate filament expression is significant because during RGC differentiation the predominant cytoskeletal proteins change from vimentin to neurofilament proteins (Alvarez-Buylla and Nottebohm, 1988; Pollerberg *et al*, 1995).

When analyzed together, the results of these immunocytochemical

experiments suggest that QNR/D cells are representative of differentiating RGC precursors in the specificity stage of their differentiation process.

Growth Hormone and Growth Hormone Receptor Expression in QNR/D Cells

The expression of both GH and GHR was observed in QNR/D cells. In both cases, immunocytochemistry showed a diffuse expression pattern throughout the cytoplasm. In the developing chick retina, GH is expressed in two different isoforms (Harvey, 2010). There is a 15-kDa isoform that is translated from mRNA identical to that which encodes the classical 22-kDa pituitary GH but the full-length protein is then proteolytically cleaved to yield a 15-kDa product. In addition, scGH is also expressed in the chick retina. This GH isoform is translated from a smaller, truncated mRNA, resulting in a protein that lacks the signal sequence required for secretion. Therefore, this isoform, if active, must signal via an intracrine mechanism. By comparison, the GH expressed in QNR/D cells is also a small isoform of approximately 15-kDa (Sanders *et al*, 2010). This isoform is likely to be derived from the GH mRNA present in these cells, which has greater than 98% homology with chicken GH mRNA (Sander et al, 2010). A siRNA directed towards chicken GH mRNA is thus able to knockdown the expression of the GH in QNR/D cells (Sanders *et al*, 2010). Furthermore, sequencing of the GH mRNA in the quail pituitary did not reveal a second truncated transcript, so it is unlikely that a scGH-like protein is present in QNR/D cells.

Electrophysiological Properties of QNR/D Cells

A number of the electrophysiological properties displayed by QNR/D cells

are consistent with developing RGCs. QNR/D cells exhibited a high input resistance, similar to that observed in mouse and rat RGCs prior to synaptogenesis with their CNS targets (Rothe *et al*, 1999; Reiff and Guenther, 1999). This high input resistance is due to low levels of ion channel expression in both RGCs and QNR/D cells. Specifically, Na^+ channels are not expressed, HVA Ca^{2+} channels are not expressed and K^+ channel expression is present at low levels or is absent in this cell line. This expression pattern has many important implications when considering the QNR/D cells line as an experimental model of RGCs.

It can be concluded that voltage-gated Na^+ channels are not expressed in QNR/D cells. Under voltage clamp conditions, Na^+ currents could not be elicited by membrane depolarization in a physiological bathing solution. Furthermore, under current clamp conditions no action potentials were observed upon current injections. This observation is curious since Pessac *et al* reported recording tetrodotoxin sensitive action potentials from QNR/D cells (Pessac *et al*, 1983). This indicates the presence of Na^+ channels since they are prerequisite for both action potentials and tetrodotoxin sensitive currents. Since these spiking observations were made in 1983, nearly 30 years ago, one possible explanation of this inconsistency is selective death of the more electrically active cells over this time period.

Examination of Ca^{2+} currents in QNR/D cells revealed only a single current type, which displayed characteristics of T-type Ca^{2+} channel derived currents. They activate at highly negative membrane potentials, rapidly inactivate and slowly deactivate, resulting in large tail-currents. Most conclusively, the

activity of these channels is blocked by mibefradil, a T-type specific Ca^{2+} channel antagonist. This Ca^{2+} channel expression pattern is consistent with that of avian RGC cells at ED7, the age at which the QNR/D cell line was immortalized. T-type Ca^{2+} channels are the first Ca^{2+} channels expressed in RGCs. They are expressed just as RGC axons reach their CNS targets at ED16 in the rat (Schmid and Guenther, 1996; Schmid and Guenther, 1999), which corresponds to approximately ED6 in the chick. HVA Ca^{2+} channels (L-type) are not expressed until ED20 in the rat (Schmid and Guenther, 1996; Schmid and Guenther, 1999), just before birth and well after the onset of dendritic outgrowth and arbourization. As the retina matures, HVA current begins to dominate the total Ca^{2+} current and by maturity the Ca^{2+} channels expressed are almost exclusively HVA (Schmid and Guenther, 1996; Schmid and Guenther, 1999).

K^+ channel expression in QNR/D cells was highly variable. Cells exhibited either A-type current, delayed rectifier current, a mixture of both or no current at all. This is reflected in the high degree of error displayed in the K^+ current histograms. Furthermore, when K^+ channels were expressed, they were present only at very low levels compared to mature RGCs, as shown by the small current densities. Again, this ion channel expression is typical of RGC precursors at ED17 in the rat (Reiff and Guenther, 1999). This is the time point at which RGC axons have just reached their CNS targets and corresponding to approximately ED6 in the chick. The presence of K^+ currents in some QNR/D cells but not others may indicate different levels of maturation/differentiation. This contention is supported by the pattern of voltage-gated K^+ channel

expression during development. As RGCs differentiate, they initially do not express voltage-gated K^+ channels (Reiff and Guenther, 1999; Skaliora *et al*, 1995). Then, once their axons have reached their central targets, RGCs proceed to express primarily A-type K^+ channels (Reiff and Guenther, 1999; Skaliora *et al*, 1995). Finally, at maturity, the delayed rectifier channel dominates K^+ channel expression (Reiff and Guenther, 1999; Skaliora *et al*, 1995). This pattern also holds true in a cell line context since RGC-5 cells display increased delayed rectifier K^+ currents upon differentiation by staurosporine (Frassetto *et al*, 2006).

These electrical characteristics of QNR/D cells are consistent with RGC precursors in the specificity stage of differentiation. The foremost inadequacy of this cell line, when used as an RGC model, is the lack of inward Na^+ current and the inability to fire action potentials. That being said, from an electrophysiological perspective, the QNR/D cell line is a much better model than the RGC-5 cell line since these cells not only lack any voltage-gated ion channel expression but also express un-gated inwardly rectifying K^+ channels, Cl^- channels and Gd^{3+} insensitive stretch-gated channels (Moorehouse *et al*, 2004). These ion channels are atypical of both mature and developing RGCs (Moorehouse *et al*, 2004) and it is significant to note that QNR/D cells do not express these inappropriate currents. QNR/D do not express any significant inwardly rectifying K^+ channels since the current-voltage relationship in Figure 11 clearly displays outward rectification. Nor do they express Cl^- channels. The high input resistance observed in QNR/D cells under voltage clamp conditions in a Cl^- rich environment contraindicates the presence of Cl^- channels. Clearly, from an electrophysiological perspective,

QNR/D cells are a better model of RGCs than RGC-5 cells.

The Effect of Growth Hormone on Ion Channel Expression in QNR/D Cells

The presence of GH and GHR in QNR/D cells suggests GH might have local electrophysiological actions in these cells, especially as GH had electrophysiological effects in GH- and GHR-positive N1E-115 cells and in the chicken brain (Lea and Harvey, 1993). However, while GH is active in promoting cell survival in QNR/D cells (Sanders *et al*, 2010), it had no electrophysiological action. This could be due to a number of factors. (1) The GH signalling system in these cells may be saturated, (2) the tyrosine kinase activity of the V-Src protein may be saturating the second messenger cascades that are required for exogenous GH signal transduction and (3) GH signalling may not modulate ion channel expression in QNR/D cells.

The level of endogenous GH expression by QNR/D cells may already saturate their GHRs. It is possible that the GH signalling system in QNR/D cultures operates in an intracrine fashion where GH binds GHR from within the secretory apparatus of the cell that synthesizes both proteins. It has been demonstrated that when both GH and GHR are synthesized within the same cell, GH-GHR binding occurs within the endoplasmic reticulum and prevents exogenous GH from binding GHR once the receptor reaches the plasma membrane (Van Den Eijnden and Strous, 2007). This intracrine saturation hypothesis is supported by intracellular distribution of GH and GHR. Both GH and GHR proteins detected by immunocytochemistry were not localized along the plasma membrane. Instead these proteins exhibited a diffuse intracellular

expression pattern. Furthermore, all of the observed effects of GH activity in these cells have been elicited by knockdown of endogenous GH (Sanders *et al*, 2010). Therefore, it is possible that the endogenous GH produced by QNR/D cells is preventing the activity of the exogenous GH applied in these experiments.

It is also important to recognize the fact that QNR/D cells are immortalized by the Rous sarcoma virus. This virus owes its oncogenic and immortalizing effects to a constitutively active v-Src protein tyrosine kinase encoded by a viral gene that has been integrated into the quail genome. This protein phosphorylates the tyrosine residues of intracellular signaling proteins, many of which are employed by the GH second messenger cascade. Most significantly, Src proteins initiate a chain of phosphorylation events by activating both ERK1 and ERK2 MAPK pathways (Zhu *et al*, 2002), as well as PI3K/Akt pathways (Liu *et al*, 1998), roles normally fulfilled by GH activated c-Src in non-transformed cells. Furthermore, v-Src has been shown to constitutively activate both Stat-3 and Stat-5, which are also normally activated by GH signaling (Rane and Reddy, 2002). This suggests that the signal transduction apparatus normally employed by GH is saturated by v-Src, thereby masking the effects of exogenous GH application.

Finally, the null hypothesis may be true. GH may not have any effect on ion channel expression in QNR/D cells.

Future Directions

The expression of a number of retinal ganglion cell markers and several types of voltage-gated ion channels makes the QNR/D cell line a useful model of

RGCs. The value of these cells as a model is further emphasized by the lack of availability of an avian Thy-1 reactive antibody, the scarcity of which makes the establishment of a RGC enriched primary culture impractical.

However, the QNR/D cell line model could be improved upon if these cells could be induced to express a phenotype that is characteristically more neural. In fact, a number of neural cell lines can be induced to differentiate by the application of a specific factor. For instance, N1E-115 cells do not express the entire range of ion channels normally present in a mature neuron but, upon exposure to DMSO, they differentiate into a mature phenotype that expresses more ion channel types and greater current densities (Moolenaar and Spector, 1978). Similarly, action potentials cannot be elicited in PC-12 cells in normal culture conditions but can be achieved after nerve growth factor (NGF) treatment (Dichter *et al*, 1977). Even more germane, it has been reported that delayed rectifier K^+ channel expression can be induced by the application of staurosporine, a non-selective protein kinase inhibitor, in the RGC-5 cell line (Frassetto *et al*, 2006). This "differentiation" effect has been replicated using the tyrosine kinase specific inhibitor succinyl-conanavalin A (Wood *et al*, 2010). Application of a tyrosine kinase inhibitor may initiate a differentiation process in QNR/D cells and induce greater ion channel expression and/or increased responsiveness to GH. If some neurotrophic agent can be found to induce Na^+ channel expression and the ability to generate action potentials in QNR/D cells, it would make these cells an ideal model of RGCs.

There are also a number of future directions for the study of GH activity in

QNR/D cells. Due to the possibility that GH signalling mechanisms may be saturated, the effect of GH would be better elucidated by methods that inhibit GH signalling rather than potentiate it. GH knock down by RNA interference has been shown to increase apoptosis in QNR/D cells (Sanders *et al*, 2010). This observation is in agreement with the well-established anti-apoptotic effects of GH in primary cultures as well as *in ovo*. Perhaps an electrophysiological effect of GH would be revealed using this approach.

Another avenue of research in the electrophysiological activities of QNR/D is the effect of GHRH. In the pituitary GHRH not only stimulates GH synthesis but also controls its release by modulation of voltage-gate calcium channels. It is possible GHRH functions in a similar capacity in the QNR/D cell line. It has already been determined that GHRH is expressed in QNR/D cells where it promotes the transcription of GH mRNA (Harvey *et al*, 2012). However the role of GHRH on voltage-gated ion channel activity has not been explored in QNR/D cells.

Conclusions

The electrophysiological properties of QNR/D cells have been characterized. Briefly, no Na^+ current or spiking activity was observed but T-type Ca^{2+} current, and both A-type and delayed rectifier K^+ currents were expressed. These currents, unexpectedly, were not affected by exposure to exogenous GH. However, since these cells express GH and GHR and respond to endogenous GH by increased cell survival, QNR/D cells provide an experimental model for investigating the physiology of RGCs in the neural retina of the chick embryo.

References

1. Alvarez-Buylla A., and Nottebohm F. Migration of Young Neurons in Adult Avian Brain. *Nature*, 335:353-354, 1988.

2. Dichter M.A., Tischler A.S. and Greene L.A. Nerve growth factor-induced increase in electrical excitability and acetylcholine sensitivity of a rat pheochromocytoma cell line. *Nature*, 268: 501–504, 1977.

3. Frassetto L.J., Schieve C.R., Lieven C.J., Utter A.A., Jones M.V., Agarwal N. and Levin L.A. Kinase-Dependent Differentiation of a Retinal Ganglion Cell Precursor. *Investigative Ophthalmology and Visual Science*, 47: 427–438, 2006.

4. Harvey S. Extrapituitary growth hormone. *Endocrinology*, 38: 335–359, 2010.

5. Harvey S., Lin W., Gliterman D., El-Abry N., Qiang W. and Sanders E.J. Release of retinal growth hormone in the chick embryo: Local regulation? *General and Comparative Endocrinology*, 2012.

6. Lea W.R. and Harvey S. Growth Hormone (GH) suppression of catecholine turnover in the chicken hypothalamus: implications for GH autoregulation. *Journal of Endocrinology*, 193: 245–251, 1993.

7. Liu A., Testa J.R., Hamilton T.C., Jove R., Nicosia S.V. and Cheng J.Q. AKT2, a Member of the Protein Kinase B Family, Is Activated by Growth Factors, v-Ha-ras, and v-src through Phosphatidylinositol 3-Kinase in Human Ovarian Epitherial Cancer Cells. *Cancer Research*, 58: 2973–2977, 1998.

8. McLoon S.C. and Barnes R.B. Early Differentiation of Retinal Ganglion Cells: An Axonal Protein Expressed by Premigratory and Migrating Retinal Ganglion Cells. *The Journal of Neuroscience*, 9:1424–1432, 1989.

9. Moolenaar W.H. and Spector I. Ionic currents in cultured mouse neuroblastoma cells under voltage-clamp conditions. *Journal of Physiology*, 278:265–286, 1978.

10. Moorhouse A.J., Li S., Vickery R.M. Hill M.A. and Morley J.W. A patch-clamp investigation of membrane currents in a novel mammalian retinal ganglion cell line. *Brain Research*, 1003: 205–208, 2004.

11. Pan L., Deng M., Xie X. and Gan L. Isl1 and Brn3b co-regulate the differentiation of murine retinal ganglion cells. *Development*, 135:1981–90, 2008.

12. Pessac B., Girard A., Romey G, Crisanti P., Lorinet A.M. and Calothy G. A neural clone derived from a Rous sarcoma virus-tranformed quail embryo neuroretina established culture. *Nature*, 302: 616–618, 1983.

13. Pollerberg G.E., Kuschel C. and Zenke. Generation of Cell Lines from Embryonic Quail Retina Capable of Mature Neuronal Differentiation. *Journal of Neuroscience Research*, 41:427–442, 1995.

14. Rane S.G. and Reddy E.P. JAKs, STATs and Src kinases in hematopoiesis. *Oncogene*, 21: 3334–3358, 2002.

15. Reiff D.F. and Guenther E. Developmental changes in voltage-activated potassium currents of rat retinal ganglion cells. *Neuroscience*, 92:1103–17, 1999.

16. Rothe T., Jüttner R., Bähring R. and Grantyn R. Ion conductances related to development of repetitive firing in mouse retinal ganglion neurons in situ. *Journal of Neurobiology*, 38:191–206, 1999.

17. Sanders E.J., Baudet M.L., Parker E. and Harvey S. Signaling mechanisms mediating local GH action in the neural retina. *General and Comparative Endocrinology*, XXX: XXX–XXX, 2009.

18. Sanders E.J., Lin W.L.., Parker E. and Harvey S. Growth hormone expression and neuroprotective activity in a quail neural retina cell line. *General and Comparative Endocrinology*, 165: 111–119, 2010.

19. Schmid S. and Guenther E. Developmental regulation of voltage-activated Na^+ and Ca^{2+} currents in rat retinal ganglion cells. *NeuroReport*, 7:677–681, 1996.

20. Schmid S. and Guenther E. Voltage-activated calcium currents in rat retinal ganglion cells in situ: changes during prenatal and postnatal development. *Journal of Neuroscience*, 19:3486–94, 1999.

21. Skaliora I., Robinson D.W., Scobey R.P. and Chalupa L.M. Properties of K^+ conductances in cat retinal ganglion cells during the period of activity-mediated refinements in retinofugal pathways. *European Journal of Neuroscience*, 7:1558–68, 1995.

22. Van Bergen N.J., Wood J.P., Chidlow G., Trounce I.A., Casson R.J., Ju W.K., Weinreb R.N. and Crowston J. Re-characterisation of the RGC-5 retinal ganglion cell line. *Investigative Ophthalmology and Visual Science*, 50:4267–4272, 2009.

23. Van Den Eijnden M.J. and Strous G.R. Autocrine Growth Hormone: Effects on Growth Hormone Receptor Trafficking and Signaling. *Molecular Endocrinology*, 21: 2832–2846, 2007.

24. Wood J.P.M., Chidlow G., Tran T., Crowston J.G. and Casson R.J. A Comparison of Differentiation Protocols for RGC-5 Cells. *Investigative Ophthalmology and Visual Science*, 51: 3774–3783, 2010.

25. Zhu T., Ling L. and Lobie P.E. Identification of a JAK2-independent Pathway Regulating Growth Hormone (GH)-stimulated p44/42 Mitogen-activated Protein Kinase Activity. *Journal of Biological Chemistry*, 227: 45592–45603, 2002.